A NUMERICAL STUDY OF SOLITON SOLUTIONS OF SOME NONLINEAR EVOLUTIONARY EQUATIONS

A Thesis

Submitted in partial fulfilment of the requirements for

the award of the degree of

DOCTOR OF PHILOSOPHY

IN

MATHEMATICS

By

Richa Rani

Registration Number: 41801038

Supervised By

Dr. Geeta Arora

(UID:18820)

Professor

Department of Mathematics

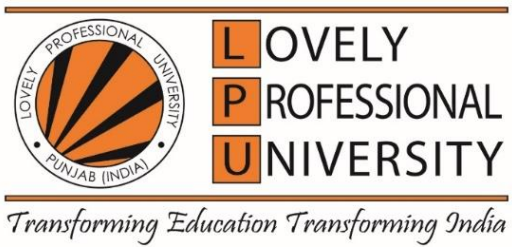

LOVELY PROFESSIONAL UNIVERSITY

PUNJAB

2023

DECLARATION

I, Richa Rani, declare that the work presented in the thesis entitled **"A NUMERICAL STUDY OF SOLITON SOLUTIONS OF SOME NONLINEAR EVOLUTIONARY EQUATIONS"** for the award of the degree of **Doctor of Philosophy (Ph.D.)**, is the outcome of research work carried out by me under the supervision of Dr. Geeta Arora, working as Professor, in the Department of Mathematics of Lovely Professional University, Punjab, India. I confirm that no part of the research work presented in this thesis has been submitted to any other University or Institute for the award of any degree.

(Signature of Scholar)
Richa Rani
Registration Number: 41801038,
Department of Mathematics,
Lovely Professional University,
Punjab, India.

CERTIFICATE

This is to certify that the work reported in the Ph.D. thesis entitled **"A NUMERICAL STUDY OF SOLITON SOLUTIONS OF SOME NONLINEAR EVOLUTIONARY EQUATIONS"** submitted by Richa Rani, has been carried out under my supervision for the award of the degree of **Doctor of Philosophy (Ph.D.)** of Mathematics, Lovely Professional University, Punjab, India. The work presented in this thesis is original and has not been submitted in any other University or Institute for the award of any degree or diploma. The work is comprehensive, complete, and fit for evaluation.

(Signature of Supervisor)
Dr. Geeta Arora
Professor,
Department of Mathematics,
Lovely Professional University,
Punjab, India.

ABSTRACT

Nonlinear evolutionary equations (NLEEs) play a crucial role for describing nonlinear phenomena across various scientific fields, including biology, physics, chemistry, pattern formation, solitons, ecology, heat transfer, and nonlinear dispersion. Solitary waves, which are solutions to NLEEs, maintain their shape while moving at a constant speed, and have received significant attention from the scientific community. This research provides, a comprehensive understanding of the origin and development of solitons and their behavior under different NLEEs. The versatility of solitons is explored, including their applications in plasma physics, nonlinear optics, biology, and nonlinear Bose-Einstein condensation. NLEEs are mathematical models used to describe the time evolution of various physical, biological, and social systems. They are partial differential equations (PDEs) that describes how a system changes over time based on the values of its variables and the relationship between them. They are often used to study the dynamics of system with multiple interacting components, where the behavior of the system as a whole cannot be understood by looking at each component separately. When these equations are mathematically modeled, it is a possibility that these equations are difficult to solve analytically. Therefore, it would be challenging for researchers to identify analytical or exact solutions to these differential equations. Advanced numerical approaches are shown to be most efficient in these situations for providing an approximate numerical solution to these differential equations.

In this research, two numerical methods are established to solve partial differential equations. These newly established numerical methods are: “Exponential modified cubic B-spline differential quadrature method (Expo-MCB-DQM) with LOOCV approach” and “Exponential modified cubic B-spline differential quadrature method (Expo-MCB-DQM) with PSO approach”.

In these methods two approaches (LOOCV and PSO) are used with the “Exponential modified cubic B-spline differential quadrature method” to identify the optimal value of the parameter ϵ that is used in the exponential cubic B-spline basis functions, that needs to provide a value which plays an important role in obtaining accurate numerical solutions. The combination of these approaches with Expo-MCB-DQM, makes it novel in the literature, that attract researchers' interest, which improves the

results of this method. Up till now, the value of parameter ϵ had been determined by the hit-and-trial approach, which leads to unstable results.

To check the authenticity of these newly developed techniques, the methods are implemented on nonlinear Schrödinger (NLS) equation and Sine-Gordon (SG) equation. These two partial differential equations (NLS equation and SG equation), have soliton-type solutions and play crucial roles in various physical applications in science and engineering. The Josephson junction and optical fiber are two significant applications of the NLS equation and SG equation, respectively, briefly discussed in the thesis.

ACKNOWLEDGEMENT

This research work is devoted to Almighty God. With the Grace of God, I could become able to complete this research.

I would like to heartily thank my respected supervisor Dr. Geeta Arora, Professor, Lovely Professional University, Punjab, India. She supervised me in the best possible way. I am truly fortunate to have the opportunity to work with her as a student. It has been an honor and a privilege to work with her. She helped me in each and every aspect of my research. I do not find enough words with which, I can express my feeling of thanks to the entire staff, Lovely Professional University, Punjab, India, for their help, which went a long way in the successful completion of my work. I thank all those who have contributed directly or indirectly to this work. Last, but not least, I would like to thank my family members, who always gave me the strength to complete my goals, which, I decided to achieve. A special thanks to my son who is 2 years old and always prays to God “Babaji mumma ka kaam jaldi finish kar do”. I would appreciate the efforts of my parents and special thanks to my husband who supported me a lot in this journey of Ph.D. and given so many sacrifices in his life, so that I can achieve my goals. The affection and care of my family members for me always gave me the inspiration to complete this research.

CONTENTS

Table of Contents

LIST OF TABLES

LIST OF FIGURES

LIST OF APPENDICES

Ordinary Differential Equations	ODEs
Nonlinear Evolutionary Equations	NLEEs
Exponential Modified Cubic B-spline	Expo-MCB
Differential Quadrature Method	DQM
Sine-Gordon	SG
Nonlinear Schrödinger	NLS
Optical Fiber Communication	OFC
Superconducting Quantum Interference Devices	SQUIDs
Strong stability-preserving time-stepping Runge-Kutta	SSP-RK43
Leave-One-Out Cross-Validation	LOOCV
Particle Swarm Optimization	PSO
Radial Basis Function	RBF
Rate of Convergence	ROC

Chapter-1

Introduction

1.1 Research Problem and Motivation

In modern life, mathematical modeling has become a powerful tool to tackle a wide range of real-world problems. However, finding exact solutions to these problems are challenging, and thus, advanced numerical techniques are often required. Finite difference, finite element, collocation, and differential quadrature methods are some examples of these techniques. I started my research journey by studying literature of differential quadrature method which used many B-spline basis functions to calculate weighing coefficients. Despite its usefulness, literature research indicates that the exponential cubic B-spline basis function is not as extensively used as compared to other B-spline basis functions. One possible reason for this is that its results can be unstable due to a randomly assigned parameter value. Our research problem stems from this issue: can we optimize this parameter value used in basis functions of exponential cubic B-spline? From studied literature, it is noticed that Radial basis functions (RBF) also faces the same type of problem. The research presented in the literature is an extension of the statistical approaches (LOOCV and PSO), that are utilized to find the optimal value of the shape parameter, which is used with different numerical techniques to solve PDEs [1-4].

Now the question arises here: can we use these statistical approaches to improve the accuracy and stability of the "exponential cubic B-spline differential quadrature method"? This problem becomes our research objective, and we aim to apply the "exponential cubic B-spline differential quadrature method" with LOOCV and PSO approaches to solve NLEEs that represent engineering and science applications.

1.2 Need of Numerical methods: Differential equations are vital mathematical tools used to explain and model various scientific phenomena, such as electromagnetic fields, quantum physics, fluid flow, diffusion processes, and structural mechanics. They play a fundamental role in many scientific disciplines, aiding researchers in developing a comprehensive understanding of the behavior of complex systems. In

the field of sciences and engineering, a wide range of ODEs and PDEs are used to explain many mathematical models. Researchers have solved a large number of ODEs and PDEs, analytically and numerically due to their importance. If an analytical solution is unavailable, then such an equation can be solved numerically. Solving nonlinear PDEs can be a challenging task due to the complexity of the equations. At that time, the importance and clarity of numerical methods are highlighted. Different numerical techniques have been developed to find the best-approximated results of such complex-natured PDEs. Numerical methods, such as the “finite difference method”, “finite element method” and “differential quadrature method”, etc. are often used to approximate the solutions to this type of PDEs. These methods involve discretizing the domain of the problem and using iterative algorithms to obtain an approximate solution that satisfies the equation within a certain error tolerance.

Numerical analysis is an area of mathematics that works with creating effective numerical techniques to solve such challenging mathematical problems. Through the use of DQM with B-spline basis functions, this study investigates improved numerical solutions of nonlinear PDEs. The objective is to develop a numerical methodology to solve nonlinear PDEs. The NLS equation and Sine-Gordon equation play a crucial role in framing various mathematical models, which further enhances their significance in scientific research. By developing a numerical technique to solve these equations, researchers can gain a better understanding of their behavior and potential applications, ultimately aiding in the development of innovative solutions for various scientific and engineering challenges.

1.3 Nonlinear evolutionary equations (NLEEs): Nonlinear evolutionary equations are called "nonlinear" because they involve nonlinear functions of the variables, which can lead to complex and often unpredictable behavior of the system. They are also called "evolutionary" because they describe how the system evolves, taking into account the effects of various factors that influence the system's behavior. NLEEs dynamically describe nonlinear sciences, the two dimensions of space and time through the nonlinear systems. NLEEs are a type of nonlinear PDE whose solution exists in the form of solitons and have several other important properties.

There are many examples of nonlinear evolutionary equations that are used to model a wide range of physical, biological, and social phenomena. Here are a few examples:

1.3.1 The Navier-Stokes equations: These are a set of nonlinear PDEs that describe the motion of fluids. They are used to model the behavior of liquids and gases in a variety of applications, including weather forecasting, aerodynamics, and oceanography.

1.3.2 The Fisher-Kolmogorov equation: This is a nonlinear PDE that is used to model the spread of a population over time. It is often used to study the dynamics of biological populations, such as the spread of a disease or the growth of a population.

1.3.3 The Korteweg-de Vries equation: This is a nonlinear PDE that describes the propagation of waves in certain types of media, such as shallow water waves. It is used in many applications, including fluid dynamics, plasma physics, and optics.

1.3.4 The Schrödinger equation: This is a nonlinear PDE that describes the behavior of quantum mechanical systems. It is used to study the behavior of particles at the atomic and subatomic level, and has applications in fields such as chemistry, materials science, and electronics.

1.3.5 The Black-Scholes equation: This is a nonlinear PDE that is used in financial mathematics to model the behavior of stock prices. It is used to value options and other financial derivatives, and has applications in portfolio optimization and risk management.

1.4 Applications of nonlinear evolutionary equations

NLEEs have a wide range of applications in various fields of science and engineering. Here are a few examples:

1.4.1 Pattern formation: NLEEs, such as reaction-diffusion equations, are used to model pattern formation in biological systems, such as the stripes on a zebra or the spots on a leopard.

1.4.2 Fluid dynamics: The Navier-Stokes equations, which are NLEEs, are used to model the behavior of fluids, such as air and water, weather patterns, blood flow, and

aircraft design. These equations have numerous applications in aerospace engineering, weather forecasting, and oceanography, among other fields.

1.4.3 Epidemiology: NLEEs, as the Susceptible-Infectious-Recovered (SIR) model, are used to model the spread of diseases and infections in populations. These equations can help predict the spread of a disease and assess the effectiveness of interventions, such as vaccination programs.

1.4.4 Materials science: The Schrödinger equation, a well-known NLEEs is used to model the behavior of materials at the atomic and subatomic level. This can help researchers design new materials with specific properties, such as strength, conductivity, and elasticity. NLEEs, such as the Ginzburg-Landau equation, are used to model the behavior of materials, such as superconductors and super fluids.

1.4.5 Finance: NLEEs, such as the Black-Scholes equation, are used in financial mathematics to model the behavior of financial instruments, such as options and futures. This can help investors make informed decisions and manage risk.

1.4.6 Climate science: Heat equation, which is a NLEE used to model the behavior of the Earth's climate system. This can help researchers understand the factors that influence climate change and make predictions about future climate patterns.

1.4.7 Quantum mechanics: NLEEs, such as the NLS equation are used to model the behavior of quantum mechanical systems, such as the behavior of atoms in a Bose-Einstein condensate.

1.4.8 Nonlinear optics: NLEEs, such as the NLS equation, are used to model the propagation of light in nonlinear media, such as optical fibers.

1.4.9 Population dynamics: Lotka-Volterra equation is a NLEE which is used to model the interactions between different species in an ecosystem.

1.4.10 Soliton: NLEEs, such as KdV equation and SG equation have important applications in the study of soliton solutions, which are localized wave-like solutions that maintain their shape and speed even after interacting with other solitons or perturbations.

These are just a few examples of the many applications of NLEEs. These equations are used in many fields of science and engineering, where they help researchers and engineers to understand complex system and design new technologies.

1.5 Different types of solutions of nonlinear evolutionary equations

NLEEs have a wide range of applications in physics, chemistry, biology, and engineering. Here are some applications of these equations based on their different types of solutions:

1.5.1 Periodic solutions: A periodic solution is a solution that repeats itself after a certain amount of time. Examples of equations with periodic solutions include Kuramoto-Sivashinsky, Ginzburg-Landau, and Swift-Hohenberg equations. They are commonly used to model natural phenomena like flame fronts, chemical reactions, and turbulence in fluid dynamics. Identifying and analyzing periodic solutions is essential in understanding the behavior of complex systems in nature.

1.5.2 Travelling wave solutions: Travelling wave solutions are type of soliton solutions that maintain their shape and speed while propagating through space. Equations such as KdV, NLS, and SG have travelling wave solutions. They are used to model the propagation of waves in water and light in optical fibers. Travelling wave solutions also explain the spread of epidemics and nerve impulses.

1.5.3 Shock waves: A shock wave is a sudden change in amplitude or speed of a wave. Equations such as the Burgers' equation and the Riemann problem have shock wave solutions. The Burgers' equation, which has shock wave solutions, is used to model traffic flow and the behavior of fluids under high pressure. In addition, shock wave solutions are also used to explain the behavior of supernovae and other explosive events.

1.5.4 Chaotic solutions: Chaotic solutions are unpredictable and exhibit complex behavior over time. Equations with chaotic solutions include the Lorenz system, Rossler system, and Henon-Heiles system. Chaotic solutions are used to study fluid turbulence, the dynamics of chemical reactions, and the behavior of financial markets.

1.5.5 Multisoliton solutions: Multisoliton are solutions consisting of multiple solitons that maintain their shape and speed over long distances. Equations with

multisoliton solutions include the KdV, NLS, and SG equations. Multisoliton solutions have applications in the study of magnetic flux tubes dynamics, Bose-Einstein condensates behavior, and quantum fluid dynamics.

In summary, NLEEs can have a variety of solution types, including periodic solutions, travelling wave solutions, shock waves, soliton solutions, chaotic solutions, and multisoliton solutions. The specific type of solution that arises depends on the physical system being modeled and the properties of the equation governing that system.

1.6 Solitons: Solitons are a unique type of long wave that does not disperse and moves as a packet with a constant velocity. They are also known as shallow water waves with a permanent form. The remarkable feature of solitons is that they maintain their shape when they collide with another soliton. This property has made solitons popular among mathematicians, physicists, and engineers due to their robustness and practical applications. Solitons are formed as a special type of solution of NLEEs, and NLEEs are a type of nonlinear PDEs.

1.7 Introduction to Differential Quadrature Method

To get approximation findings of nonlinear PDEs, several numerical approaches have been developed during the last few decades, for example “finite difference (FD) method”, “finite element (FE) method”, “finite volume (FV) method”, “collocation method”, etc. However, one of the most advanced and useful numerical approaches for obtaining the results of various nonlinear PDEs is DQM.

DQM is a well-known numerical technique, is employed to solve partial differential equations (PDEs). Bellman and Casti [5, 6] presented this technique in the 1970s. This technique underwent revision in the 1980s [7] and shown to be a useful numerical approach to issues in the physical and engineering sciences [8]. Due to its properties of quick convergence, high accuracy, and computational power, it is currently a well-known numerical approach. Professor Chang Shu [9] has produced a book on DQM and its use in general engineering up to the year 1999. The weighting coefficient formulation enhanced by Quan and Chang [10] is the most important component of DQM. It is effectively applied to estimate the weighting coefficients

using a variety of basis functions, including B-spline functions [11], Lagrange interpolation polynomials, Fourier expansion-based functions, polynomial-based functions [12], radial basis functions [13], trigonometric B-spline functions [14], exponential B-spline functions [15], hyperbolic B-spline functions, sinc function etc.

1.8 Literature Review of Differential Quadrature Method (DQM)

A number of basis functions have been used in literature with DQM. The B-spline DQM is a significant numerical approach to obtain solutions of PDEs. There has been a lot of work described in the literature for obtaining numerical approximations of nonlinear PDEs using various types, orders, and degrees of B-spline DQM, some of which are presented here. Bashan et al. presented modified cubic B-spline [16, 17], modified quintic B-spline [18], and Crank-Nicolson quintic B-spline [19] with DQM. Korkmaz and Dag presented cubic B-Spline [20], quartic B-spline [21] and sinc functions [22] with DQM. Tamsir et al. [23, 24] presented exponential modified cubic B-spline with DQM. Arora et al. [25-28] presented modified trigonometric B-spline with DQM. Shukla et al. presented cubic B-splines [29], and exponential modified cubic B-spline [30] with DQM. Kapoor et al. presented modified uniform algebraic hyperbolic (UAH) tension B-spline [31], modified quartic hyperbolic B-spline [32], and Barycentric Lagrange interpolation basis [33] with DQM. Kumar et al. [34] used radial basis functions with DQM.

1.9 Spline Functions: The theory of splines is explained in detail by Carl de Boor [35]. Splines are widely used by draftsmen and shipbuilders to draw curves that pass-through points in a continuous manner, as well as in numerical techniques. These functions are commonly used in numerical analysis, computer-aided design, computer graphics, and other fields where the accurate representation of curves and surfaces is important. They provide a flexible and computationally efficient way to interpolate or approximate data, and can be used to construct curves and surfaces of arbitrary shape and complexity.

Spline functions are mathematical functions used in the interpolation and approximation of data. These are piecewise-defined functions that consist of polynomial segments of a certain degree that are smoothly connected at a set of points

called knots. The polynomial segments are chosen to ensure that the spline is smooth and continuous across the knots.

In numerical analysis, a spline is a function defined piecewise using polynomial functions. It is a polynomial of degree k in each interval $[\mathcal{V}_i, \mathcal{V}_{i+1}], i = 0,1,2, \dots, n-1$, with the property that the polynomial and its first to k-1th derivatives are continuous in the domain $[\mathcal{V}_i, \mathcal{V}_{i+1}]$. The knots or node points are the known abscissas x_i on a uniform mesh $\mathcal{V}_0 < \mathcal{V}_1 < \dots\dots < \mathcal{V}_n$ in the computational domain [a, b], where, $\mathcal{V}_0 = a$ and $\mathcal{V}_n = b$. The spline function $S(\mathcal{V})$ on the computational domain [a, b], is defined as the sum of the polynomial functions $P(\mathcal{V}_i)$ over all sub-domains that is:

$$S(\mathcal{V}) = \sum_{i=1}^{n} P(\mathcal{V}_i)$$

The concept of spline originated from the problem of fitting a polynomial to a set of data points with known functional values. For example, a linear polynomial can be used with two data points, a quadratic polynomial with three, and a cubic polynomial with four. However, as the number of data points increases, the degree of the polynomial required also increases, making it challenging to work with higher degree polynomials. The most commonly used spline functions are cubic splines, which consist of cubic polynomial segments that are joined smoothly at the knots. To construct a cubic spline, the data points are first divided into a set of intervals, with each interval containing two adjacent knots. A cubic polynomial is then fitted to the data within each interval, subject to certain continuity and smoothness conditions at the knots. These conditions ensure that the spline is smooth and continuous across the knots, and that its first and second derivatives are also continuous. Once the cubic spline is constructed, it can be evaluated at any point within the interval by using the appropriate polynomial segment. This allows the spline to interpolate or approximate the data with a high degree of accuracy, even if the data is noisy or irregularly spaced.

1.10 Different types of spline functions

Here are some examples of different types of spline functions:

(a) Linear spline: A simple example of a linear spline is a straight line connecting two adjacent data points. For example, if we have the data points (1,2) and (3,4) the linear spline connecting them is: $y = 1 + \frac{x}{2}$.

(b) Quadratic spline: A quadratic spline is a parabolic curve or piecewise quadratic function that connects adjacent data points smoothly. They are more flexible than linear splines but are still relatively simple. For example, if we have the data points (1, 2), (2, 1), and (3, 4), a quadratic spline that fits these points is: $y = -\frac{x^2}{4} + \frac{3x}{2} - 1$.

(c) Cubic spline: A cubic spline is a cubic polynomials or piecewise cubic function that connects adjacent data points smoothly. They are the most commonly used type of spline function and provide a good balance between flexibility and simplicity. For example, for the data points (1, 2), (2, 1), and (3, 4), a cubic spline that fits these points is given by: $y = -\frac{x^3}{2} + 3x^2 - 3x + 2$.

(d) Quartic splines: Quartic splines are spline functions of degree four. They are used in situations where a higher degree of accuracy is required, but cubic splines are not sufficient. Quartic splines are defined by piecewise quartic polynomials that are joined smoothly at the knots.

(e) Quintic splines: Quintic splines are spline functions of degree five. They are used in situations where even greater accuracy is required than with quartic splines. Quintic splines are defined by piecewise quintic polynomials that are joined smoothly at the knots.

(f) Higher-order splines: Higher-order splines are spline functions of degrees higher than three. They are less commonly used than cubic splines but can provide greater flexibility and accuracy in some situations.

(g) B-spline: B-splines are a type of piecewise polynomial function that are widely used in computer graphics and geometric modeling. An example of a B-spline is the cubic B-spline, which is a piecewise cubic function that is defined by a set of control points and a set of basis functions. The basis functions determine the shape of the curve, while the control points determine its position.

(h) Non-Uniform Rational B-Splines (NURBS): NURBS are a type of spline function that are commonly used in computer-aided design (CAD) and computer graphics. An example of a NURBS curve is a Bezier curve, which is a cubic NURBS curve that is defined by a set of control points and a set of weights. The weights determine the degree of influence that each control point has on the shape of the curve. They are similar to B-splines but allow for more complex shapes and can represent curves and surfaces with a high degree of accuracy.

Overall, spline functions are a powerful and versatile tool for the interpolation and approximation of data, and the choice of spline function depends on the specific requirements of the application. These are just a few examples of the different types of spline functions. There are many other types of spline functions, each with their own unique properties and applications.

1.11 Different types of B-splines functions

B-spline basis functions are powerful techniques used in computer aided geometry design (CAGD) and approximation theory. B-splines are piecewise polynomials that exhibit global smoothness. The points at which these pieces are connected are known as knot points or grid points. The term "B-spline" was first introduced in 1946 by Schoenberg [36] as a short form of basis spline, which is a piecewise polynomial approximation that is smooth.

B-spline is a spline function that achieves minimal support for a given degree, smoothness, and partition domain. The basis function is the fundamental concept of the B-spline. A knot sequence is a non-decreasing sequence of knot points, where each knot point is denoted by $\mathcal{V}_i$. The interval between each knot point, $[\mathcal{V}_i, \mathcal{V}_{i+1})$, is the i^{th} knot span. When knots are equally spaced, the knot sequence is known as a uniform knot sequence, and when knots are not equally spaced, it is a non-uniform knot sequence. A B-spline function with degree k covers $(k+1)$ knot points or k intervals.

In the 1972, Cox and Boor [35] gave a recurrence relation for attaining the B-spline basis function. Using Leibnitz's Theorem, Boor derived the n^{th} B-spline basis function with k^{th} degree in the form of a recurrence relation:

$$C_{i,k}(\mathcal{V}) = Z_{i,k}C_{i,k-1}(\mathcal{V}) + \big(1 - Z_{i+1,k}\big)C_{i+1,k-1}(\mathcal{V})$$

where $Z_{i,k}$ is given by:

$$Z_{i,k} = \left(\frac{\mathcal{V} - \mathcal{V}_i}{\mathcal{V}_{i+k} - \mathcal{V}_i}\right)$$

The above recursion formula is known as the Cox de Boor formula, and $Z_{i,k}$ is the i^{th} B-spline function with degree k. The set $\{\mathcal{V}_i\}$ is the non-decreasing set of knot points. By using the Cox de Boor formula, we can easily observe that the B-spline function of an arbitrary degree can be evaluated as a linear combination of lower degree B-splines.

Here are some examples of different types of B-splines:

(a) Zero Degree B-splines: By setting k = 0, the basis function of zero degree B-splines simplifies to a step function, making it a straightforward and uncomplicated basis function. Thus, a B-spline of zero degree is constructed as follows:

$$C_{i,0}(\mathcal{V}) = \begin{cases} 1, & \mathcal{V}\epsilon\,[\mathcal{V}_i\,\mathcal{V}_{i+1}) \\ 0, & otherwise \end{cases}$$

(b) Linear B-spline: If we substitute k = 1 in the equation and utilize the concept of B-spline of 1st degree, which is commonly referred to as the linear B-spline. The construction of the linear B-spline is as follows:

$$C_{i,1}(\mathcal{V}) = \begin{cases} \dfrac{\mathcal{V} - \mathcal{V}_i}{\mathcal{V}_{i+1} - \mathcal{V}_i,} & \mathcal{V}\epsilon\big[\mathcal{V}_i,\mathcal{V}_{i+1}\big) \\ \dfrac{\mathcal{V}_{i+2} - \mathcal{V}}{\mathcal{V}_{i+2} - \mathcal{V}_{i+1},} & \mathcal{V}\epsilon[\mathcal{V}_{i+1},\mathcal{V}_{i+2}) \\ 0, & otherwise \end{cases}$$

(c) Quadratic B-spline: To obtain the B-spline of 2nd degree, also known as the quadratic B-spline, we can substitute k = 2 in formula and incorporate the concept of the B-spline of the first degree.

The construction of the quadratic B-spline is as follows:

$$C_{i,2}(\mathcal{V}) = \frac{1}{h^2}\begin{cases} \dfrac{(\mathcal{V}-\mathcal{V}_i)^2}{(\mathcal{V}_{i+2}-\mathcal{V}_i)(\mathcal{V}_{i+1}-\mathcal{V}_i)}, & \mathcal{V}\epsilon[\mathcal{V}_i,\mathcal{V}_{i+1}) \\ \dfrac{(\mathcal{V}-\mathcal{V}_i)(\mathcal{V}_{i+2}-\mathcal{V})}{(\mathcal{V}_{i+2}-\mathcal{V})(\mathcal{V}_{i+2}-\mathcal{V}_{i+1})} + \dfrac{(\mathcal{V}_{i+3}-\mathcal{V})(\mathcal{V}-\mathcal{V}_{i+1})}{(\mathcal{V}_{i+3}-\mathcal{V}_{i+1})(\mathcal{V}_{i+2}-\mathcal{V}_{i+1})}, & \mathcal{V}\epsilon[\mathcal{V}_{i+1},\mathcal{V}_{i+2}) \\ \dfrac{(\mathcal{V}_{i+3}-\mathcal{V})^2}{(\mathcal{V}_{i+3}-\mathcal{V}_{i+1})(\mathcal{V}_{i+3}-\mathcal{V}_{i+2})}, & \mathcal{V}\epsilon[\mathcal{V}_{i+2},\mathcal{V}_{i+3}) \\ 0, & otherwise \end{cases}$$

(d) Cubic B-spline: The B-spline of degree 3, also referred to as the cubic B-spline, can be obtained by utilizing the recurrence relation and the B-spline of degree 2. The construction of the cubic B-spline is as follows:

$$C_{i,3}(\mathcal{V}) = \frac{1}{h^3}\begin{cases} (\mathcal{V}-\mathcal{V}_{i-2})^3, & \mathcal{V}\epsilon[\mathcal{V}_{i-2},\mathcal{V}_{i-1}) \\ (\mathcal{V}-\mathcal{V}_{i-2})^3 - 4(\mathcal{V}-\mathcal{V}_{i-1})^3, & \mathcal{V}\epsilon[\mathcal{V}_{i-1},\mathcal{V}_i) \\ (\mathcal{V}_{i-2}-\mathcal{V})^3 - 4(\mathcal{V}_{i+1}-\mathcal{V})^3, & \mathcal{V}\epsilon[\mathcal{V}_i,\mathcal{V}_{i+1}) \\ (\mathcal{V}_{i+2}-\mathcal{V})^3, & \mathcal{V}\epsilon[\mathcal{V}_{i+1},\mathcal{V}_{i+2}) \\ 0, & otherwise \end{cases}$$

(e) Quartic B-spline: The B-spline of degree 4, also known as the quartic B-spline, can be constructed by utilizing the recurrence relation and the B-spline of degree 3 to obtain the B-spline of degree 4. The construction of the quartic B-spline is as follows:

$$C_{i,4} = \frac{1}{h^4}\begin{cases} (\mathcal{V}-\mathcal{V}_{i-2})^4, & \mathcal{V}\epsilon[\mathcal{V}_{i-2},\mathcal{V}_{i-1}) \\ (\mathcal{V}-\mathcal{V}_{i-2})^4 - 5(\mathcal{V}-\mathcal{V}_{i-1})^4, & \mathcal{V}\epsilon[\mathcal{V}_{i-1},\mathcal{V}_i) \\ (\mathcal{V}-\mathcal{V}_{i-2})^4 - 5(\mathcal{V}-\mathcal{V}_{i-1})^4 + 10(\mathcal{V}-\mathcal{V}_i)^4, & \mathcal{V}\epsilon[\mathcal{V}_i,\mathcal{V}_{i+1}) \\ (\mathcal{V}_{i+3}-\mathcal{V})^4 - 5(\mathcal{V}_{i+2}-\mathcal{V})^4, & \mathcal{V}\epsilon[\mathcal{V}_{i+1},\mathcal{V}_{i+2}) \\ (\mathcal{V}_{i+3}-\mathcal{V})^4, & \mathcal{V}\epsilon[\mathcal{V}_{i+2},\mathcal{V}_{i+3}) \\ 0, & otherwise \end{cases}$$

(f) Quintic B-spline: The B-spline of degree 5, also referred to as the quintic B-spline, can be established by utilizing the recurrence relation and the B-spline of degree 4.

The construction of the quintic B-spline is as follows:

$$C_{i,5} = \frac{1}{h^5}\begin{cases} (\mathcal{V} - \mathcal{V}_{i-3})^5, & \mathcal{V}\epsilon[\mathcal{V}_{i-3}, \mathcal{V}_{i-2}) \\ (\mathcal{V} - \mathcal{V}_{i-3})^5 - 6(\mathcal{V} - \mathcal{V}_{i-2})^5, & \mathcal{V}\epsilon[\mathcal{V}_{i-2}, \mathcal{V}_{i-1}) \\ (\mathcal{V} - \mathcal{V}_{i-3})^5 - 6(\mathcal{V} - \mathcal{V}_{i-2})^5 + 15(\mathcal{V} - \mathcal{V}_{i-1})^5, & \mathcal{V}\epsilon[\mathcal{V}_{i-1}, \mathcal{V}_i) \\ (\mathcal{V}_{i+3} - \mathcal{V})^5 - 6(\mathcal{V}_{i+2} - \mathcal{V})^5 + 15(\mathcal{V}_{i+1} - \mathcal{V})^5, & \mathcal{V}\epsilon[\mathcal{V}_i, \mathcal{V}_{i+1}) \\ (\mathcal{V}_{i+3} - \mathcal{V})^5 - 6(\mathcal{V}_{i+2} - \mathcal{V})^5, & \mathcal{V}\epsilon[\mathcal{V}_{i+1}, \mathcal{V}_{i+2}) \\ (\mathcal{V}_{i+3} - \mathcal{V})^5, & \mathcal{V}\epsilon[\mathcal{V}_{i+2}, \mathcal{V}_{i+3}) \\ 0, & otherwise \end{cases}$$

(g) Uniform B-spline: A uniform B-spline is a B-spline where the knots are equally spaced. Uniform B-splines are commonly used in numerical analysis because they have desirable mathematical properties.

(h) Non-uniform B-spline: A non-uniform B-spline is a B-spline where the knots are not equally spaced. Non-uniform B-splines are used in situations where more control over the shape of the curve is needed.

(i) Periodic B-spline: A periodic B-spline is a B-spline where the curve is closed, meaning it has the same value at the beginning and end points. Periodic B-splines are used in situations where the curve needs to be continuous and smooth at the endpoints.

These are just a few examples of the different types of B-splines. There are many other types of B-splines with different orders, continuity, and knot vectors, each with their own unique properties and applications.

1.12 Exponential cubic B-spline

The exponential cubic B-spline basis functions are a type of spline function used in numerical analysis and computer graphics to approximate curves and surfaces. Expo-MCB basis functions also available in literature for solving various equations such as Burgers equation [23], multi-dimensional convection-diffusion equations [30], Sine-Gordon equation [15], Fisher's reaction-diffusion equation [24], telegraph equation [37], nonlinear Schrödinger equation [26], etc. However, compared to other basis functions, Expo-MCB-DQM is still not often found in the literature. This is because

there exists a parameter ϵ in exponential cubic B-spline basis functions that needs to provide a value which plays an important role in finding the numerical solutions.

1.13 The algorithm of DQM with B-spline basis functions

The DQM is a numerical technique for solving nonlinear PDEs using B-spline functions as the basis functions. The algorithm for the DQM with B-spline basis functions is as follows:

Step 1 Discretize the domain: Divide the domain of the nonlinear PDEs into a set of discrete points. The points should be evenly spaced to simplify the calculations.

Step 2 Choose appropriate basis functions: A suitable basis functions are required to approximate the unknown function and its derivatives at the discrete points.

Step 3 Approximation: Approximate the unknown function and its derivatives at each of the discrete points using a weighted sum of the function values at these points. In this study the weighting coefficients are determined by the exponential cubic B-spline basis functions.

Step 4 Derivative evaluation: Evaluate the derivatives of the unknown function using the approximation obtained in step 3.

Step 5 System of equations: Substituting the derivatives, the PDE transformed the PDE into a system of ODEs.

Step 6 Solve the system of equations: Solve the system of algebraic equations to obtain the values of the unknown function at the discrete points.

1.14 Modified Exponential Cubic B-spline Differential Quadrature Method

DQM is a numerical method for approximating the function derivative as a linear sum of the function value on the discrete node points inside the problem's solution space. This technique takes into consideration the grid distribution, where a given interval $[a, b]$ is divided into a set of discrete grid points $a = x_1 < x_2 < \cdots < x_N = b$.

Assuming that the function $u(x)$ is sufficiently smooth within the region of the solution, the value of the derivatives at the discrete points $x_i$can be written in the form as follows:

$$\frac{d^{(r)}u}{dx^{(r)}}|_{x_i} = \sum_{j=1}^{N} p_{i,j}^{(r)} u(x_j), \quad i = 1,2,\dots,N, \quad r = 1,2,\dots,N-1 \tag{1.1}$$

here r signifies the order of derivative, $p_{i,j}^{(r)}$ are the weighing coefficients and N are the total points consider for approximation solution in the domain.

The objective of the DQM approach is to estimate the weighting coefficients that can be obtained using a set of basis functions that covers the domain. While calculating the weighting coefficients, various types of basis functions may be applied as per the context.

This research employs the exponential form of B-spline in third degree as the basis functions for calculating the weighting coefficients. The exponential cubic B-spline basis functions are defined as follows [23]:

$$C_m(x) = \frac{1}{h^3}\begin{cases} \alpha_3\,(x_{m-2}-x) - \frac{\alpha_3}{\epsilon(\sinh(\epsilon(x_{m-2}-x)))}, & x\epsilon[x_{m-2}, x_{m-1}) \\ \alpha_1 + \alpha_2(x_m - x) + \alpha_4 e^{\epsilon(x_m-x)} + \delta_1 e^{-\epsilon(x_m-x)}, & x\epsilon[x_{m-1}, x_m) \\ \alpha_1 + \alpha_2(x - x_m) + \alpha_4 e^{\epsilon(x-x_m)} + \delta_1 e^{-\epsilon(x-x_m)}, & x\epsilon[x_m, x_{m+1}) \\ \alpha_3(x - x_{m+2}) - \frac{\alpha_3}{\epsilon(\sinh(\epsilon(x-x_{m+2})))}, & x\epsilon[x_{m+1}, x_{m+2}) \end{cases} \tag{1.2}$$

where $h = x_n - x_{n-1}$ for all n.

$$\alpha_1 = \frac{\epsilon h c_1}{\epsilon h c_1 - c_2}, \alpha_2 = \frac{\epsilon}{2}\left(\frac{c_1(c_1-1)+{c_2}^2}{(\epsilon h c_1 - c_2)(1-c_1)}\right), \alpha_3 = \frac{\epsilon}{2(\epsilon h c_1 - c_2)}, \alpha_4 = \frac{1}{4}\left(\frac{(1-c_1+c_2)e^{-\epsilon h}-c_2}{(\epsilon h c_1 - c_2)(1-c_1)}\right),$$

$$\delta_1 = \frac{1}{4}\left(\frac{(-1+c_1+c_2)e^{\epsilon h}-c_2}{(\epsilon h c_1 - c_2)(1-c_1)}\right), c_1 = \cosh(\epsilon h), c_2 = \sinh(\epsilon h).$$

The parameter (ϵ) that has to be optimized is used here, which is necessary for finding the solutions.

The numerical values of the exponential cubic B-spline functions $C_m(x)$ and their derivatives at different nodal points can be obtained with the help of Table 1.1.

Table 1.1. The exponential cubic B-spline functions $C_m(x)$ and their derivatives at the different grid points.

	x_{n-2}	x_{n-1}	x_n	x_{n+1}	x_{n+2}
$C_m(x)$	0	$\frac{c_2-\epsilon h}{2(\epsilon h c_1-c_2)}$	1	$\frac{c_2-\epsilon h}{2(\epsilon h c_1-c_2)}$	0
$C'_m(x)$	0	$\frac{\epsilon(c_1-1)}{2(\epsilon h c_1-c_2)}$	0	$\frac{\epsilon(1-c_1)}{2(\epsilon h c_1-c_2)}$	0
$C''_m(x)$	0	$\frac{\epsilon^2 c_2}{2(\epsilon h c_1-c_2)}$	$\frac{-\epsilon^2 c_2}{(\epsilon h c_1-c_2)}$	$\frac{\epsilon^2 c_2}{2(\epsilon h c_1-c_2)}$	0

When utilizing exponential cubic B-spline as the basis functions in the fundamental DQM equation (1.1), the resultant equation is as follows:

$$\frac{\partial^{(r)}C_m(x_i)}{\partial x^{(r)}} = \sum_{j=m-2}^{m+2} p_{i,j}^{(r)} C_m(x_j), \quad m = -1, 0, \dots, N+2, \quad i = 1, 2, \dots, N. \tag{1.3}$$

Utilizing exponential cubic B-spline leads to the appearance of two additional points on both the left and right sides, resulting in a total of four additional points. These extra points are eliminated by modified form of the basis functions. The modified exponential cubic B-splines can be calculated as shown below at the mesh points [23]:

$$\begin{aligned} G_1(x) &= C_1(x) + 2C_0(x), \\ G_2(x) &= C_2(x) - C_0(x), \\ G_k(x) &= C_k(x) for \quad k = 3,4, \dots, N-2, \\ G_{N-1}(x) &= C_{N-1}(x) - C_{N+1}(x), \\ G_N(x) &= C_N(x) + 2C_{N+1}(x), \end{aligned} \tag{1.4}$$

When r=1 in equation (1.1), the resulting equation is:

$$G'_k(x_i) = \sum_{j=1}^{N} p_{i,j}^{(1)} G_k(x_j), \ for \quad i = 1,2, \dots, N, \quad k = 1,2, \dots, N. \tag{1.5}$$

$$A\vec{p}^{(1)}[i] = \vec{T}[i] \ for \quad i = 1,2, \dots, N. \tag{1.6}$$

The coefficient matrix $A = [G_{ij}]$ of order N, is expressed as:

$$A = \begin{bmatrix} \frac{\epsilon h c_1 - \epsilon h}{\epsilon h c_1 - c_2} & \frac{c_2 - \epsilon h}{2(\epsilon h c_1 - c_2)} & 0 & 0 & 0 & \cdots & 0 \\ 0 & 1 & \frac{c_2 - \epsilon h}{2(\epsilon h c_1 - c_2)} & 0 & 0 & \cdots & 0 \\ 0 & \frac{c_2 - \epsilon h}{2(\epsilon h c_1 - c_2)} & 1 & \frac{c_2 - \epsilon h}{2(\epsilon h c_1 - c_2)} & 0 & \cdots & 0 \\ \ddots & \ddots & \ddots & \ddots & \ddots & \ddots & \ddots \\ 0 & 0 & \cdots & \frac{c_2 - \epsilon h}{2(\epsilon h c_1 - c_2)} & 1 & \frac{c_2 - \epsilon h}{2(\epsilon h c_1 - c_2)} & 0 \\ 0 & 0 & \cdots & 0 & \frac{c_2 - \epsilon h}{2(\epsilon h c_1 - c_2)} & 1 & 0 \\ 0 & 0 & \cdots & 0 & 0 & \frac{c_2 - \epsilon h}{2(\epsilon h c_1 - c_2)} & \frac{\epsilon h c_1 - \epsilon h}{\epsilon h c_1 - c_2} \end{bmatrix}$$

The weighing coefficient vector $\vec{p}^{(1)}[i] = \left[p_{i1}^{(1)}, p_{i2}^{(1)}, \dots, p_{iN}^{(1)}\right]^T$ which corresponds to grid point x_i, and the coefficient vector $\vec{T}[i] = \left[G'_{1,i}, G'_{2,i} \dots, G'_{N-1,i}, G'_{N,i}\right]^T$ also corresponding to grid point x_i, are calculated for $i = 1,2, \dots, N$ as follows:

$$T[1] = \begin{bmatrix} \frac{\epsilon(1-c_1)}{(\epsilon h c_1 - c_2)} \\ \frac{\epsilon(1-c_1)}{(\epsilon h c_1 - c_2)} \\ 0 \\ 0 \\ \vdots \\ 0 \\ 0 \end{bmatrix}, \; T[2] = \begin{bmatrix} \frac{\epsilon(1-c_1)}{2(\epsilon h c_1 - c_2)} \\ 0 \\ \frac{\epsilon(1-c_1)}{2(\epsilon h c_1 - c_2)} \\ 0 \\ \vdots \\ 0 \\ 0 \end{bmatrix}, \dots, \; T[N-1] = \begin{bmatrix} 0 \\ 0 \\ \vdots \\ 0 \\ \frac{\epsilon(1-c_1)}{(\epsilon h c_1 - c_2)} \\ 0 \\ \frac{\epsilon(c_1-1)}{(\epsilon h c_1 - c_2)} \end{bmatrix}, \; T[N] = \begin{bmatrix} 0 \\ 0 \\ \vdots \\ 0 \\ 0 \\ \frac{\epsilon(1-c_1)}{(\epsilon h c_1 - c_2)} \\ \frac{\epsilon(c_1-1)}{(\epsilon h c_1 - c_2)} \end{bmatrix}$$

After implementing the developed program on MATLAB the values of weighting coefficients are obtained. These values can then be utilized to determine the weighting coefficients for the second-order derivatives using the following relationship:

$$p_{ij}^{(2)} = \begin{cases} -\sum_{i=1}^{N} p_{ij}^{(2)} & for\ i = j \\ 2p_{ij}^{(1)}\left(p_{ii}^{(1)} - \frac{1}{x_i - x_j}\right) & for\ i \neq j \end{cases}$$

A strong stability-preserving time-stepping Runge-Kutta (SSP-RK43) scheme [38] is then after applied to calculate the numerical solution to the resulting ODE system.

1.15 Strong stability-preserving time-stepping Runge-Kutta (SSP-RK43) scheme

The SSP-RK43 is a numerical method to solve the given ordinary differential equations (ODEs). In the proposed research work, the reduced system of ODE can be presented by the following equation:

$$\frac{du}{dt} = L(u)$$

where L denotes a spatial nonlinear differential operator and to solve this system of ODE following are the steps as outlined below:

$$u^{(1)} = u^{(m)} + \frac{\Delta t}{2} L\left(u^{(m)}\right)$$

$$u^{(2)} = u^{(1)} + \frac{\Delta t}{2} L\left(u^{(1)}\right)$$

$$u^{(3)} = \frac{2}{3} u^{(m)} + \frac{u^{(2)}}{3} + \frac{\Delta t}{6} L\left(u^{(2)}\right)$$

$$u^{(m+1)} = u^{(3)} + \frac{\Delta t}{2} L\left(u^{(3)}\right),$$

and consequently, the solution $u(x,t)$ at a particular time level is completely known.

1.16 Convergence analysis

A numerical method for solving a differential equation is considered convergent if the approximate solution approaches the exact solution as the step size (h) tends to zero, given that rounding errors from initial conditions approach zero. This implies that as the method is refined with smaller step sizes, the sequence of approximate solutions should converge to the exact solution.

1.16.1 Rate of Convergence (ROC)

The rate of convergence (p) characterizes how quickly the iterates approach the exact solution as the number of iterations increases in an iterative numerical method.

- $p \approx 1$ suggests linear convergence, where the error decreases by a constant factor in each iteration, and the number of correct digits roughly doubles.

- If p is close to 2, it indicates quadratic convergence. Here, the error decreases by a squared factor in each iteration, resulting in roughly quadrupling the number of correct digits.
- Higher p values denote faster convergence, and the associated interpretations hold for higher orders of convergence.

The rate of convergence of the numerical scheme used in the chapters is calculated by the formula [39]:

$$p \approx \frac{\log\left(\frac{E_N}{E_{2N}}\right)}{\log\left(\frac{2N}{N}\right)}$$

where, E_N, and E_{2N} are the L_∞ errors with the number of partitions as N and 2N respectively.

- $\frac{E_N}{E_{2N}}$: Represents the ratio of errors between two successive iterations (N and $2N$). And reflects how much the error decreases from one iteration to the next.
- $\log\left(\frac{E_N}{E_{2N}}\right)$: The logarithm (natural log is used, denoted by "ln" and is expressed with base e) of the error ratio amplifies differences in errors.
- $\log\left(\frac{2N}{N}\right)$: The logarithm of 2 serves as a normalization factor.
- $\frac{\log\left(\frac{E_N}{E_{2N}}\right)}{\log\left(\frac{2N}{N}\right)}$: Gives a numerical estimate of the rate of convergence (p). The numerator measures how errors decrease, and the denominator normalizes this measurement.

1.17 Stability of method

In the context of numerical methods, stability denotes how an algorithm or method behaves when confronted with minor errors, or uncertainties. A numerical method is deemed stable if it consistently delivers accurate and reliable results, demonstrating resilience in the face of slight variations in input data, initial conditions, or computational parameters.

The stability of the DQM method has undergone scrutiny in the literature, assessed by various authors [25-28]. Observations reveal that the DQM method exhibits

conditional stability, signifying its stability contingent on specific conditions, such as particular choices of time step or grid size.

By utilizing the differential quadrature method on partial differential equations, we can obtain a set of ordinary differential equations that can be solved using numerical methods such as the Runge-Kutta method. To ensure stability when using the Runge-Kutta method, conditions for eigenvalues are provided by M.K. Jain [40] in his book. Consider the equation of the form:

$$u_t(x,t) = M + f\big(u(x,t)\big),$$

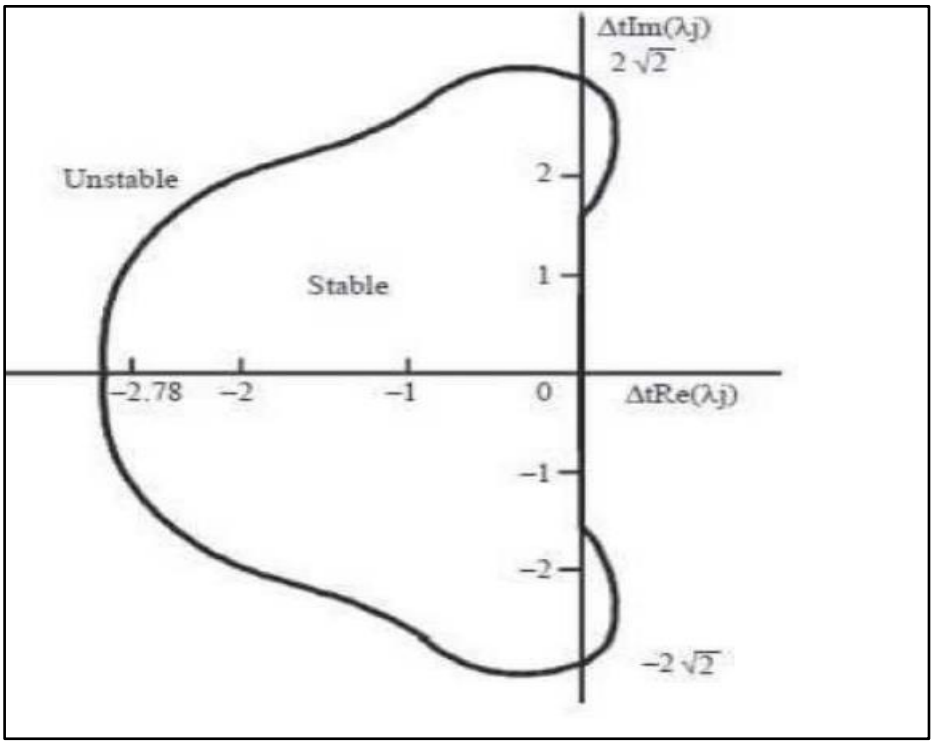

Figure 1.1. Region of Stability

where M is a matrix derived from the partial differential equation and $f\big(\mathrm{u(x,t)}\big)$ represents the nonlinear terms. The stability of the system depends on the eigenvalues of matrix M, which must satisfy specific conditions depending on the value of time step Δt as defined below:

(a) Real λ_j : $-2.78 < \Delta t\lambda_j < 0$

(b) Pure Imaginary λ_j: $-2\sqrt{2} < \Delta t\lambda_j < -2\sqrt{2}$

(c) Complex λ_j: $\Delta t\lambda_j$, lies inside the region (shown in Figure 1.1)

The system is stable only if the eigenvalues fall within certain ranges, as shown in Figure 1.1. It is essential to consider the time step value when determining the stability of the system.

1.18 Optimization

The process of minimizing or maximizing an objective function by choosing the best values for each of its variables from within the permitted range of values is referred to as "optimization". Any real-world application can often be turned into an optimization task.

1.18.1 Applications of optimization techniques

Optimization techniques have a variety of applications. Some of the applications of optimization techniques include:

Operations research: Optimization techniques are widely used in operations research to solve problems such as resource allocation, inventory management, and scheduling. For example, linear programming can be used to optimize production and transportation schedules to minimize costs in a manufacturing company.

Engineering: Optimization techniques are used in engineering to optimize the designing of complex problems, such as airplanes, bridges, and electronic circuits. For example, genetic algorithms can be used to optimize the shape of a wing for a given set of designs and nonlinear programming (NLP) can be used to optimize the shape of an aircraft wing to minimize drag while maximizing lift.

Finance: Optimization techniques are used in finance to optimize investment portfolios, risk management, and trading strategies. For example, quadratic programming can be used to minimize the risk of an investment portfolio while maximizing its return.

Machine learning: Gradient descent is an optimization technique that is widely used in machine learning to optimize the parameters of a model. It is used to minimize the loss function of a model, which measures the difference between the predicted and

actual output. Gradient descent is used in many machine learning algorithms, such as linear regression, logistic regression, and neural networks.

Energy systems: Optimization techniques are used in energy systems to optimize the operation and control of power grids, renewable energy systems, and energy storage systems. An example is optimal power flow, which is an optimization problem that aims to minimize the operating cost of a power system while satisfying various constraints, such as the demand for electricity and the capacity of transmission lines.

Overall, optimization techniques have numerous applications across different fields, and they are an essential tool for solving complex problems and improving efficiency and performance.

1.18.2 Resampling techniques

Resampling is a technique used in statistics and machine learning to create new datasets from an existing dataset by drawing samples with or without replacement. The goal of resampling is to improve the accuracy and reliability of statistical estimates and to reduce the risk of overfitting by generating multiple independent samples from the original dataset. There are several important resampling techniques such as cross-validation, LOOCV, Jackknifing, Bootstrapping, etc. By creating multiple independent samples from the original dataset, resampling allows researchers to obtain more accurate estimates of statistical parameters and to test the robustness of their results.

LOOCV is not a specific algorithm, but rather a technique used in machine learning and statistical analysis to evaluate the performance of a model on a given dataset and parameter tuning. LOOCV trains the model on all the data except for one observation, which serves as the validation set. Every observation in the dataset goes through this procedure once, ensuring that every observation is utilized as the validation set precisely once. The algorithm's performance is tracked after each cycle, and the final estimation of the algorithm's performance on the full dataset is based on the average performance across all cycles. When the dataset is small or there is a shortage of data, LOOCV is often utilized. It may also be used to evaluate the effectiveness of many algorithms or adjust the hyperparameters of a single method. For estimating the

model's performance on new, untested data, LOOCV is very helpful since the dataset is limited. Nevertheless, since LOOCV involves fitting the model several times, it may be computationally costly, particularly for large datasets.

1.18.3 Nature inspired algorithms

Nature-inspired algorithms are a class of optimization algorithms that simulate the behavior of natural systems. These algorithms are widely used to solve complex optimization problems in engineering, computer science, and other fields. Some of the most popular nature-inspired algorithms are genetic algorithms, particle swarm optimization, ant colony optimization, artificial bee colony, differential evolution, firefly algorithm, harmony search, grey wolf optimizer, cuckoo search, and bat algorithm etc. One of them is briefed here i.e., particle swarm optimization (PSO).

A computational worldwide optimization technique called PSO was initially suggested by Kennedy and Eberhart in 1995 [41]. It is based on research into the movement patterns of fish and bird flocks and derives from swarm intelligence. The birds are either separated or clustered together during their search until they pinpoint the spot where they could find food. One bird consistently has a good sense of smell, suggesting that it is aware of the position of the food and is more knowledgeable about the source of the food, while the other birds fly from one site to another in quest of food. Since the birds are constantly sharing information, particularly useful information as they migrate from one area to another in quest of food, they will ultimately assemble at the location where food can be obtained. Excellent information is like the most optimistic solution, and food supplies are like the most optimistic solution throughout the whole course. In terms of the particle swarm optimization approach, the solution swarm is like a flock of birds flying from one place to another. Each participant might work together to discover the most upbeat solution using the PSO method. A particle without quality or volume assumes the role of each individual and a simple behavioral pattern is regulated for each particle to demonstrate the complexity of the complete particle swarm. One may use this strategy to resolve the difficult optimist problems.

1.19 Error norms

To ensure the accuracy of developed numerical technique, the findings are verified by comparing the approximations to both exact solutions and previously published numerical solutions. To accomplish this developed technique, various measures of error norms are utilized in the proposed research, and some of the most important formulas used to compute numerical errors are:

$$L_\infty = \max\left(\left|u_{exact}(x_i,t) - u_{numerical}(x_i,t)\right|\right),$$

$$L_2 = \sqrt{h\sum_{i=1}^{N}\left|u_{exact}(x_i,t) - u_{numerical}(x_i,t)\right|^2},$$

$$RMS = \sqrt{\frac{1}{\mathrm{N}\sum_{\mathrm{i}=1}^{\mathrm{N}}\left|u_{exact}(x_i,t) - u_{numerical}(x_i,t)\right|^2}},$$

where u_{exact} and $u_{numerical}$ represents the exact and numerical solutions respectively and N represents the number of partitions of the domain.

1.20 Objectives of the proposed research work

- To explore the importance of applications of solitons in various fields of science.
- To study the solitons for their behavior that are existing as a result of solving the mathematical models which have significant role in the field of science and engineering.
- To implement the differential quadrature method on nonlinear wave equations resulting in solitons using the LOOCV approach.
- To implement the differential quadrature method on nonlinear wave equations resulting in solitons using the PSO approach.

1.21 Layout of the Thesis

This thesis is structured into six chapters, providing a comprehensive and impressive exploration of solitons and their application in science and engineering.

In chapter 1, a comprehensive introduction to NLEEs, solitons theory, SSP-RK45, optimization techniques, and other related topics have been discussed. This chapter also includes the literature regarding the origin of the differential quadrature method. Furthermore, the developed formulae of "Exponential modified cubic B-spline DQM" and its related methodology is also mentioned in this chapter. The error formulae to check the robustness of the schemes are also mentioned in this chapter. This chapter provides an overview of the concepts that are employed throughout the thesis.

In chapter 2, literature regarding the history of solitons along with the development of solitons solutions, and the behavior of the solutions of NLEEs are discussed. The types of soliton are briefly explained, along with the significance of their applications in many branches of science and engineering.

In chapter 3, an introduction to LOOCV along with its advantages, disadvantages, and algorithm has been discussed. A numerical technique "Exponential modified cubic B-spline differential quadrature method (Expo-MCB-DQM) with LOOCV approach" has been developed. To check the authenticity of developed technique, it is implemented on two important equations which are nonlinear Schrödinger (NLS) equation and nonlinear Sine-Gordon (SG) equation in one dimension. The authenticity and effectiveness of this methodology are shown by the findings, which are equivalent to those found in the literature and near to exact solution. The work is presented in form of figures and tables.

In chapter 4, an introduction to PSO along with its advantages, disadvantages, and algorithm has been discussed. A numerical technique "Exponential modified cubic B-spline differential quadrature method (Expo-MCB-DQM) with PSO approach" has been developed. To check the authenticity of developed technique, it is implemented on two important equations which are NLS equation and nonlinear SG equation in one dimension. The authenticity and effectiveness of this methodology is shown by the findings, which are equivalent to those found in the literature and near to exact solution. The work is presented in the form figures and tables.

Soliton solutions have practical applications that are highly relevant to various fields of science and engineering. Optical fibers and Josephson junctions are just two examples of how solitons can be used in real-world scenarios to achieve technological

advancements. Chapter 5, briefly explains two critical applications of solitons: optical fibers and Josephson junctions, out of several applications that have a significant role in the field of science and engineering.

In Chapter 6, the conclusion and future scope of this research work is presented.

Chapter-2

Overview of soliton and its applications in various field of science

2.1 Introduction

A soliton is a type of wave that maintains its shape while traveling through a medium, instead of dissipating or spreading out like most waves do. This means that a soliton will remain localized in space and time, moving as a single, self-reinforcing wave packet that retains its shape and velocity even after interacting with other waves or obstacles. Solitons are often observed in nonlinear systems, such as in shallow water waves, optical fibers, and plasma physics, and they have various applications in fields like telecommunications, signal processing, and quantum computing. Solitons are characterized by their ability to maintain their shape and amplitude over long distances, making them useful for long-range communication and energy transfer. This property arises from a balance between the nonlinear and dispersive effects in a system, which leads to a soliton's ability to counteract the dispersive spreading of its waveform by the nonlinear focusing of energy towards its center.

2.2 History

John Scott Russell [42], a Scottish naval architect, observed a "Great Translation Wave" in the shallow waters of the Great Britain Canal in 1834.

Figure 2.1: John Scott Russell*

*https://images.app.goo.gl/gDrohxPgKeitREvp7

He attempted to demonstrate a constant wave by constructing a channel so that the wave could travel a great distance with the channel. He placed the boat in the canal with a rope to which he tied the horses on either side. He found that the wave came to rest due to the obstruction of the wave propagation by the boat, but continued to move at a constant speed without losing its shape. He followed the wave for about 8 miles and found that the wave moves at a constant speed for up to 2 miles without losing its shape.

Figure 2.2 Solitary wave observed by the Scott Russell on the Great Britain Canal.*

He continued his research and briefly described the properties of translational waves as follows:

(a) The waves can travel large distances with constant speed.

(b) They never merge, unlike normal waves.

(c) The speed of a wave depends on its size and its width depends on the depth of water.

(d) The higher waves travel faster than the smaller waves.

*https://images.app.goo.gl/i3Nb8ypDEne3UygY9

(e) The velocity of waves can be formulated by an equation which is as follows:

$$V = \sqrt{G(H + A)} \qquad (2.1)$$

Where G is the acceleration due to gravity, A is the amplitude of solitary waves; H is the height of shallow water channel and V is the velocity of travelling waves.

The results of Russell were not appreciated by the mathematical society and also denied by a researcher named Array. In 1845, Array published his book "Tides and Waves", in which he presented a theory of long waves and focused on the speed of waves which depends on their height and amplitude. This theory indicated that solitary waves by Russell could not exist [43].

In the 1870s, two great physicists, Joseph Boussinesq and Lord Rayleigh, independently further illuminated Russell's observations in the form of a mathematical model [44]. Boussinesq and Rayleigh observed the velocity of a solitary wave and related its height to distance, discussing the properties of high and small waves.

In 1895 [45], the Dutch mathematician Diederik Korteweg, together with Gustav de Vries, formulated a nonlinear PDE, called as the KdV equation, recognizing soliton solutions to describe shallow water waves. This equation mathematically proves solitary water waves.

In 1955, Fermi, Pasta, and Ulam [46] studied a computer simulation of a one-dimensional nonlinear lattice to discuss its equilibrium state. They believed that the nonlinear interactions with respect to the normal modes of the linear system resulted in the energy of the system being uniformly distributed among all modes. But when they examined the KdV equation numerically, the results reversed this notion. The energy was again distributed unevenly among all modes, but the system returned to its initial position after some time. The problem later became known as the FPU problem.

To understand this recursion phenomenon, Zabusky and Martin Kruskal [47] studied the FPU problem again in 1965. They solved the KdV equation numerically in terms of a nonlinear grid. Further, they noted the surprising property that the interaction of two solitary waves of the KdV equation exhibits elastic behaviour. When two solitary

waves collide, they reappear without changing their original shape, size, and velocity. These properties of elastic collision between two particles make them behave like stable particles. They called these solitary waves 'solitons' because of their particle-like behaviour like protons, electrons, photons, etc. This is how the soliton was invented.

When the soliton was discovered, there was no mathematical tool to solve the initial value problem of nonlinear integrable PDEs. Later, Gardner, Kruskal, Miura, and Greene (GKMG) invented a technique for solving nonlinear PDEs known as inverse scattering (IST). A year later, another mathematical approach for dealing with nonlinear problems was developed by Lax [48]. In it, an integrable PDE can be put into a standard form called a Lax pair. Then, Zakharov and Shabat [49] generalized this as a linear matrix eigenvalue problem and solved the nonlinear Schrödinger (NLS) equation using IST and obtained a soliton solution.

Another scheme, known as the AKNS scheme, was developed by Ablowitz, Kaup, Newell, and Segur [50], who identified solitons with nonlinear evolution equations. This scheme was first used to numerically solve the SG equation, which was later used to solve several other nonlinear PDEs. There are several other methods such as the bilinear Hirota method and the Backlund transform that are commonly used to solve integrable nonlinear PDEs.

2.3 Types of solitons

Here are some important types of solitons depending on their shapes:

2.3.1 Kink soliton: Kink soliton is a one-dimensional solitary wave, which signifies a change in the solution value due to the transition from one state to another [51, 52]. They are also known as topological solitons because their velocity does not depend on the wave amplitude.

Topological solitons [53] are defined as a localized lumps of energy in a nonlinear system. They are stable particle-like objects with finite mass, have a smooth structure and appear like monopoles in the nonlinear classical field theory.

The collision properties of solitons are observed in both kinks and anti-kinks solutions. The KdV, SG, Burger's, Ostrovsky equations [54], and many more

equations admits a kink type soliton solutions. Kink waves rise or fall from one asymptotic state to another and approach a constant level at infinity. The Kink-type soliton has been presented by the SG equation in section 2.5.2 of this chapter.

2.3.2 Breather: A breather is a nonlinear wave in which energy accumulates in an oscillatory and bounded manner. They oscillate in both time and space, but sometimes exhibit oscillations in space and can localize in time. Once a breather reaches its maximum amplitude, it decays symmetrically and eventually disappears. The SG [55] and the NLS equation [56] are examples of one-dimensional PDEs that contain breather-type soliton solutions. The Breather-type soliton has been presented by the SG equation in section 2.5.2 of this chapter.

2.3.3 Gap solitons: These are the solitons that occur in finite gaps in the domain of continuous systems. These types of solitons have been discussed by the NLS equation with periodic solutions observed experimentally in nonlinear optics and Bose-Einstein condensation [57]. Optical gap solitons [58], which exist in nonlinear optical media, are electromagnetic field structures.

The difference between a regular soliton and a gap soliton is due to the dispersion of the group velocity of the photonic band structure. The gap solitons are presented by NLS equation in section 2.5.3 of this chapter.

2.3.4 Envelope solitons: Envelope solitons are solitary wave solutions that occur in a dispersive nonlinear medium [59-61]. Envelope solitons can be divided into light and dark solitons. Bright solitons occur with a localized intensity peaking over a constant wave background, while dark solitons are described as a concavity in the continuous background. From the NLS equation bright soliton solutions are derived in the anomalous dispersion regime and dark soliton solutions are derived in the normal dispersion regime [62]. The dark solitons are more stable and less affected by background noise and interference compared to the light solitons. Apart from NLS equation the Chaffee-Infante equation [63] and Kaup-Kupershmidt equation [64] also admits bright and dark soliton solutions. The envelope soliton resulting from the NLS equation has been presented in section 2.5.3 of this chapter.

2.3.5 Solitary waves with discontinuous derivatives: There are solitary waves with discontinuous derivatives, which can be classified as peakons, cuspons, and compactons [65].

(a) Peakons are solitary waves whose peaks have a discontinuous first derivative [66, 67]. This type of solitary wave solution is smooth, except for a peak at one corner of its vertex. In particular, peakons maintain their velocity and shape after colliding with other peakons. The equation of Camassa-Holm (CH) and the integral equation of Degasperis Procesi (DP) have peakon-type solutions. The peakon solution for the equation CH is presented in section 2.5.4 of this chapter.

(b) Cuspons are soliton solutions where the solutions have cusps at crests [68]. In some special cases, the solutions of the CH and DP equation are of cuspons type. Cuspons have a variety of applications in physics, including in the study of fluid dynamics, plasma physics, and optics. They can be used to model the behavior of waves in nonlinear media, and their ability to maintain their shape over long distances makes them useful for transmitting information over long distances. The coupons solution for the DP equation has been presented in section 2.5.4 of this chapter.

(c) Compactons are solitary waves that have a finite wavelength, are free of exponential tails, and have robust soliton-like solutions. They are special solitary waves that have the property of maintaining their shape and travelling at the same speed after colliding with other compactons. The nonlinear dispersive K(n,n) equation, which is a family of nonlinear KdV-like equations, yields a soliton solution of the compacton type presented in section 2.5.1 of this chapter.

Each type of soliton has its own unique characteristics and is often associated with specific physical phenomena.

2.4 Applications of solitons

Solitons have a broader application perspective in various fields such as biophysics, field theory, plasma physics, fluid dynamics, photonic crystal fibers, optical fibers, condensed matter physics, Josephson junction and Bose-Einstein condensates, surface waves, etc.

Some of the above applications are briefly discussed below:

2.4.1 Biophysics: Study of solitons is used in biophysics in the DNA lattice. When a protein comes near to soliton, some conformational changes occur, which cause intracellular communication. This communication of solitons on the DNA lattice is described by Feynman diagrams, which describe the survival of cellular life. The solitary wave is also used to study various biophysical phenomena.

The Davydov soliton [69] is one such soliton that exists as a solution to an equation describing the energy distribution in hydrogen-bonded spines. The DNA molecules also reveal the presence of solitary waves [70], which arose in the process of splitting double-stranded DNA into single strands [71].

Solitons have been also observed in biological systems, including in the propagation of nerve impulses and in the motion of protein molecules. Understanding the properties of solitons in these systems can help us better understand the behavior of biological systems. For example, solitons have been observed in the propagation of nerve impulses in the squid giant axon, and they can be used to study the properties of ion channels in the axon, it can be modeled by the Fitz Hugh-Nagumo equation. Envelope solitons and breather solitons have also been observed in biological systems.

Solitons can be used in medical imaging for example, MRI. Mathematical models are used to simulate the behavior of solitons in the human body, which can help to optimize imaging techniques and improve diagnosis.

2.4.2 Field theory: Solitons appear in both classical and quantum field theory [51]. Topological solitons exist in field theory [53] in the form of kinks, monopoles, vortices, and skyrmions. In two-dimensional quantum field theory, the SG equation has solutions for topological solitons that can be mapped onto the elementary excitations of an exactly solvable quantum field theory [72].

2.4.3 Plasma physics: Solitons in the KdV equation and the modified KdV equation have applications in plasma physics, including in the study of magnetic reconnection and turbulence. Solitons can also be used to generate and accelerate high-energy particles in plasma-based accelerators. For example, solitons can be used to create

shocks in the plasma, which can accelerate particles to high energies. The study of solitary waves is also related to the study of plasma physics, which contains charged particles in large numbers [73]. For example, the KdV equation reflects the change of charge from neutrality. Another equation describing solitons and solitary-wave solutions for the study of plasma physics is the KP equation, variants of KdV. In addition, the soliton in plasma is studied in various contexts, e.g., to discuss the interaction of solitons in collisionless plasma [47], in Langmuir wave collapse for plasma [74], in the study of soliton stability in plasma and hydrodynamics [72], and in ionic-acoustic solitons in plasma [76, 77] etc. Benjamin-Bona-Mahony (BBM) [78] is considered as an improvement of the KdV equation and used to describe the properties of the long surface gravity wave, acoustic-gravity waves in compressible fluids, hydromagnetic waves in a cold plasma, and acoustic waves in an harmonic crystals.

Example of plasma solitons in day-to-day life, is in the phenomenon known as aurora borealis, or the Northern Lights. Auroras occur when charged particles from the sun, called the solar wind, interact with the Earth's magnetic field and atmosphere. This interaction can generate plasma waves, including solitons, in the Earth's magnetosphere, which can produce the beautiful and colorful light displays that is seen in the night sky.

Another example is in plasma processing, where solitons are used to control and manipulate plasma in order to produce thin films, microelectronics, and other industrial products. In this application, solitons are used to create patterns and structures in the plasma, which can be transferred onto a surface to create the desired product.

Solitons are also used in laser-plasma acceleration, which is a technique for accelerating charged particles using a high-power laser pulse and a plasma. In this application, solitons can be used to create highly intense and localized electric fields, which can accelerate particles to very high energies in a short distance.

2.4.4 Fluid dynamics: Solitary waves are also among the characteristics of fluid dynamics. The "translational wave" described by Russell was a water wave [79] and Korteweg and de Vries described a shallow water wave by the KdV equation, which

also occurs in a long-wavelength limit. Solitary waves also exist in deep water, as shown by the work of Vladimir Zakharov [80], who set up the NLS equation to study these waves. Solitary wave solutions have been constructed in many models of fluid dynamics. For example, tidal wells have been explained using dispersive shock waves, the theory of non-propagating surface-wave solitons [81], the small-amplitude gravity capillary wave as an envelope soliton [82], and the soliton mean-field theory in macroscopic flow hydrodynamics [83], etc.

2.4.5 Fiber Optic Communications and optical fibers: Soliton pulses are widely used in fiber-optic communications to transmit data over long distances. These pulses maintain their shape and amplitude over long distances, which allows high-speed data transmission without signal distortion. Since solitons travel at a speed equal to that of light, they provide high-speed connectivity and a high-bandwidth network [84]. This property feature of optical solitons makes them useful for high-speed communication over an optical fiber [85]. Soliton pulses are used in submarine cables, where they can transmit data over thousands of kilometers with minimal signal loss. The soliton solution of the NLS equation is widely used in fiber optic communications. Both bright and dark solitons are used for signal transmission. There are applications in a variety of fields related to fiber optics, such as soliton photonic switches, which are used for optical switching by using the process of position shifting of the spatial soliton after collision [86]. In addition, trapping solitons in optical fibers can be used to develop optical logic gates [87]. Solitons are used in nonlinear optics to study optical switching, pulse compression, and pulse shaping. For example, solitons can be used to compress a long pulse into a much shorter pulse, which is useful in high-speed data transmission and in ultrafast laser systems. Solitons are used in laser technology to generate ultra-short laser pulses. Solitons can be generated in laser cavities, and they have extremely short durations, on the order of picoseconds or femtoseconds. These ultra-short laser pulses are used in a variety of applications, such as laser eye surgery, laser machining, and laser spectroscopy. Solitons are also used in pulse shaping to create customized waveforms that can be used in variety of applications. The propagation of solitons in fibers can be modeled by the NLS equation. In the study of optical solitons, the NLS equation [85] is crucial, which are used in pulse compression and shaping . The Fokas-Lenells (FL) equation [89, 90] has been derived

as an alternate model equation of the Schrödinger equation for the higher-order terms, and it represents the propagation of short pulses in optical fibers. Complex perturbed Gerdjikov-Ivanov equation [91] describes the physical characterization of the optical soliton waves to mitigate internet bottlenecks with many different applications in the telecommunication industry. Additionally, the telegraph equation [92, 93] has an important application electromagnetic waves in communication.

2.4.6 Josephson junctions: A Josephson junction [94] is a device that consists of two superconducting electrodes separated by a thin insulating barrier. When a current is applied to the junction, a supercurrent can flow across the barrier, which is a quantum mechanical effect that occurs because of the way that electrons behave in superconductors. Specifically, solitons can be used to carry information in the form of binary digits, or bits, in superconducting digital circuits. In a Josephson junction, a soliton corresponds to a specific pattern of supercurrent flow that travels across the junction without dissipating. By carefully controlling the current applied to the junction, it is possible to create and manipulate solitons in order to encode and decode information. One example of a practical application of soliton solutions in Josephson junctions is in the design of high-speed data communication systems. By using solitons to encode and transmit digital information, it is possible to achieve extremely high data rates with low power consumption and minimal interference from other signals. Another example of a potential application of soliton solutions in Josephson junctions is in the design of quantum computing systems. Solitons could be used to carry and manipulate quantum information in the form of qubits, which are the basic building blocks of quantum computers.

2.4.7 Bose-Einstein condensates (BEC): In 1924, Bose and Einstein demonstrated the process of Bose-Einstein condensates. Solitons have been observed in Bose-Einstein condensates, which are ultra-cold atoms that behave like a single, coherent wave. Solitons in Bose-Einstein condensates can be used to manipulate the behavior of the atoms and to study the properties of superfluid. For example, solitons can be used to create vortices in the superfluid, which can be used to study the behavior of turbulence. At a very low temperature, a finite fraction of particles in a dilute base gas can assume the same quantum state known as BEC. The macroscopic dynamics of

BEC near temperature zero is modelled by the Gross-Pitaevskii equation [95, 96]. BECs were experimentally detected in 1995 by trapping atoms of dilute alkali vapours in a magnetic trap, which was then cooled to an extremely low temperature on the order of micro-Kelvins [97, 98]. Rogue waves in nonlinear Schrödinger models with variable coefficients are also an important application for Bose-Einstein condensates [99, 100]. The soliton solutions of the Gross-Pitaevskii equation, KdV equation and the modified KdV equation are also used in the study of the dynamics of Bose-Einstein condensates.

2.4.8 Oceanography: In oceanography, solitons are used to study ocean waves and tsunamis. Solitons can propagate over long distances without losing their shape, which makes them ideal for studying the behavior of waves in the open ocean. For example, solitons have been observed in the Indian Ocean tsunami of 2004, and they can be used to predict the behavior of tsunamis and other ocean waves. The KdV equation is a mathematical model used to study long, surface waves in shallow water. It includes nonlinear and dispersive terms that cause waves to behave differently from simple harmonic waves. In particular, the nonlinear term causes the wave to self-modulate, resulting in the formation of soliton-like waves known as internal waves. Internal waves have been observed in the ocean and in laboratory experiments. They can travel great distances without significant attenuation, making them an important factor in the study of ocean dynamics. Internal waves affect the distribution of temperature and salinity in the ocean and the mixing of different water masses. Tsunamis, which are large, long-period waves that can cause significant damage, can also be modeled using soliton solutions. The soliton solutions of the nonlinear shallow water wave equation have been used to study tsunamis. These solutions can be used to predict the propagation of tsunamis and their effects on the coastal environment.

Overall, nonlinear evolutionary equations have a wide range of applications in various fields of science and engineering, and they continue to be an active area of research.

2.5 Relation between soliton solutions and nonlinear evolutionary equations

NLEEs are mathematical models that describe how a system changes over time. NLEEs are characterized by their nonlinearity, which means that the relationship between the dependent and independent variables is not linear. NLEEs are of great

interest to researchers in various fields because they can exhibit a wide range of complex behaviors such as chaos, bifurcations, solitons, and pattern formation. Studying these behaviors can provide insight into the underlying mechanisms of the system being modeled and lead to the development of new technologies and applications.

Soliton solutions are an important class of solutions for certain types of NLEEs. NLEEs are partial differential equations that describe how a system evolves over time and exhibit nonlinear behavior. The existence of soliton solutions in NLEEs is a result of the balance between nonlinear and dispersive effects. They are considered a unique tool for describing nonlinear phenomena in science and engineering. Soliton solutions of NLEEs are important because they exhibit unique properties, such as stability, non-dispersiveness, and the ability to maintain their shape and speed over long distances. The soliton solutions of NLEEs have many important applications in science and engineering. Soliton solutions are useful in various applications, which has been already discussed in this chapter briefly. A brief discussion is done on the type of solution and the physical behavior using MATLAB, which are briefly described below:

2.5.1 Korteweg-de Vries Equation: The KdV is a very simple model of the wave equation, which is hyperbolic in nature. It is a nonlinear equation that links dispersion and nonlinearity. It is the most important class of NLEEs with various applications in engineering and natural sciences. It was originally discovered by Lord Rayleigh in 1812; subsequently, it was mathematically introduced by Joseph Boussinesq in 1877 and rediscovered by Diedrik Korteweg and Gustav de Vries in 1905, who introduced this equation in modelling shallow water waves. The KdV equation plays an important role in compressible fluids of fluid mechanics, description of the properties of electron plasmas, oceanic water waves, and mass transport problems associated with chemical compounds [101]. A simple generalization of the KdV equation is given as:

$$u_t + \alpha u u_x + u_{xxx} = 0, -\infty < x < \infty, \quad 0 \le t < \infty \qquad (2.2)$$

Where variables *x*, *u*, and *t* represent wave amplitude, space, and time respectively and the subscripts represent differentiation with respect to the relevant variable. A

travelling wave solution of permanent form occurs due to a balance between the dispersive term and the nonlinear term.

The nonlinear dispersive K(n,n) equation, which is a family of nonlinear KdV like equations give compactons type soliton solution is given as:

$$u_t + a(u^n)_x + (u^n)_{xxx} = 0, -\infty < x < \infty, \quad 0 \le t < \infty \qquad (2.3)$$

where $a = 1$ results in compact solitary travelling soliton. The compactons soliton solution obtained for the K(n,n) equation is presented in Figure 2.3 for the exact solution given as [101]:

$$u(x,t) = \sqrt{\cos(x-t)}, 0 < x < 1.5, \quad 0 \le t \le 1.5. \qquad (2.4)$$

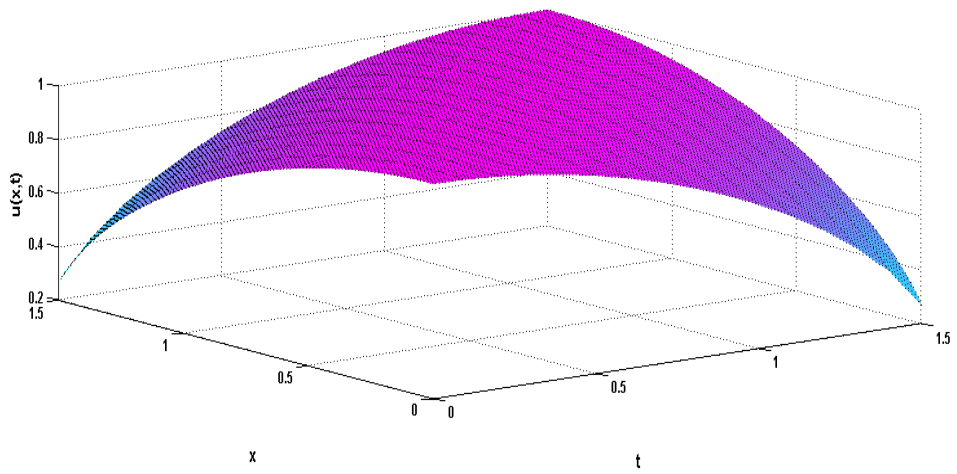

Figure 2.3: Compacton soliton from K(n,n) equation.

2.5.2 Sine-Gordon Equation: The SG is a nonlinear PDE of hyperbolic in nature that has soliton solutions. It is named after its trigonometric sine function and Scottish mathematician James Gordon, who first introduced it in 1971. The structure of the soliton solutions is the same as that of the KdV equations. It was originally introduced by Edmond Bour in 1862 and rediscovered by Frenkel and Kontorova in 1939 while studying crystal dislocations [102]. The Sine-Gordon equation is given as:

$$u_{tt} - u_{xx} + \sin(u) = 0, -\infty < x < \infty, \quad 0 \le t < \infty \qquad (2.5)$$

where u is a function, t represents the time and x denotes the space coordinate in the direction of propagation. The SG equation admits the soliton solution as presented as in Figure 2.4 and 2.5.

The breather soliton solution obtained for the SG equation is presented in Figure 2.4 for the exact solution given as [102]:

$$u(x,t) = 4\arctan\left(\frac{vsinh\left(\frac{x}{1-v^2}\right)}{\cosh\left(\frac{vt}{1-v^2}\right)}\right), -20 < x < 20,\ 0 \le t \le 30. \quad (2.6)$$

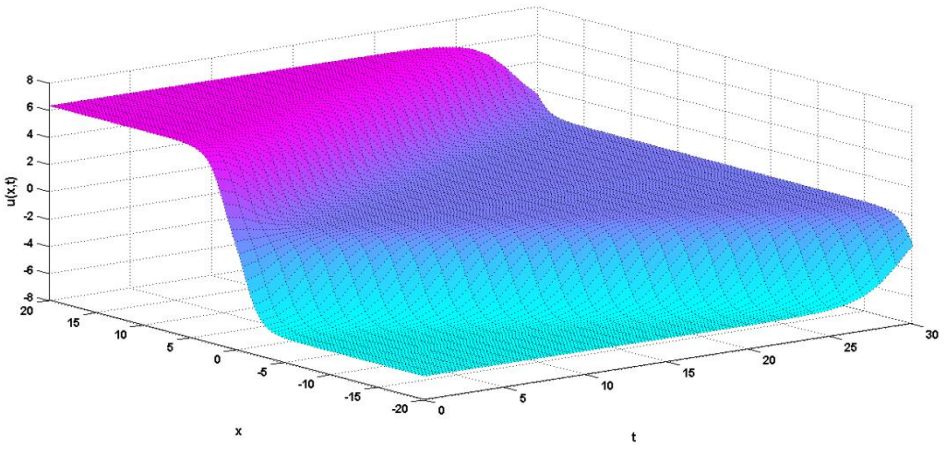

Figure 2.4: Breather soliton from SG equation.

The kink solitons that occurred for the SG equation is presented in Figure 2.5 for the exact solution given as [102]:

$$u(x,t) = 4\tan^{-1}\left(e^{\frac{x-vt}{d}}\right), -15 < x < 15,\ 0 \le t < 10 \text{ for } v = 0.5. \quad (2.7)$$

where *v* represents the velocity of soliton with $d = \sqrt{1-v^2}$ is the Lorenz contraction factor.

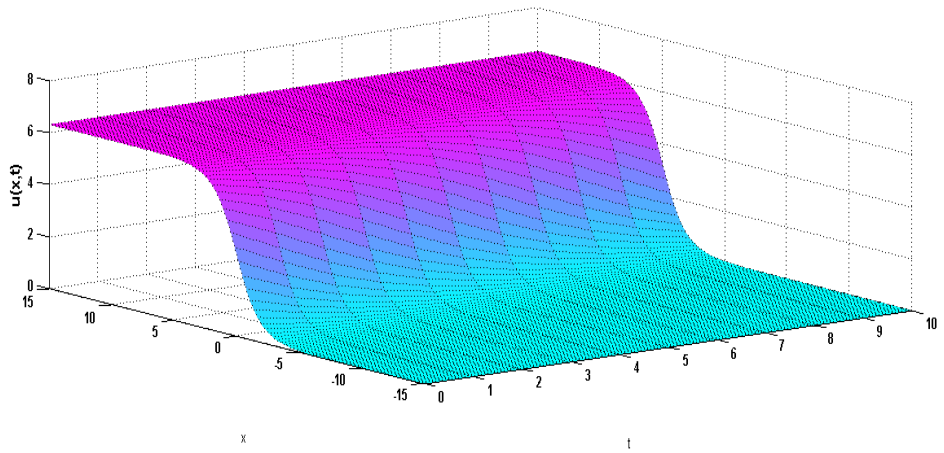

Figure 2.5: Kink soliton from SG equation.

This equation has a wide range of application in physics, not only in relativistic field theories but also in study of solid-state physics, nonlinear optics, shape waves, mechanical transmission lines and Josephson junction, Bloch wall motion of magnetic crystals and nonlinear dynamics of DNA etc.

2.5.3 Nonlinear Schrödinger Equation: NLS equation is an important dynamical model in nonlinear physics, which presents the function of wave in nonlinear and dispersive motion and is given by:

$$iu_t = u_{xx} + g|u|^2 u, -\infty < x < \infty, \quad 0 \le t < \infty \tag{2.8}$$

where u is the complex field function and g is a constant. The first function of wave i.e., dispersion effect makes the waveform spread and the second function causes the steepening of waveform due to its nonlinear effect. The NLS equation admits the soliton solution as presented as in Figure 2.6 and 2.7.

The gap solitons that occurred for NLS equation is presented in Figure 2.6 for the exact solution given as [26]:

$$u(x,t) = \sin(x)\, e^{-i1.5t}, -4 < x < 4, \ 0 \le t \le 2. \tag{2.9}$$

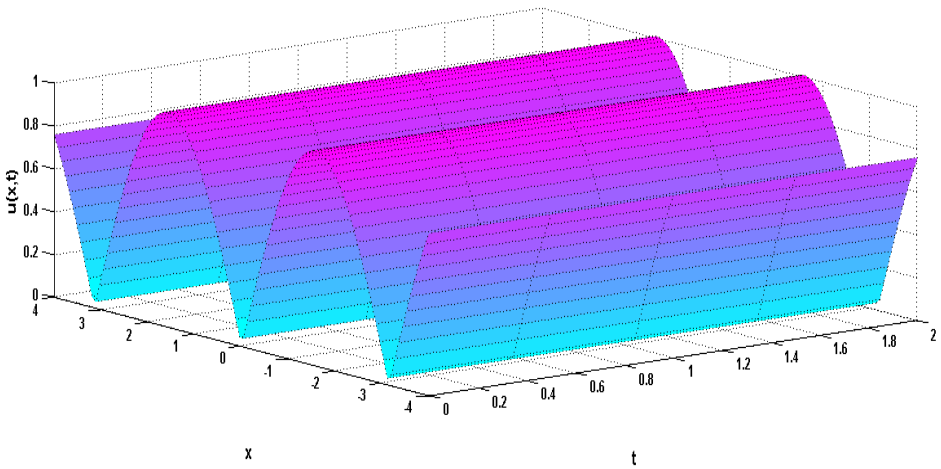

Figure 2.6: Gap solitons from NLS equation.

The envelope soliton that occurred for NLS equation is presented in Figure 2.7 for the exact solution given as [26]:

$$u(x,t) = \sqrt{2}\cos(2x - 3t)\,\mathrm{sech}(x - 4t), -10 < x < 10, \ 0 \le t \le 1. \tag{2.10}$$

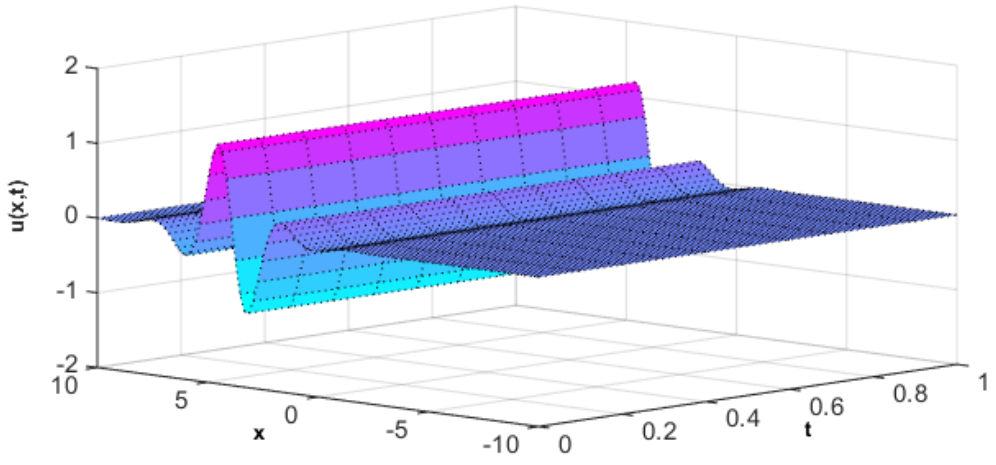

Figure 2.7: Envelope soliton from NLS equation.

NLS equation has localized solutions which have applications in many fields such as plasmas, electromagnetism and many other instability phenomena. It is also helpful in problem of optical pulse propagation in asymmetric, twin core optical fibers etc. Optical solitons, which are one of the most important solutions of NLSE, are used in optical fiber communication [84, 88, 103-108].

2.5.4 Camassa-Holm equation: This equation is first introduced by Camassa and Holm [109] by the use of Hamiltonian method. The Camassa-Holm (CH) equation of the form:

$$u_t + 2ku_x - u_{xxt} + 3uu_x = 2u_xu_{xx} + uu_{xxx} \qquad (2.11)$$

where u denotes the fluid velocity and the parameter k is a constant related to the critical shallow water wave speed. This is an entirely integrable dispersive water wave equation for all k and for $k = 0$, it has travelling solution of the form $ce^{-|x-\alpha|}$, which are called peakons because they have a discontinuous first derivative at the peak. The CH equation has peakon type solutions.

The peakon solution for CH equation is shown in Figure 2.8 with exact solution [110]:

$$u(x,t) = \sqrt{\frac{3}{2}}e^{-|x-t|}, -6 < x < 6, \;\; 0 \le t \le 1. \qquad (2.12)$$

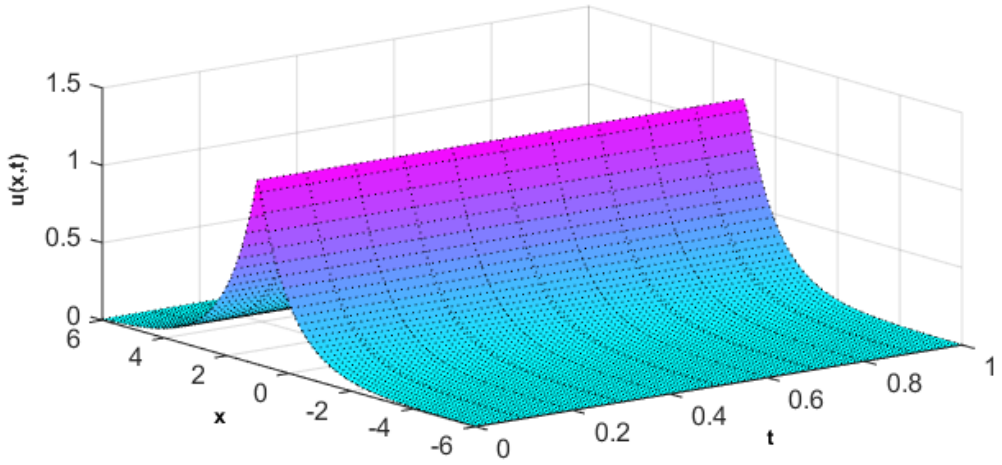

Figure 2.8: Peakon soliton from CH equation.

The DP equation also describes shallow water nonlinear waves and its asymptotic accuracy resembles as that of CH equation:

The DP equation is given by:

$$m_t + m_x u + 3mu_x = 0, m = u - u_{xx}. \qquad (2.13)$$

The cuspons solution for DP equation is shown in Figure 2.9 with exact solution [23]:

$$u(x,t) = \sqrt{1 - e^{-2|x|}}, -2 < x < 2, \quad 0 \le t \le 1. \qquad (2.14)$$

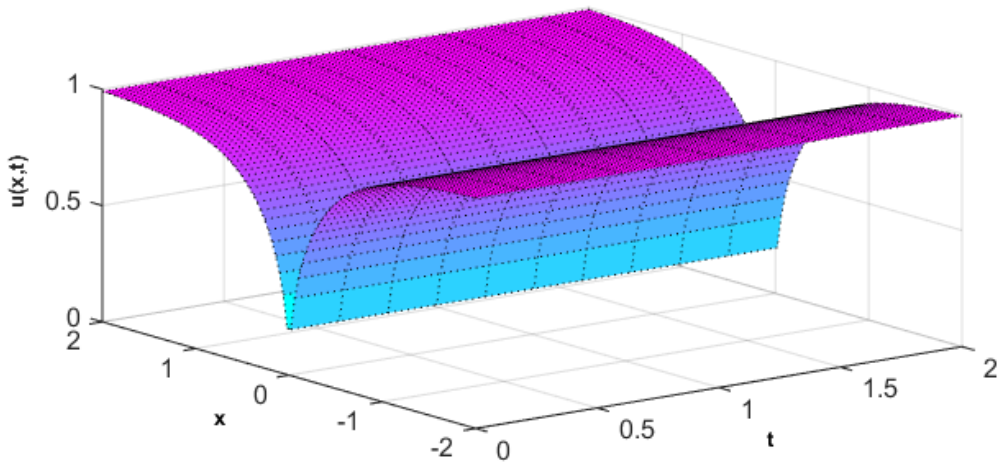

Figure 2.9: Cuspons soliton from DP equation.

In addition to the above equations, there are many equations that admits soliton type solutions i.e., Kolmogorov-Petrovskii-Piskunov equation [111], generalized (2+1)-dimensional shallow water waves equation [112], human immunodeficiency virus infection of CD4+ T-cells fractional biomathematical model for constructing novel solitary wave solutions [113], Fokas-Lenells equation [89], Klein-Fock-Gordon equation [114] relates to Schrödinger equation, phi-four equation [115] which is a particular case of the Klein-Fock-Gordon equation, telegraph equation [92], Chaffee-Infante equation [63], Benjamin-Bona-Mahony (BBM) [78], Cahn-Allen equation [116], Klein-Gordon-Zakharov equation [77, 117], Kaup-Kupershmidt equation [64], Fisher-Kolmogorov-Petrovskii-Piskunov [118], Kadomtsev-Petviashvili equation [119], Ginzburg–Landau equation [120], Hirota-Satsuma-Shallow water wave equation [121], (2+1)-dimensional Kadomtsev-Petviashvili-Benjamin-Bona-Mahony equation [122], cubic-quintic nonlinear Helmholtz model [123], Ostrovsky equation [54], Vakhnenko-Parkes equation which is reduced from the Ostrovsky equation [124], complex perturbed Gerdjikov-Ivanov (CPGI) equation [91], etc.

2.6 Summary

In recent decades, nonlinear equations have emerged in various forms to study the behavior of complex natural phenomena across different branches of science and technology. Nonlinear systems exhibit outputs that are not proportional to their inputs. As a result, most nonlinear phenomena are modeled using NLEEs due to both dispersion and nonlinear effects.

Solitons, a type of solitary wave, have significant importance in real life as they occur in various natural phenomena such as water waves, optics, and plasma. They also have practical applications in fields like communication, transportation, and medicine. For example, solitons are used in fiber optic communication to transmit data over long distances with minimal distortion. In transportation, solitons help to model traffic flow, while in medicine, they are used to study the dynamics of nerve impulses. Their ability to maintain their shape and energy over long distances makes them a valuable tool for transmitting and processing information, studying complex systems, and understanding the behavior of natural phenomena.

This chapter focuses on solitons, providing a brief history of their existence. Additionally, the applications of soliton solutions in various scientific and engineering fields are discussed. To generate reader interest, the types of solitons with the help of well-known NLEEs are also presented.

Chapter-3

Numerical solutions of nonlinear partial differential equations using “Exponential modified cubic B-spline differential quadrature method (Expo-MCB-DQM) with LOOCV approach”

3.1 Introduction

Optimization is the process of determining the optimum feasible values for a model's parameters in order to minimize a specified cost or objective function. Optimization is also a key aspect of machine learning, and selecting the appropriate optimization method and hyperparameters that may greatly enhance a model's performance.

Machine learning is a subfield of artificial intelligence (AI) that involves developing algorithms and statistical models that enable computer systems to automatically learn from and improve upon their performance in a specific task, without being explicitly programmed to do so.

In other words, machine learning algorithms use statistical techniques to analyze and learn from patterns in large amounts of data, and then use this knowledge to make predictions or take actions without human intervention. Machine learning is used in a wide range of applications, including image and speech recognition, natural language processing, recommender systems, fraud detection, and many others.

Machine learning models must be trained using this procedure in order to learn from the data and produce reliable predictions. There must establish an objective function that measures how well a machine learning model performs on the data in order to improve the model. The model parameters are then iteratively updated by the optimization process to minimize this objective function. To prevent overfitting, it's also crucial to keep an eye on the training procedure and assess the model's performance on a validation set. To get the best results, there may also have to adjust the optimization algorithm's hyperparameters, including learning rate and regularization.

Resampling optimization techniques are a class of techniques used in machine learning and statistical analysis to improve model performance by iteratively training and testing a model on multiple subsamples of the available data. Resampling techniques can be used for various purposes, such as model selection, hyperparameter tuning, and estimating the model's generalization error. The goal of resampling techniques is to create multiple, independent subsets of the data to train and validate the model, with the aim of obtaining a more accurate estimate of the model's performance.

Some commonly used resampling techniques include:

Cross-validation: In cross-validation, the available data is randomly partitioned into k subsets or folds. The model is trained on k-1 folds and evaluated on the remaining fold, and this process is repeated k times, with each fold being used as the validation set once.

Bootstrap: Bootstrap is a resampling technique that involves creating multiple random samples of the available data by drawing data points with replacement. A model is trained on each of these bootstrap samples, and the results are averaged to provide an estimate of the model's performance.

Leave-One-Out Cross-Validation (LOOCV): LOOCV is a special case of cross-validation where each data point is used as the validation set once, and the model is trained on the remaining data. This process is repeated for all data points, and the results are averaged to provide an estimate of the model's performance.

Monte Carlo Cross-Validation: Monte Carlo Cross-Validation is a resampling technique that involves randomly sampling the available data to create new datasets. A model is trained on each of these datasets, and the results are averaged to provide an estimate of the model's performance.

Resampling techniques are widely used in machine learning and statistical analysis to optimize model performance, select the best model or set of hyperparameters, and estimate the model's generalization error.

3.2 Leave-One-Out Cross-Validation

Several optimization techniques, such as gradient descent, LOOCV, stochastic gradient descent, Adam, and Adagrad, are often used in machine learning. The

selection of one of these techniques will rely on the particular issue and data since they vary in how they update the model parameters during training which is known as LOOCV.

3.2.1 Advantages of LOOCV algorithm

LOOCV algorithm has several advantages, including:

No information loss: LOOCV uses all the data points available for training and testing the model. It leaves out only one data point at a time and trains the model using the remaining data points. Therefore, LOOCV does not result in any information loss.

Low bias: LOOCV has a low bias as it uses almost all the available data for training. This ensures that the model is trained on a representative sample of the data.

Low variance: Since LOOCV trains the model on almost all the available data, it ensures that the model is not affected by the variance that may result from different partitions of the data.

Provides a reliable estimate of model performance: LOOCV provides a reliable estimate of the model's performance as it tests the model on all the available data points. This ensures that the estimate is not affected by the randomness that may occur in the partitioning of the data.

Applicable to small datasets: LOOCV is particularly useful for small datasets where partitioning the data into training and testing sets may result in a small sample size for either the training or testing set.

Overall, the LOOCV algorithm is a useful tool for model selection and performance evaluation, particularly when dealing with small datasets or when there is a concern about bias or variance in the model.

3.2.2 Disadvantages of LOOCV algorithm

Although LOOCV has several advantages, it also has some disadvantages, including:

High computational cost: LOOCV requires running the model on the entire dataset multiple times, which can be computationally expensive, particularly for large datasets.

Prone to overfitting: LOOCV may lead to overfitting if the model is too complex or if there are outliers or noise in the dataset. In such cases, the model may memorize the training data and perform poorly on new data.

Unstable estimates: LOOCV estimates may be unstable if the model is sensitive to the particular data point left out during each iteration. This may result in high variance in the estimate of the model's performance.

Not suitable for some models: LOOCV may not be suitable for some models, such as those with a high computational cost or those that require the use of specialized optimization algorithms.

Not suitable for some types of data: LOOCV may not be suitable for certain types of data, such as time series data, where the order of the data points is important.

Overall, LOOCV is a useful tool for model selection and performance evaluation, but it is important to consider its limitations and use it in conjunction with other methods to ensure the best results.

3.2.3 LOOCV algorithm

Estimating how well a machine learning algorithm will perform when asked to make predictions on data can be done with the LOOCV method. Rippa [125] suggested the application of the LOOCV to get the best possible value for the shape parameter in his mathematical work. Rippa determined that the shape parameter can be obtained by minimizing the error function l, which is defined as $l = [l_1, l_2, l_3, \dots, l_n]^t$,

where $l_k = |u(x_k) - v^k(x_k)|$, And $v^k(x_k)$ is the radial basis function that plays an important role to interpolate all the data points except x_k. Rippa presented the approach in a closed form which is given as

$$l_k = \frac{p_k}{A_{kk}^{-1}},$$

where p_k is the kth coefficient of the interpolation and A_{kk}^{-1} is the kth diagonal element of the inverse of the interpolation matrix.

The procedure of LOOCV can be defined in the following steps:

- In LOOCV, the dataset is divided into n subsets, where n is the total number of observations in the dataset.

- For each iteration, one observation is chosen as the test set, and the remaining observations are used to train the model.
- The model is then tested on the observation that is left out, and the process is repeated n times, with each observation being left out once.
- The performance of the model is then evaluated by calculating the average error rate over all the iterations.

LOOCV is a reliable technique for estimating the performance of a model because it uses all the data available for training and testing, and it minimizes bias in the evaluation of the model's performance. This is an expansion of the statistical methodology that has been used successfully in the literature to choose the shape parameter in RBF [1, 4].

3.3 Numerical Scheme

In this chapter "Exponential modified cubic B-spline differential quadrature method (Expo-MCB-DQM) with LOOCV approach" is being used to find the numerical solutions of two nonlinear PDEs (NLS equation and SG equation) with eight numerical problems. Figure 3.1 shows graphical representation of the numerical scheme implemented on these two partial differential equations

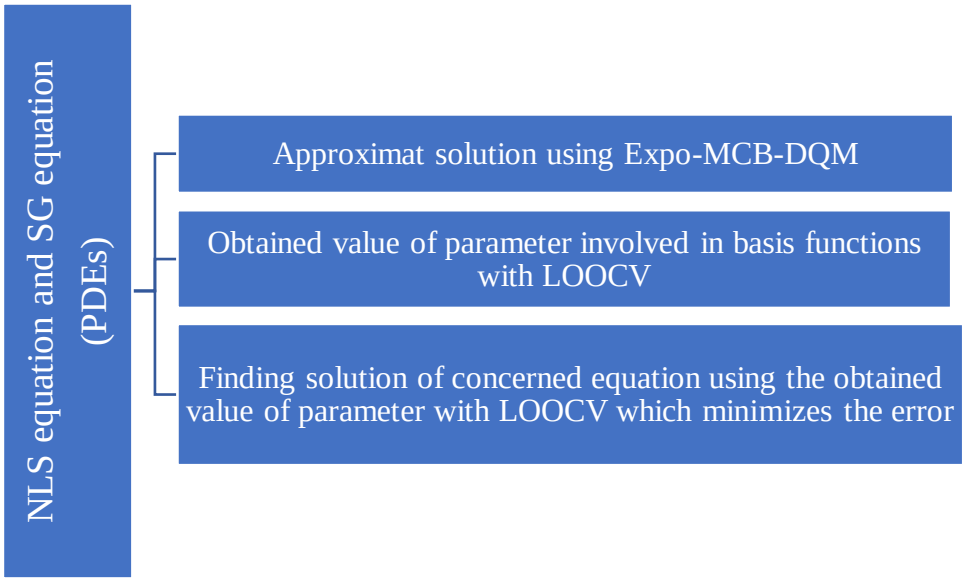

Figure 3.1: Graphical representation of the numerical scheme.

3.4 Introduction to nonlinear Schrödinger equation

The one-dimensional NLS equation is given by [26]:

$$iu_t = \alpha u_{xx} + \beta|u|^2u + g(x,t)u, x \in [a,b], t \geq 0, \quad (3.1)$$

with initial: $u(x,0) = u_0(x)$,

with boundary conditions: $\lim_{|x\to\infty|} u(x,t) = 0$.

Where α, β are arbitrary real numbers, $g(x,t)$ denotes a bounded real-valued function, i is the imaginary unit and $u = c + id$ denotes the complex-valued wave function. The variables x and t indicate space and time variables, respectively.

The nonlinear Schrödinger equation is a variant of the Schrödinger equation that describes the propagation of non-dispersive waves in certain physical systems, including optical fibers. The NLS equation was first introduced by the Russian mathematician Andrei N. Kolmogorov and the Japanese physicist Yasushi Akaike in the 1960s.

The NLS equation has become an essential tool for understanding the behavior of light waves in optical fibers and has led to the development of new technologies, including soliton transmission and dispersion compensation.

3.4.1 Applications of nonlinear Schrödinger equations

NLS equation is a fundamental equation in many areas of science and engineering. The nonlinear Schrödinger equation has applications in many fields, e.g., quantum mechanics, Bose-Einstein condensates [100], ocean dynamics [127], and nonlinear optics [84], etc. A key component of optical fiber communication is the utilization of optical solitons, one of the most significant solutions to the NLS equation [73, 84, 88, 103-106, 128]. Here are some applications of the NLS equation:

Soliton theory: The NLS equation is one of the fundamental equations in soliton theory, which is the study of wave phenomena that maintain their shape and velocity as they propagate. The NLS equation admits soliton solutions, which are localized wave packets that arise in certain nonlinear systems.

Nonlinear optics: The NLS equation is used to describe the propagation of light in nonlinear media, such as optical fibers and waveguides. The equation is used to model phenomena such as self-focusing, self-phase modulation, and soliton formation in optical fibers.

Bose-Einstein condensates: The NLS equation is used to describe the dynamics of ultracold atoms in a Bose-Einstein condensate. The equation is used to model the behavior of the condensate order parameter, and it is a fundamental tool for understanding phenomena such as soliton formation and coherence collapse.

Fiber optics communications: The NLS equation is used to model the transmission of data over long distances in optical fibers. The equation is used to study the nonlinear effects that can degrade the quality of the transmitted signal, such as self-phase modulation, cross-phase modulation, and four-wave mixing.

High-energy physics: The NLS equation arises in the study of certain quantum field theories in high-energy physics, such as the nonlinear sigma model. The equation is used to study the dynamics of solitons and other nonlinear excitations in these systems.

Quantum field theory: The NLS equation arises in the study of certain quantum field theories, such as the Gross-Pitaevskii equation for Bose-Einstein condensates and the nonlinear sigma model in high-energy physics.

Overall, the NLS equation is a versatile equation with many applications in various fields of physics and engineering. Its study continues to be an active area of research, with new applications and analytical techniques being developed.

3.4.2 Role of soliton solutions in applications of nonlinear Schrödinger equations

The soliton solution of the NLS equation is a fundamental concept in the study of nonlinear wave phenomena. Solitons are stable, localized wave packets that maintain their shape and velocity as they propagate through a nonlinear medium. Here are some applications of solitons in the context of the NLS equation:

Optical communications: Solitons are used in optical communications to transmit data over long distances without distortion. In optical fibers, solitons can be generated by modulating the input signal and then allowing the solitons to propagate through the fiber without any additional modulation.

Fiber optic amplifiers: Solitons are used in fiber optic amplifiers to enhance the signal-to-noise ratio of the transmitted signal. The solitons are generated by a process called mode-locking, where a laser is operated in a way that produces a train of solitons.

Bose-Einstein condensates: Solitons can be formed in Bose-Einstein condensates by manipulating the trapping potential of the atoms. These solitons can be used to study the dynamics of ultracold atoms and to create atom-based quantum devices.

Condensed matter physics: The NLS equation is used to model the behavior of excitons, polarons, and other quasiparticles in condensed matter systems. The equation is used to study the formation and propagation of solitons and other nonlinear excitations in these systems.

Nonlinear optics: Solitons are used in nonlinear optics to study phenomena such as self-focusing, self-phase modulation, and four-wave mixing. Solitons can be generated in nonlinear media by using a pump laser to excite a nonlinear response.

Oceanography: Solitons are used in oceanography to study internal waves, which are waves that propagate beneath the ocean surface. Solitons can be formed in oceanographic systems by the interaction of currents and temperature gradients.

Overall, solitons are a versatile concept that has many applications in various fields of physics and engineering. The soliton solution of the NLS equation is a fundamental tool for understanding nonlinear wave phenomena, and its study continues to be an active area of research.

3.4.3 Literature Review of NLS equation: Many mathematicians and engineers have solved the nonlinear Schrödinger problem due to such important applications. By using the technique of unknown coefficients, Biswas et al. [129] investigated

the optical characteristics of the cubic quartic NLS equation. Kumar et al. [130] solved NLSE to find the optical soliton solution. Remizov and Starodubtseva [131] used quasi-Feynman formulae to resolve the multidimensional Schrödinger problem. Remizov [132] solved the NLS equation problem using a translation operator. Abdel Wahed [73] has solved the (n+1) dimensional NLS equation for an analytical answer. Malik et al. [105] used analytical methods to find novel optical solitons, including the Lie symmetry analysis and two iterations of the new extended generalized Kudryashov approach. Osman et al. [106] used two techniques for the perturbed NLS equation in nonlinear optical fibers: the first is the extended modified auxiliary equation, and the second is a generalized Riccati equation approach. In addition, the extended trial equation method [133], spectral collocation method [134], split step finite difference method [135], trigonometric cubic B-spline with DQM [26], finite difference method, and the quartic B-spline DQM [136], Crank-Nicolson based quintic B-spline DQM [19], modified cubic B-spine DQM [16], quintic B-spline Galerkin finite element method [137], exponential cubic B-spline collocation method [138], and exponential cubic B-spline DQM [88], are few further effective numerical methods to the NLS equation.

3.4.4 Implementation of the proposed scheme on numerical of the nonlinear Schrödinger equation

Example 3.1: Consider the NLS equation (3.1) with $\alpha = -0.5$, $\beta = 1$, $g(x,t) = cos^2(x)$, domain $x \in [0,2\pi]$ and $t > 0$.

The exact solution is given as [26]:

$$u(x,t) = \sin(x)\exp\left(-3it/2\right),$$

with the initial conditions $u(x,0) = \sin(x)$,

and boundary conditions $u(0,t) = 0 = u(2\pi,t)$.

The physical representation of numerical and exact solution is shown in the figures 3.2-3.5. The calculations are performed using $\Delta t = 0.0001$, and $N = 51$ (node points). The findings show that the current method is effective and similar to results

reported in the literature for the parameter $\epsilon = 0.051436$. The L_∞ error norm are shown in Table 3.1 and compared with the research findings [26] in order to verify the outcomes. The result of this method is better even when N is exactly half to the compared one in literature.

Table 3.1: Comparative analysis of solutions of Example 3.1 with error norm.

Time	**Arora et al. [26] ($N = 100$)**	**Present ($N = 51$)**
t	L_∞	
1	1.69e-04	8.0091e-05
5	6.57e-04	3.8471e-04
10	2.17e-03	1.7641e-03
20	8.26e-03	7.5851e-03

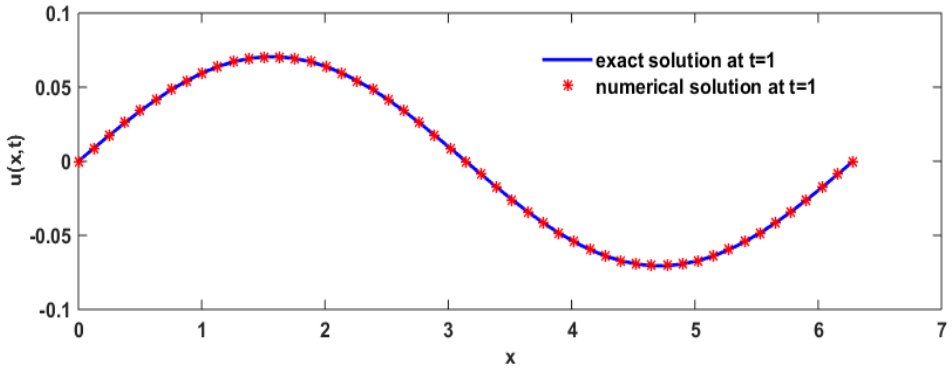

Figure 3.2: The physical representation of comparison of exact and numerical solutions of Example 3.1 for N=51 at t=1.

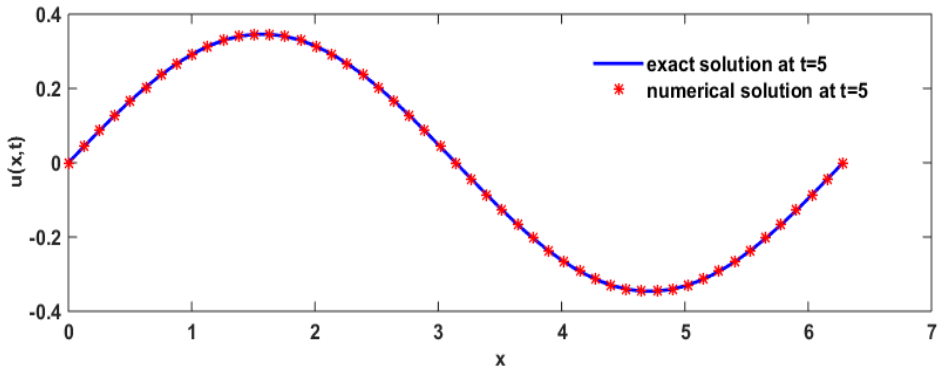

Figure 3.3: The physical representation of comparison of exact and numerical solutions of Example 3.1 for N=51at t=5.

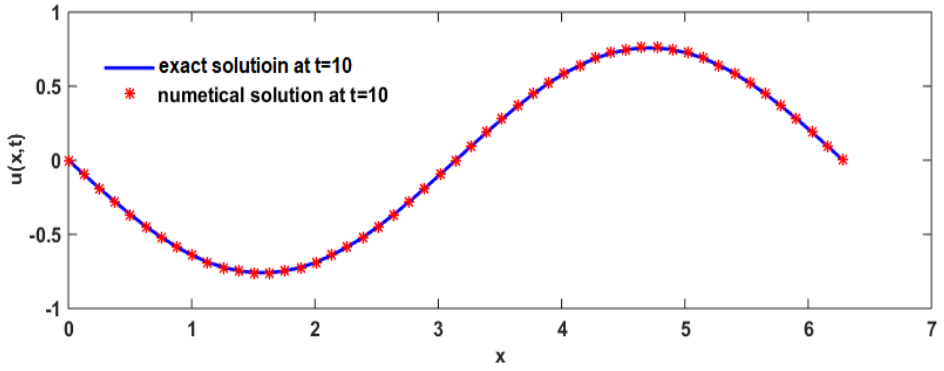

Figure 3.4: The physical representation of comparison of exact and numerical solutions of Example 3.1 for N=51 at t=10.

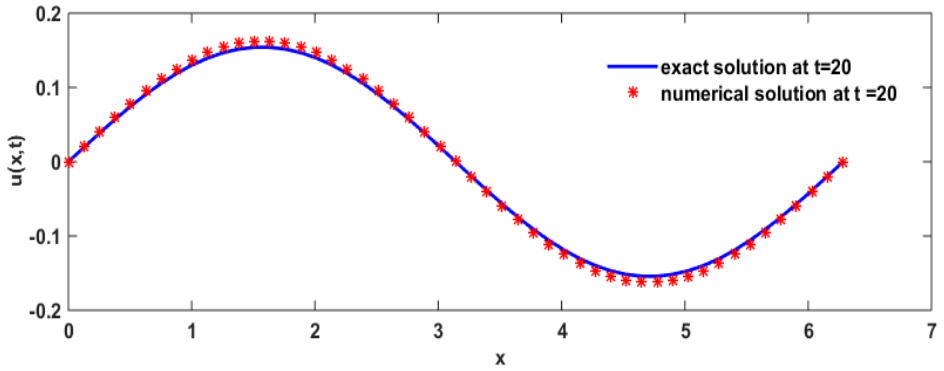

Figure 3.5: The physical representation of comparison of exact and numerical solutions of Example 3.1 for N=51 at t=20.

Example 3.2: Consider the NLS equation (3.1) with $\alpha = 1$, $\beta = 2$, $g(x,t) = 0$, domain $x \in [-15,15]$ and $t > 0$.

The exact solution is given as [26]:

$$u(x,t) = \exp\big(-i(2x + 4 - 3t)\big)\,\mathrm{sech}(x + 2 - 4t),$$

with the initial conditions: $u(x,0) = \exp\big(-i(2x + 4)\big)\,\mathrm{sech}(x + 2)$,

and boundary conditions: $u(-15,t) = 0 = u(15,t)$.

The physical representation of numerical and exact solution is shown in Figure 3.6-3.8. The calculations are performed using $\Delta t = 0.0001$, and $N = 301$ (node points). The findings show that the current method is effective and similar to results reported in the literature for the parameter $\epsilon = 3.000066$. The L_∞ error norm are shown in

Table 3.2 and compared with the research findings [26] in order to verify the outcomes. Results are comparable that the results available in literature.

Table 3.2: Comparative analysis of solutions of Example 3.2 with error norm.

Time	**Arora et al. [26] (N = 200)**	**Present (N= 301)**
t	L_∞	
0.5	2.54e-04	2.4820e-04
1.0	1.97e-04	1.8289e-04
1.5	2.32e-04	1.3055e-04
2.0	3.40e-04	1.2879e-04
2.5	4.49e-04	2.0734e-04
3.0	6.68e-04	3.1204e-04

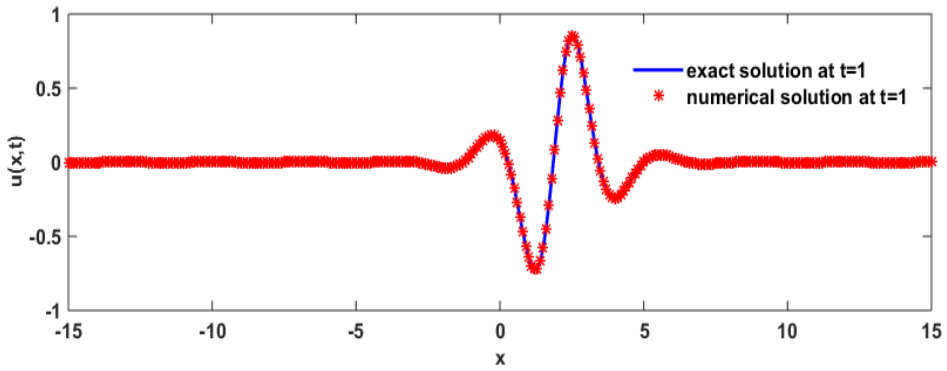

Figure 3.6: The physical representation of comparison of exact and numerical solutions of Example 3.2 for N=301 at t=1.

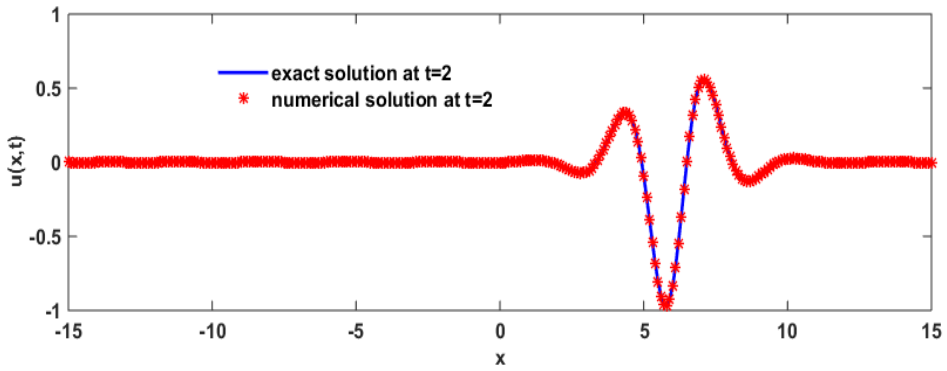

Figure 3.7: The physical representation of comparison of exact and numerical solutions of Example 3.2 for N=301 at t=2.

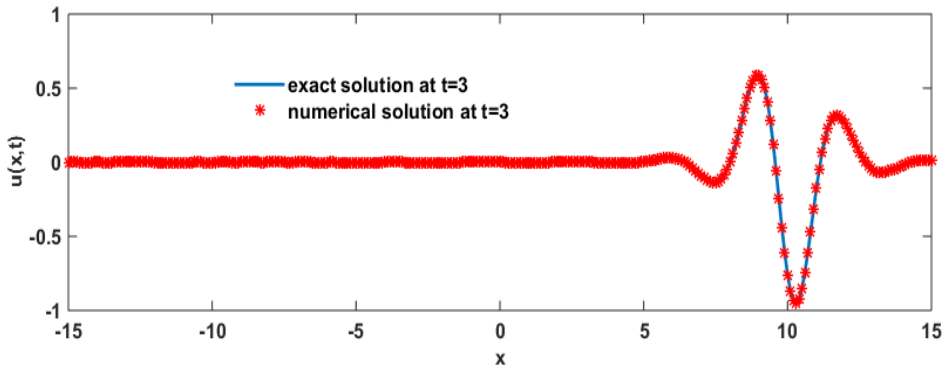

Figure 3.8: The physical representation of comparison of exact and numerical solutions of Example 3.2 for N=301 at t=3.

3.5 Introduction to nonlinear Sine-Gordon equation

The SG equation is given by:

$$u_{tt} + \alpha\, u_t = \beta\ u_{xx} + \eta(x)\sin(u) \qquad (3.2)$$

initial conditions:

$$u(x,0) = \phi_1(x)\ and\ u_t(x,0) = \phi_2(x)$$

and values defined at the boundaries.

Here, α and β are real constants and $\eta(x,y)$ parameter depicts the Josephson current density. The constant α represents the dissipative term that plays an important role in converting equation from damped $(\alpha \geq 0)$ to undamped for $(\alpha = 0)$.

The SG equation has been studied extensively since its introduction in 1834 by James Clerk Maxwell, and it has found applications in many areas of physics, including the study of the behavior of magnetic flux lines in superconductors, the dynamics of vortices in fluid dynamics, and the study of topological defects in field theory. The equation has also been studied in mathematics, where it has been used to study the geometry of surfaces, integrable systems, and nonlinear waves.

3.5.1 Applications of Sine-Gordon equation

The SG equation is a second order nonlinear partial PDE with several applications in science and engineering, including mechanical transmission, Josephson junction, condensed matter physics, field theory, magnetic crystals, and mathematical physics. It appears as a remedy for the traditional Maxwell systems in the study of optics

[139]. Additionally, the geometrical analysis of the soliton in light of the canonical field uses this equation in the literature [140]. A mathematical model to show the fault dynamics of the phenomena of strain waves and earthquakes is also presented by the SG equation [141]. It is crucial to comprehend the impact of seismic distortion on the earth's crust and the idea underlying the origin of defective natural elements. The kinks form of the equation's soliton solution makes it a good tool for understanding the ideas behind various events. Here are some applications of the SG equation:

Soliton theory: The SG equation is a prototypical example of a soliton equation, which means that it admits solutions that are localized and have the property of particle-like behavior. These solutions are known as solitons, and they have a remarkable property of being able to maintain their shape and velocity after colliding with other solitons or obstacles.

Condensed matter physics: The SG equation describes the dynamics of the phase of a one-dimensional superfluid or superconducting system. It is also used to model the behavior of magnetic domain walls and dislocations in crystals.

Classical mechanics: The SG equation arises in the study of certain classical mechanical systems, such as the motion of a pendulum in a dissipative medium.

Integrable systems: The SG equation is one of the integrable systems, which means that it can be solved exactly using techniques from algebraic geometry and complex analysis. This property makes it a useful tool for studying other integrable systems in physics and mathematics.

3.5.2 Role of solitons in applications of Sine-Gordon equation

The soliton solution of the SG equation is a fundamental concept in the study of nonlinear wave phenomena. Solitons are stable, localized wave packets that maintain their shape and velocity as they propagate through a nonlinear medium. Here are some applications of solitons in the context of the SG equation:

Condensed matter physics: The SG equation arises in the study of certain condensed matter systems, such as Josephson junction arrays and spin chains. Solitons can be formed in these systems, and they are used to study the dynamics of topological defects and other nonlinear excitations.

High-energy physics: The SG equation arises in the study of certain quantum field theories in high-energy physics, such as the Thirring model and the Gross-Neveu model. Solitons can be formed in these systems, and they are used to study the dynamics of particles and other nonlinear excitations.

Nonlinear optics: The SG equation is used to model the propagation of light in nonlinear media, such as optical fibers and waveguides. Solitons can be formed in these systems, and they are used to study the dynamics of self-trapping, self-phase modulation, and other nonlinear effects.

Fluid mechanics: The SG equation arises in the study of certain fluid dynamics problems, such as shallow water waves and surface waves on a fluid interface. Solitons can be formed in these systems, and they are used to study the dynamics of wave breaking, rogue waves, and other nonlinear effects.

Nonlinear acoustics: The SG equation is used to model the propagation of sound waves in nonlinear media, such as acoustic metamaterials and photonic crystals. Solitons can be formed in these systems, and they are used to study the dynamics of nonlinear wave propagation and scattering.

Overall, the soliton solution of the SG equation is an active area of research.

3.5.3 Literature Review of SG Equation: The SG problem has been resolved by the researchers due to such important applications using a number of analytical and numerical methods for its soliton solutions including the modified decomposition method [142] for solving this equation 2D, homotopy analysis method [143], collocation and radial basis function [144], tension spline-based approximation scheme [145], modified cubic B-spline collocation technique [102], Legendre spectral element method [146], virtual element method [147], Barycentric rational interpolation and RBF [148], fourth-order collocation scheme [149], cubic B-spline DQM [29], modified trigonometric B-spline DQM [27], and rational radial basis function [153].

3.5.4 Implementation of the proposed scheme on numerical of the nonlinear Sine-Gordon equation

Example 3.3: Consider the SG equation (3.2) in domain $x \in [-20,20]$ for $\alpha = 0$, $\beta = 1$ and $\eta(x) = -1$,

with initial conditions:

$$\phi_1(x) = 4\tan^{-1}(c\sinh(\gamma x)),$$

and

$$\phi_2(x) = 0$$

The exact solution of the equation is given by:

$$u(x,t) = 4\tan^{-1}(c\sinh(\gamma x)\,\mathrm{sech}(\gamma c t))$$

here, γ is a parameter that depends on speed of a solitary wave is expressed as:

$$\gamma = \frac{1}{\sqrt{1-c^2}}$$

and the boundary conditions are calculated from exact solutions.

The calculations are performed using parameters of $c = 0.5, k = 0.001$, and $N = 301$ (node points). The findings show that the current method is effective and similar to results reported in the literature for the parameter $\epsilon = 0.011702$. The errors are shown in Table 3.3 and compared with the research findings [27] in order to verify the outcomes. Figure 3.9 shows the results at different times to show compression of exact solution and numerical solution. Figure 3.10 shows the surface plot of exact solution for $0 \leq t \leq 20$.

Table 3.3: Comparative analysis of solutions of Example 3.3 with different error norms.

Time	**Present results**			**Arora et al.** [27]		
t	L_2	L_∞	***RMS***	L_2	L_∞	***RMS***
1	8.5768e-06	5.6434e-06	1.3516e-06	4.53e-06	3.36e-06	7.13e-07
2	8.3200e-06	6.0814e-06	1.3111e-06	4.67e-06	3.36e-06	7.36e-07
5	1.2807e-05	1.0619e-05	2.0183e-06	9.67e-06	6.88e-06	1.52e-06
10	2.2668e-05	1.4979e-05	3.5722e-06	2.08e-05	1.23e-05	3.28e-06
15	3.3615e-05	2.0633e-05	5.2974e-06	---	---	---
20	4.4854e-05	2.6284e-05	7.0685e-06	---	---	---

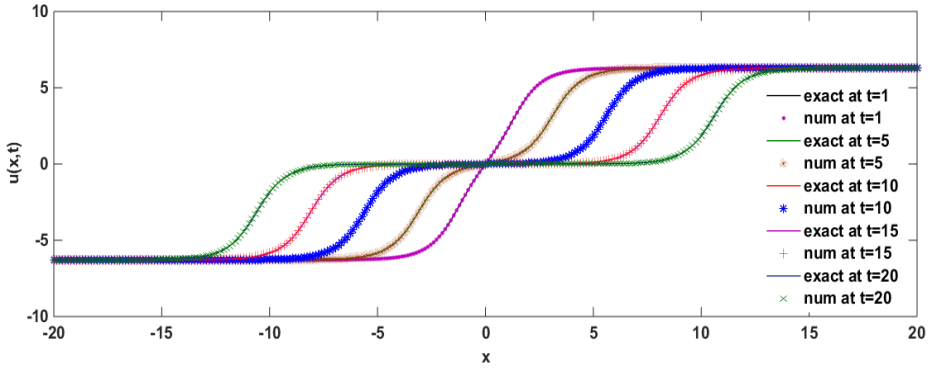

Figure 3.9: The physical representation of comparison of exact and numerical solutions of Example 3.3 at t=1, 5, 10, 15, 20.

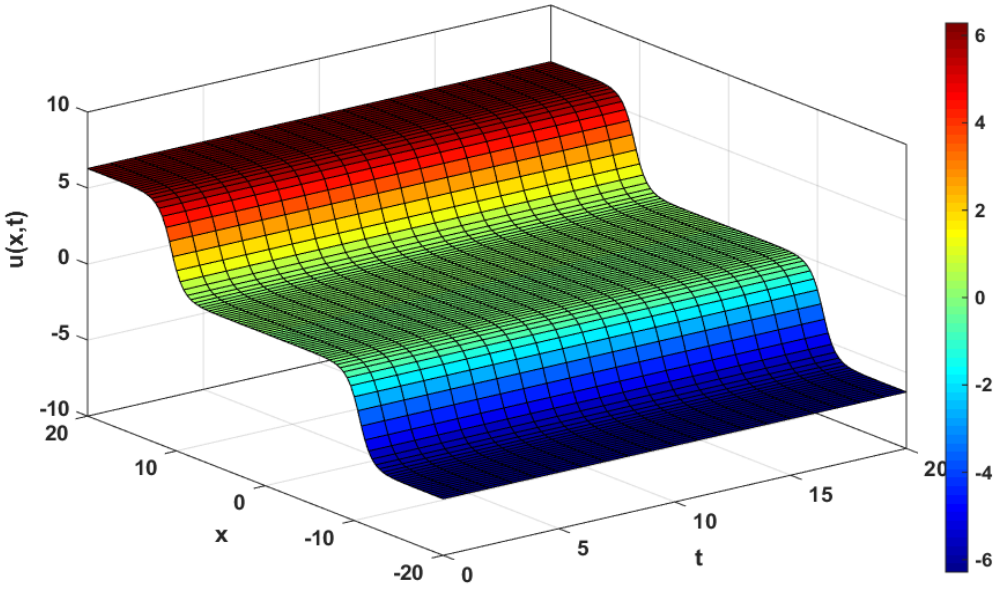

Figure 3.10: Surface plot of exact solution of Example 3.3 for $0 \leq t \leq 20$.

Example 3.4: Consider the SG equation (3.2) in domain $x \in [-3,3]$ for $\alpha = 0$, $\beta = 1$ and $\eta(x) = -1$,

with initial conditions:

$$\phi_1(x) = 4\tan^{-1}(\exp(\gamma x)),$$

and

$$\phi_2(x) = \frac{-4\gamma \exp(\gamma x)}{1 + \exp(2\gamma x)}$$

The exact solution of the equation is given by:

$$u(x,t) = 4\tan^{-1}\left(\exp\left(\gamma(x - 0.5t)\right)\right)$$

here, γ is a parameter that depends on speed of a solitary wave is expressed as:

$$\gamma = \frac{1}{\sqrt{1-c^2}}$$

and the boundary conditions are calculated from exact solutions.

The calculations are performed using parameters of $c = 0.5, k = 0.0001$, space step size is $h = 0.04$, and $N = 151$ (node points). The findings show that the current method is effective and similar to results reported in the literature for the parameter $\epsilon = 0.040996$. The errors are shown in Table 3.4 and compared with the research findings [29,102] in order to verify the outcomes. Figure 3.11 shows the results at different times to show compression of exact solution and numerical solution. Figure 3.12 shows the surface plot of exact solution for $0 \leq t \leq 1$.

Table 3.4: Comparative analysis of solutions of Example 3.4 with different error norms.

Time	**Present results**			**Mittal and Bhatia** [102]		**Shukla and Tamsir** [29]	
t	L_2	L_∞	RMS	L_2	L_∞	L_2	L_∞
0.25	6.4671e-06	1.3759e-05	2.1273e-07	3.66e-05	4.90e-05	5.67e-06	9.61e-06
0.50	8.6897e-06	1.4149e-05	2.8584e-07	9.00e-05	7.55e-05	8.39e-06	1.10e-05
0.75	9.9927e-06	1.4242e-05	3.2871e-07	1.60e-04	1.43e-04	1.05e-05	1.26e-05
1.0	1.0807e-05	1.4056e-05	3.5549e-07	2.27e-04	2.10e-04	1.24e-05	1.44e-05

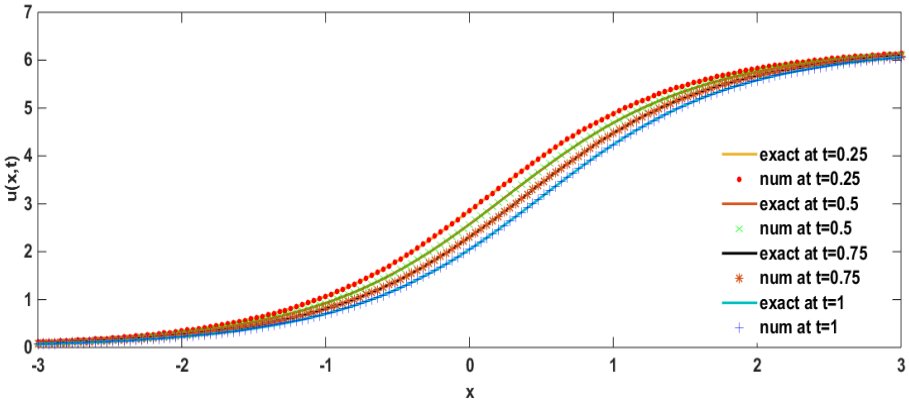

Figure 3.11: The physical representation of comparison of exact and numerical solutions of Example 3.4 at t=0.25, 0.5, 0.75, 1.

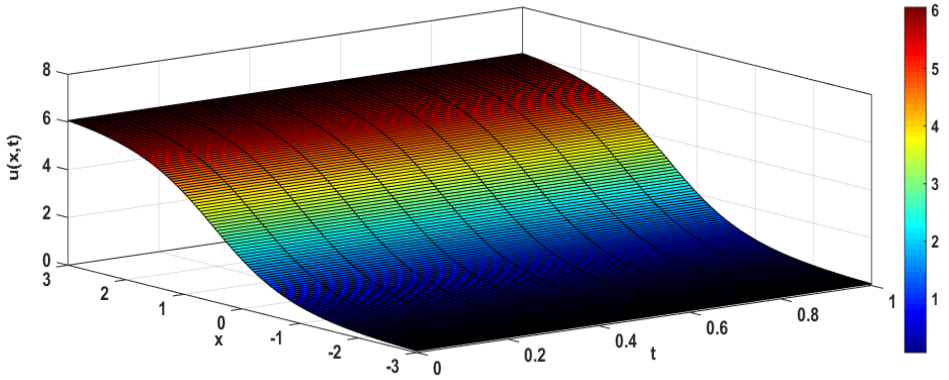

Figure 3.12: Surface plot of exact solution of Example 3.4 for $0 \leq t \leq 1$.

Example 3.5: Consider the SG equation (3.2) in domain $x \in [-20,20]$ for $\alpha = 0$, $\beta = 1$ and $\eta(x) = -1$,

with initial conditions:

$$\phi_1(x) = 4\tan^{-1}(\exp(\gamma x)),$$

and

$$\phi_2(x) = \frac{-4\gamma c exp(\gamma x)}{1 + \exp(2\gamma x)}$$

The exact solution of the equation is given by:

$$u(x,t) = 4\tan^{-1}\big(\exp\big(\gamma(x - ct)\big)\big)$$

here, γ is a parameter that depends on speed of a solitary wave is expressed as:

$$\gamma = \frac{1}{\sqrt{1-c^2}}$$

and the boundary conditions are calculated from exact solutions.

The calculations are performed using parameters of $c = 0.5, k = 0.01$, and $N = 501$ (node points). The findings show that the current method is effective and similar to results reported in the literature for the parameter $\epsilon = 0.012557$. The errors are shown in Table 3.5 and compared with the research findings [150] in order to verify the outcomes. Figure 3.13 shows the results at different times to show compression of exact solution and numerical solution. Figure 3.14 shows the surface plot of exact solution for $0 \leq t \leq 10$.

Table 3.5: Comparative analysis of solutions of Example 3.5 with different error norms.

Time	**Present results**			**Shiralizadeh et al.** [150]		
t	L_2	L_∞	RMS	L_2	L_∞	RMS
0.25	1.1209e-07	1.2617e-07	1.7688e-08	2.4100e-04	1.1894e-04	1.0778e-05
0.50	3.5654e-07	3.9927e-07	5.6261e-08	3.4300e-04	1.2227e-04	1.5339e-05
0.75	5.6832e-07	6.3866e-07	8.9680e-08	4.1281e-04	1.2225e-04	1.8461e-05
1	7.0289e-07	8.2197e-07	1.1092e-07	4.6189e-04	1.2046e-04	2.0657e-05
2	9.9756e-07	1.1835e-06	1.5741e-07	5.1809e-04	1.1437e-04	2.3170e-05
5	1.6328e-06	1.4574e-06	2.5765e-07	4.3038e-04	1.3423e-04	1.9247e-05
10	3.2190e-06	2.7674e-06	5.0795e-07	5.1966e-04	1.7801e-04	2.3240e-05
15	5.2748e-06	4.2855e-06	8.3235e-07	6.5199e-04	2.3543e-04	2.9158e-05
20	7.8827e-06	6.1400e-06	1.2439e-06	8.4070e-04	3.1339e-04	3.7579e-05

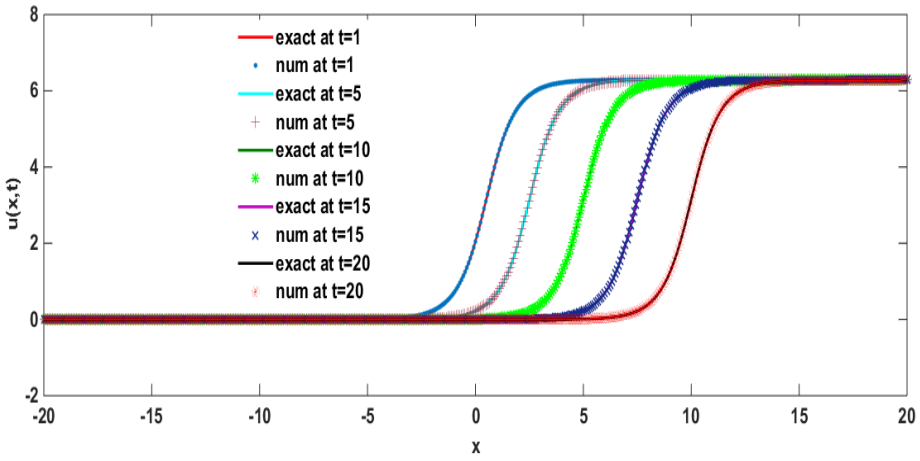

Figure 3.13: The physical representation of comparison of exact and numerical solutions of Example 3.5 at t=1, 5, 10, 15, 20.

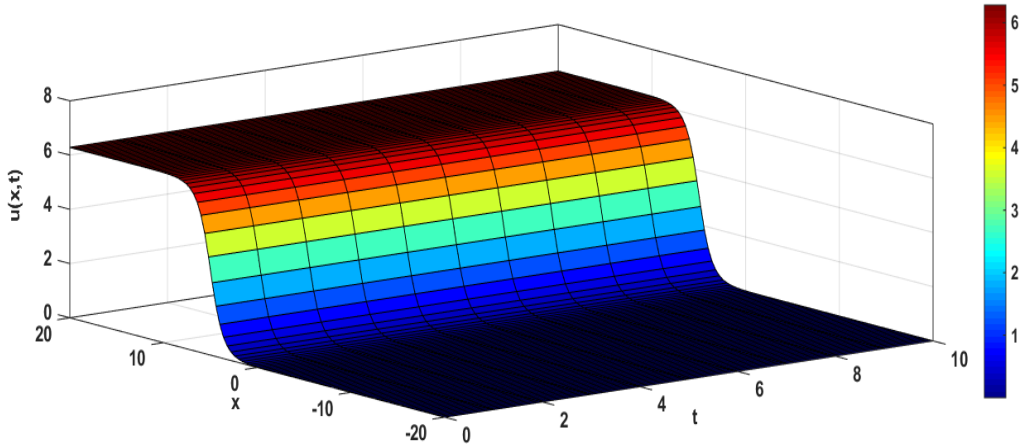

Figure 3.14: Surface plot of exact solution of Example 3.5 for $0 \leq t \leq 10$.

Example 3.6: Consider the SG equation (3.2) in domain $x \in [-20,20]$ for $\alpha = 0$, $\beta = 1$ and $\eta(x) = -1$,

with initial conditions:

$$\phi_1(x) = 4\tan^{-1}(\exp(\gamma x)),$$

and

$$\phi_2(x) = \frac{-4\gamma c exp(\gamma x)}{1 + \exp(2\gamma x)}$$

The exact solution is given and the boundary conditions are calculated from that:

$$u(x,t) = 4\tan^{-1}\left(\exp\left(\gamma(x-ct)\right)\right)$$

here, γ is a parameter that depends on speed of a solitary wave is expressed as:

$$\gamma = \frac{-1}{\sqrt{1-c^2}}$$

and the boundary conditions are calculated from exact solutions.

The calculations are performed using parameters of $c = 0.95, k = 0.01$, and $N = 501$ (node points). The findings show that the current method is effective and similar to results reported in the literature for the parameter $\epsilon = 0.012557$. The errors are shown in Table 3.6 and compared with the research findings [150] in order to verify the outcomes. Table 3.7 displays the rate of convergence of the proposed scheme, evaluated using the L_∞ error norm at different time level. Figure 3.15 shows the results at different times to show compression of exact solution and numerical solution. Figure 3.16 shows the surface plot exact solution for $0 \leq t \leq 10$.

Table 3.6: Comparative analysis of solutions of Example 3.6 with different error norms.

Time	**Present results**			**Shiralizadeh et al.** [150]		
t	L_2	L_∞	RMS	L_2	L_∞	RMS
0.25	1.7667e-05	3.4727e-05	1.2443e-07	3.9330e-04	1.3086e-04	1.7589e-05
0.50	3.1706e-05	6.9928e-05	2.2330e-07	4.9815e-04	1.4274e-04	2.2278e-05
0.75	4.7193e-05	1.0470e-04	3.3238e-07	5.9493e-04	1.9470e-04	2.6606e-05
1	6.2698e-05	1.3951e-04	4.4158e-07	7.0399e-04	2.5476e-04	3.1483e-05
5	3.0092e-04	6.0438e-04	2.1193e-06	1.2000e-03	5.1335e-04	5.1525e-05
10	5.9195e-04	8.0423e-04	4.1690e-06	3.2000e-03	1.4000e-03	1.4163e-04
15	8.6128e-04	1.1118e-03	6.0659e-06	7.4000e-03	2.6000e-03	3.3026e-04
20	2.2213e-03	4.8656e-03	1.5644e-05	1.2000e-03	4.9000e-03	5.3738e-04

Table 3.7: The ROC of numerical scheme with Example 3.6 at t = 0.25, 1, and 2.

	t=0.25		t=1		t=2	
N	L_∞	**ROC**	L_∞	**ROC**	L_∞	**ROC**
50	1.18e-01	---	4.75e-01	---	4.40e-01	---
100	3.26e-02	1.862840	3.99e-02	3.574814	1.22e-01	1.853453
200	1.44e-03	4.495112	6.13e-03	2.700139	1.17e-02	3.373211
400	9.31e-05	3.955621	3.63e-04	4.076814	7.21e-04	4.025600
800	5.06e-06	4.201838	2.07e-05	4.136676	4.28e-05	4.073538

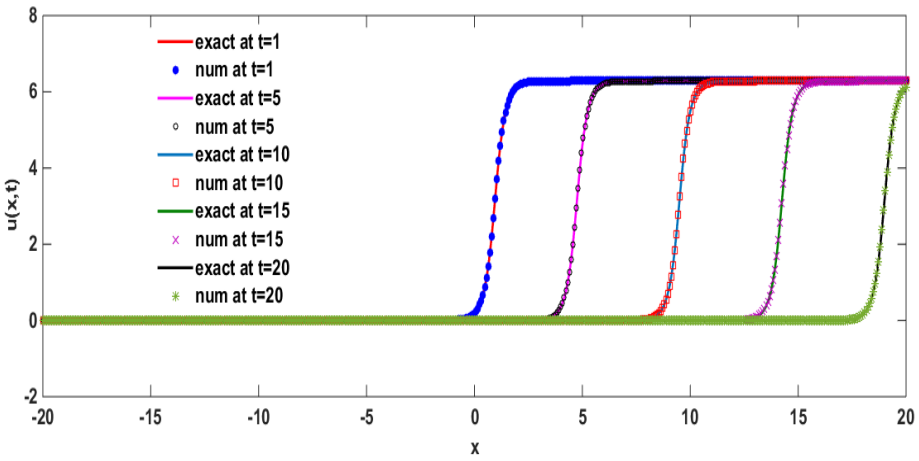

Figure 3.15: The physical representation of comparison of exact and numerical solutions of Example 3.6 at t=1, 5, 10, 20.

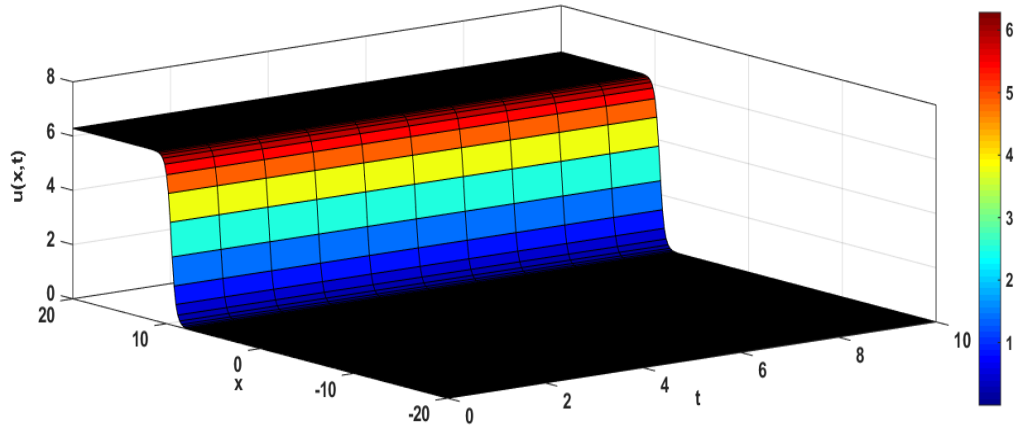

Figure 3.16**:** Surface plot of exact solution of Example 3.6 for $0 \leq t \leq 10$.

Example 3.7: Consider the SG equation (3.2) in domain $x \in [-10,10]$ for $\alpha = 0$, $\beta = 1$ and $\eta(x) = -1$,

with initial conditions:

$$\phi_1(x) = 0$$

and

$$\phi_2(x) = 4\,\mathrm{sech}(x)$$

The exact solution of the equation is given by:

$$u(x,t) = 4\tan^{-1}(\mathrm{sech}(x)\,t)$$

and the boundary conditions are calculated from exact solutions.

The calculations are performed using parameters of $k = 0.01$, and $N = 401$ (node points). The findings show that the current method is effective and similar to results reported in the literature for the parameter $\epsilon = 0.999934$. The errors are shown in Table 3.8 and compared with the research findings [150] in order to verify the outcomes. Table 3.9 displays the rate of convergence of the proposed scheme, evaluated using the L_∞ error norm at different time level. Figure 3.17 shows the results at different times to show compression of exact solution and numerical solution. Figure 3.18 shows the surface plot exact solution for $0 \leq t \leq 20$.

Table 3.8: Comparative analysis of solutions of Example 3.7 with different error norms.

Time	**Present results**			**Shiralizadeh et al.** [150]		
t	L_2	L_∞	RMS	L_2	L_∞	RMS
0.25	1.9450e-06	3.6320e-06	4.3383e-07	1.4400e-04	3.0169e-05	7.1908e-06
0.50	2.5475e-06	3.6320e-06	5.6822e-07	2.4339e-04	4.6806e-05	1.2154e-05
0.75	2.9748e-06	3.6320e-06	6.6354e-07	3.0422e-04	5.1706e-05	1.5192e-05
1	3.2777e-06	3.6320e-06	7.3108e-07	3.5484e-04	5.2994e-05	1.7720e-05
2	3.6014e-06	3.6320e-06	8.0328e-07	6.7163e-04	7.8976e-05	3.3540e-05
5	2.9577e-06	3.6320e-06	6.5971e-07	3.0000e-03	3.2159e-04	1.4923e-04
10	4.0544e-06	3.6320e-06	9.0432e-07	1.2600e-02	1.4000e-03	6.2974e-04
15	7.0675e-06	3.6320e-06	1.5764e-06	2.8900e-02	3.2000e-03	1.4000e-03
20	1.1713e-05	5.6180e-06	2.6126e-06	5.1700e-02	5.8000e-03	2.6000e-03

Table 3.9: The ROC of numerical scheme with Example 3.7 at t = 1, 2, and 5.

	t=1		**t=2**		**t=5**	
N	L_∞	**ROC**	L_∞	**ROC**	L_∞	**ROC**
25	1.65e-02	---	1.85e-02	---	1.66e-02	---
50	3.32e-04	5.638675	6.27e-04	4.883128	4.27e-04	5.283404
100	2.53e-05	3.716241	4.15e-05	3.916740	2.96e-05	3.852788
200	3.63e-06	2.797904	3.63e-06	3.514449	3.63e-06	3.024371

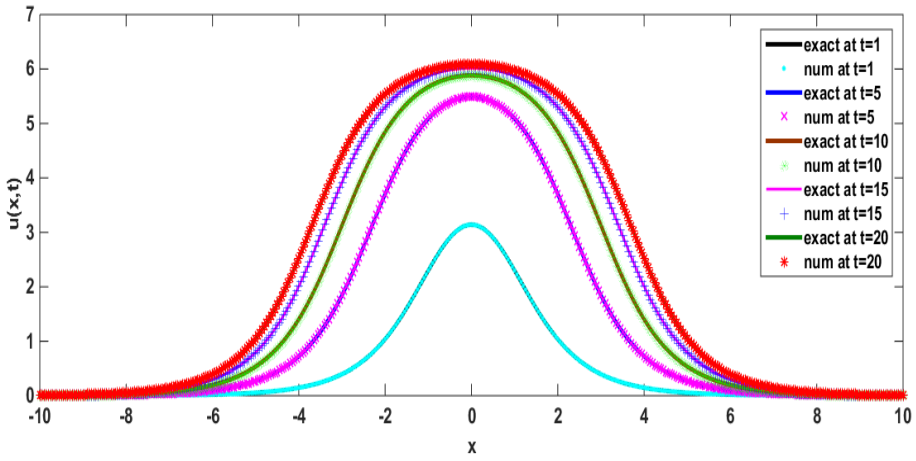

Figure 3.17: The physical representation of comparison of exact and numerical solutions of Example 3.7 at t=1, 5, 10, 15, 20.

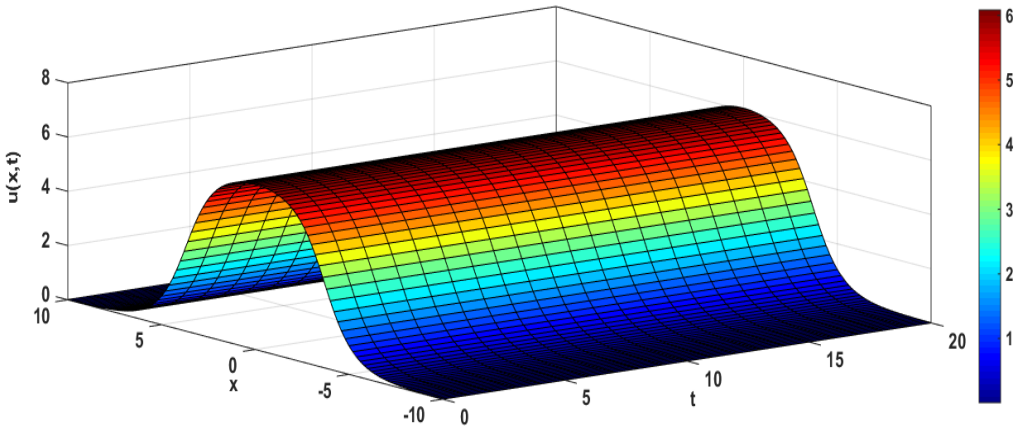

Figure 3.18: Surface plot of exact solution of Example 3.7 for $0 \leq t \leq 20$.

Example 3.8: Consider the SG equation (3.2) in domain $x \in [-2,2]$ for $\alpha = 0$, $\beta = 1$ and $\eta(x) = -1$,

with initial conditions:

$$\phi_1(x) = 0,$$

and

$$\phi_2(x) = 4\,\mathrm{sech}(x)$$

The exact solution of the equation is given by:

$$u(x,t) = 4\tan^{-1}(\text{sech}(x)\,t)$$

and the boundary conditions are calculated from exact solutions.

The calculations are performed using parameters of $k = 0.0001$, and $N = 101$ (node points). The findings show that the current method is effective and similar to results reported in the literature for the parameter $\epsilon = 0.999934$. The errors are shown in Table 3.10 and compared with the research findings [27] in order to verify the outcomes. Figure 3.19 shows the results at different times to show compression of exact solution and numerical solution. Figure 3.20 shows the surface plot exact solution for $0 \leq t \leq 20$.

Table 3.10: Comparative analysis of solutions of Example 3.8 with different error norms.

Time	**Present results**			**Arora et al.** [27]		
t	L_2	L_∞	***RMS***	L_2	L_∞	***RMS***
0.3	5.5495e-05	1.0565e-04	2.7474e-05	5.55e-05	1.05e-04	2.72e-06
0.6	6.6124e-05	1.0368e-04	3.2736e-05	6.61e-05	1.03e-04	3.24e-06
1	7.0836e-05	9.9306e-05	3.5069e-05	7.08e-05	9.93e-05	3.47e-06
1.5	7.6557e-05	9.1739e-05	3.7901e-05	---	---	---
2	8.7977e-05	8.2896e-05	4.3555e-05	---	---	---

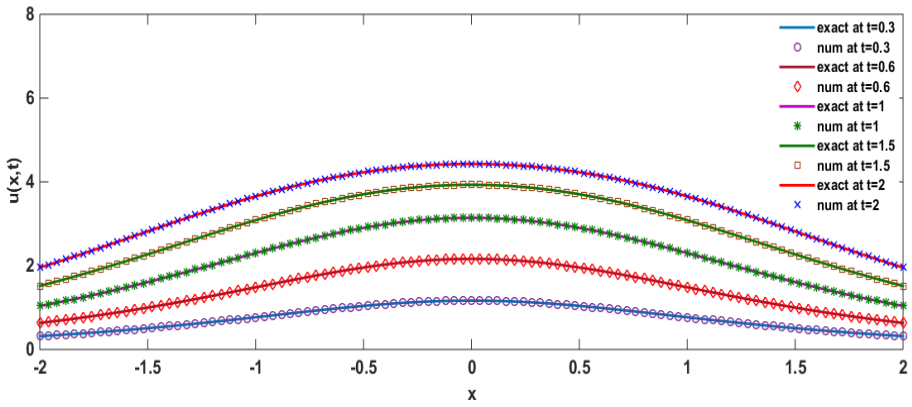

Figure 3.19: The physical representation of comparison of exact and numerical solutions of Example 3.8 at t=0.3, 0.6, 1, 1.5, 2.

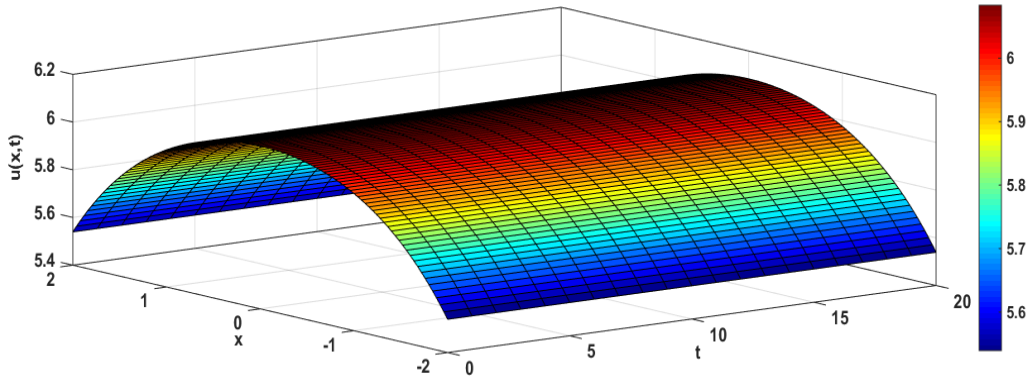

Figure 3.20: Surface plot of exact solution of Example 3.8 for $0 \leq t \leq 20$.

It may be said that the findings acquired are in excellent agreement with each other and even outperform those reported by other studies [27, 29, 102, 150].

3.6 Summary

This chapter presents an impressive approach for finding solutions of the NLEEs using the "Exponential modified cubic B-spline differential quadrature method with LOOCV approach". In addition, the LOOCV technique is briefly described, along with its advantages and disadvantages.

The use of the exponential cubic B-spline basis functions is limited in the literature due to assigned random value to parameter ϵ, that often leads to unstable results. This chapter presents a methodology that combines LOOCV approach with the exponential modified cubic B-spline differential quadrature method. The LOOCV strategy is used to find the optimal value of the parameter ϵ, occurs in the basis functions, which improves the accuracy of results. To check the authenticity and effectiveness of the proposed method, the method is implemented on examples of NLS equation and SG equation and results are shown in form of figures and tables. The success of this combined methodology, has been verified by calculated L_2, L_∞, and RMS error norms, shows that the results are close to exact solutions and comparable to other numerical methods that are already published in literature. The rate of convergence of the numerical scheme is also calculated by the L_∞ error norm, which is on an average 4. It seems that the proposed approach has a fast convergence rate.

The idea of optimizing the value of any parameter available in method with the help of LOOCV approach provides an attractive research idea for future studies.

Chapter-4

Numerical solutions of nonlinear partial differential equations using "Exponential modified cubic B-spline differential quadrature method (Expo-MCB-DQM) with PSO approach"

4.1 Introduction

Nature-inspired algorithms are a class of optimization algorithms that are based on the principles observed in nature. These algorithms are designed to solve complex optimization problems by mimicking the behavior of natural systems such as biological organisms, social insects, and physical systems.

Nature-inspired algorithms are typically based on probabilistic and stochastic models that mimic the processes of natural selection, mutation, reproduction, and survival of the fittest. These algorithms are often used in optimization problems where traditional optimization techniques may not be effective, such as in highly nonlinear, non-convex, or multi-modal optimization problems.

Some common examples of nature-inspired algorithms include:

Genetic Algorithms (GA): GA is an optimization technique inspired by the principles of natural selection and genetics. It involves generating a population of candidate solutions, evaluating their fitness based on a fitness function, and then applying selection, crossover, and mutation operators to create new candidate solutions. GA is commonly used in optimization problems where the solution space is large and complex.

Particle Swarm Optimization (PSO): PSO is an optimization technique inspired by the behavior of social insects such as birds flocking or fish schooling. In PSO, a population of particles moves through the solution space, guided by their own experience and the experience of their neighbors, to search for the optimal solution. PSO is commonly used in optimization problems with continuous variables.

Ant Colony Optimization (ACO): ACO is an optimization technique inspired by the behavior of ants. In ACO, a colony of ants searches for the shortest path between a source and a destination using pheromone trails. The pheromone trail is updated based on the quality of the solution found by the ants. ACO is commonly used in optimization problems involving graphs, such as the traveling salesman problem.

Artificial Bee Colony (ABC): ABC is an optimization technique inspired by the behavior of honeybees. In ABC, a population of artificial bees searches for the optimal solution by exploring the solution space and communicating their experience to their peers. ABC is commonly used in optimization problems with continuous variables.

Overall, nature-inspired algorithms are a powerful tool for solving complex optimization problems in a variety of domains, and they are widely used in research and practical applications.

4.2 Particle Swarm Optimization (PSO)

PSO is one of important nature-inspired optimization algorithm that belongs to the category of swarm intelligence algorithms. Swarm intelligence algorithms are based on the collective behavior of groups of simple agents, called "particles" or "swarm", that interact with each other and with the environment to solve complex optimization problems. PSO algorithm was inspired by the social behavior of bird flocking or fish schooling, where individual members of a group learn from their own and their peers' experience to adapt to changing environmental conditions and find the best path towards a common goal.

It is a computational method used to optimize complex problems by simulating the social behavior of swarms of organisms, such as birds or fish. In PSO, a group of particles moves through a multidimensional search space, with each particle representing a candidate solution to the problem being optimized. The particles adjust their positions based on their own experience and the experience of their neighbors, with the goal of finding the optimal solution. PSO has been successfully applied to a wide range of optimization problems, including engineering design, financial

forecasting, and data mining. Its advantages include its simplicity, ease of implementation, and ability to handle complex, high-dimensional search spaces.

PSO is a computer technique used in computational mathematics to optimize problems by repeatedly attempting to raise the quality of possible answers. This chapter of thesis describes the algorithm, advantages, and disadvantages of PSO, and its important applications.

4.2.1 Algorithm of PSO technique

The collective activities of birds while searching for food served as the inspiration for the development of the PSO algorithm [151]. In this technique, particles are considered entities, and their location affects how they behave. There is a component of the solution that has to be optimized at each location. The search process is driven by the updating of particle positions and velocities at each time step. There is a location for each particle in the swarm that can be resolved in D-dimensional space. Each particle moves according to its best-known locations both locally and across the search space, which are updated when new locations are discovered by other particles. With the use of a simple mathematical formula, the updating guidelines for each particle's location and speed by:

$$u_{ib}^{t+1} = \chi\left[u_{ib}^{t} + d_1\ r_1(p_{ib}^{t} - x_{ib}^{t}) + d_2\ r_2\left(p_{gb}^{t} - x_{ib}^{t}\right)\right]$$

$$x_{ib}^{t+1} = x_{ib}^{t} + u_{ib}^{t+1}$$

Where x_{ib}^{t}, represents particle's position and u_{ib}^{t} represents i^{th} particle's velocity in D dimension at time step t, p_{gb} represents the particle having the best fitness value, p_{ib} is the particle's best position visited so far, d_1, d_2 are acceleration coefficients which quantify particle personal and global experience respectively, χ is called constriction coefficient which evaluates a value in the range [0,1] and is given by

$$\chi = \frac{2\kappa}{\left|2 - \theta - \sqrt{\theta(\theta - 4)}\right|}$$

With $\theta = \theta_1 + \theta_2, \theta_1 = d_1 r_1, \theta_2 = d_2 r_2$ and $\kappa \approx 1$.

The procedure of PSO can be defined in the following steps:

Step 1. Initialize the parameters: Define the number of particles and their positions in the search space. Assign random velocities to each particle.

Step 2. Evaluate fitness: Calculate the fitness value for each particle based on its position.

Step 3. Update particle's best-known positions: Compare the fitness value of each particle with its best-known fitness value. If the current fitness value is better, update the particle's best-known position.

Step 4. Update global best-known position: Compare the fitness value of each particle with the global best-known fitness value. If the current fitness value is better, update the global best-known position.

Step 5. Update particle velocities and positions: Update the velocity of each particle based on its current velocity, best-known position, and global best-known position. Update the position of each particle based on its current position and velocity.

Step 6. Repeat steps 2-5 until a termination condition is met: Termination conditions can be a maximum number of iterations, reaching a satisfactory fitness level, or a predefined error threshold.

M. K. Heri coded this PSO algorithm in MATLAB, Yarpiz, 2015.*

The PSO algorithm is simple to implement. It is a computational technique used to determine parameter values that iteratively optimizes for minimizing error. The solution thus obtained by the implementation of the approach is reliable as it is being searched for the number of iterations with the selected number of parameters with a predetermined population (or swarm) size and range of optimize parameter. This approach has also been successfully used in literature to compute the good shape parameter using in radial basis functions [2].

*(https://yarpiz.com/50/ypea102-particle-swarm-optimization)

4.2.2 Applications of PSO technique

A number of papers have been published on applications of PSO. PSO is a potential global optimization technique that has been widely used to address problems in a variety of fields such as health care, business, smart cities and general aspects [152]. Robinson and Rahmat-Samii [153] introduced PSO to the field of electromagnetics. Wang et al. [154] developed a novel technique for electrical impedance tomography based on PSO-RBF neural network. Kulkarni et al. [155] presented the application of PSO in wireless se networks. Perracchione and Stura [3] provide a novel method based on combining PSO with a mesh-free interpolation method to predict the values of the parameters indicating the disease (Prostate Cancer) risk level. Some PSO applications for acoustic filter optimization were presented by Barbieri et al. [156]. A numerical simulation of seismic wave impedance inversion based on the PSO was presented by Haijun et al. [157]. Kalatehjari et al. [158] presented the application of PSO in geotechnical engineering. Koupaei et al. [2] integrated the PSO with RBF-collocation techniques. Pham et al. [159] used PSO to calculate the soil's undrained shear strength, which is a crucial topic for civil engineering. To solve the existing model with five objectives for the generation of green coal, Cui et al. [160] developed a multi-objective particle swarm optimization algorithm. Abed and Aladool [151] proposed the PSO technique based on a discrete least square weighted function (DLSWF) and an expansion approximant as a fitness function for the minimal optimization problem.

4.2.3 Advantages of PSO technique

Advantages of the PSO are as follows [161]:

Simplicity: PSO is a relatively simple and easy-to-implement optimization algorithm compared to other more complex algorithms. It takes up greater optimization space and is easy to execute.

Convergence: PSO is good at finding global optima, even in complex search spaces with many local optima.

Efficiency: PSO is a fast algorithm that can converge to a solution quickly, even for large-scale optimization problems. The PSO is built on intelligence. It can be used in engineering as well as scientific research.

Robustness: PSO is robust to noisy and complex objective functions, and can handle non-linear and non-convex optimization problems. PSO do not calculate mutations or overlap. The particle's speed can be used to conduct the search. Over the course of several generations, only the most optimistic particle may transmit information to the other particles, and research proceeds very quickly.

Flexibility: PSO can be easily adapted and customized to fit different types of optimization problems and objectives. PSO makes a decision immediately based on the response and a real-number code. The constant of the solution and the dimension have the same number.

4.2.4 Disadvantage of PSO technique

Disadvantages of the PSO are as follows [161]:

Lack of dimensionality: This method cannot be used to solve non-coordinate system problems like the rules for how particles move in an energy field since it lacks dimensionality.

Premature convergence: PSO can converge prematurely to a sub-optimal solution, especially for more complex optimization problems.

Difficulty in tuning parameters: PSO has several parameters that need to be tuned carefully to achieve good performance. Selecting appropriate values for these parameters can be challenging and requires domain expertise.

Limited memory: PSO has a limited memory of the best particle positions, which can prevent it from exploring new regions of the search space effectively.

Lack of diversity: PSO particles can converge to the same region of the search space, which can limit the diversity of the search.

4.3 Numerical Scheme

In this chapter “Exponential modified cubic B-spline differential quadrature method (Expo-MCB-DQM) with PSO approach” is being used to find the numerical solutions

of two nonlinear PDEs (NLS equation and SG equation) with eight numerical problems. Authenticity and effectiveness of the proposed method tested by calculating the errors norms. Figure 4.1 shows graphical representation of the numerical scheme implemented on these two partial differential equations.

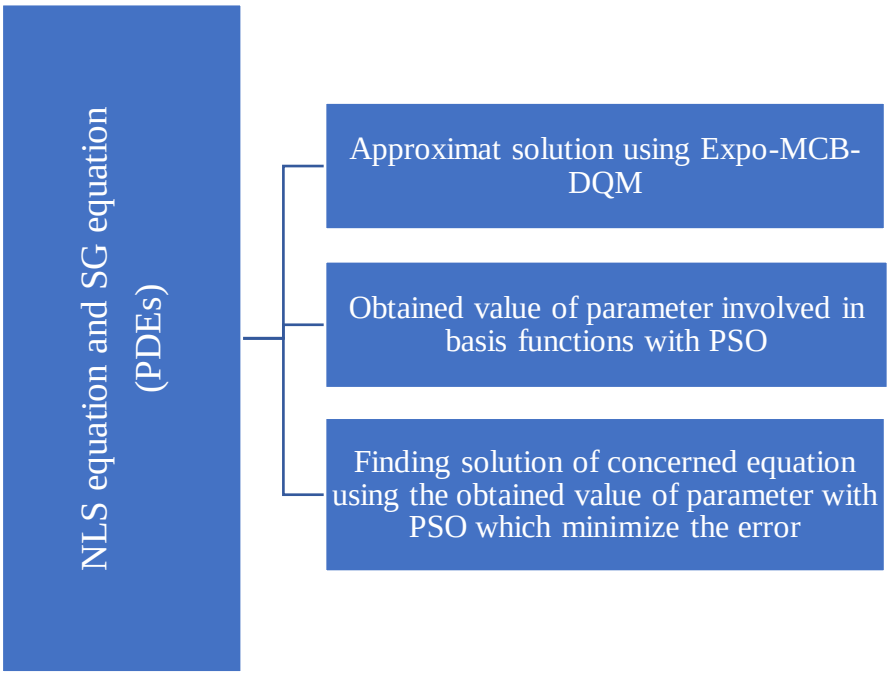

Figure 4.1: Graphical representation of the numerical scheme.

4.3.1 Implementation of the proposed scheme on numerical of the nonlinear Schrödinger equation

The one-dimensional NLS equation is expressed as [26]:

$$iu_t = \alpha u_{xx} + \beta|u|^2u + g(x,t)u, \qquad x \in [a,b], t \geq 0, \tag{4.1}$$

with an initial: $u(x,0) = u_0(x)$,

with boundary conditions: $\lim_{|x\to\infty|} u(x,t) = 0$.

Where α, β are arbitrary real numbers, $g(x,t)$ denotes a bounded real-valued function, i is the imaginary unit and $u = c + id$ denotes the complex-valued wave function. The subscripts x and t represents partial derivatives for space and time, respectively, and u_t is the amplitude of the pulse envelope.

Applications and literature review of the NLS equation is already presented in chapter 3 briefly where this equation is solved numerically by another technique.

Example 4.1: Consider NLS equation (4.1) with $\alpha = -0.5,\ \beta = 1,\ g(x,t) = cos^2(x),\ x \in [0,2\pi]$ and $t > 0$.

The exact solution is given as [26]:

$$u(x,t) = \sin(x)\exp\left({}^{-3it}/_{2}\right),$$

with the initial condition: $u(x,0) = \sin(x)$,

and boundary conditions $u(0,t) = 0 = u(2\pi,t)$.

The physical representation of comparison of numerical and exact solutions is shown in the figures 4.2-4.5 at different times. The results presented in Table 4.1 has been calculated by L_∞ error norm using $\Delta t = 0.0001$, and $N = 51$ (node points). It can be seen that the present methodology is effective, for the ideal value of parameter, $\epsilon = 1$ that has been calculated with the help of PSO approach, which helps to minimize the errors and is comparable to results available in literature [26]. This approach yields superior results even when N is exactly half of the one compared in the literature. Table 4.2 represents the comparative analysis of PSO and LOOCV with parameter value $\epsilon = 1$ and $\epsilon = 0.011702$ respectively by calculated L_∞ error norm at different time level. The results of LOOCV approach is better than PSO approach.

Table 4.1: Comparative analysis of solutions of Example 4.1 with error norm.

Time	**Arora et al. [26]** $(N = 100)$	**Present** $(N = 51)$
t	L_∞	
1	1.69e-04	8.0553e-05
5	6.57e-04	3.8156e-04
10	2.17e-03	1.7590e-03
15	---	4.2000e-03
20	8.26e-03	7.5760e-03

Table 4.2: Comparative analysis of PSO and LOOCV of Example 4.1 by calculated different error norms.

Time	**PSO ($\epsilon = 1$)**	**LOOCV ($\epsilon = 0.051436$)**
t	L_∞	
1	8.0553e-05	8.0091e-05
5	3.8156e-04	3.8471e-04
10	1.7590e-03	1.7641e-03
20	7.5760e-03	7.5851e-03

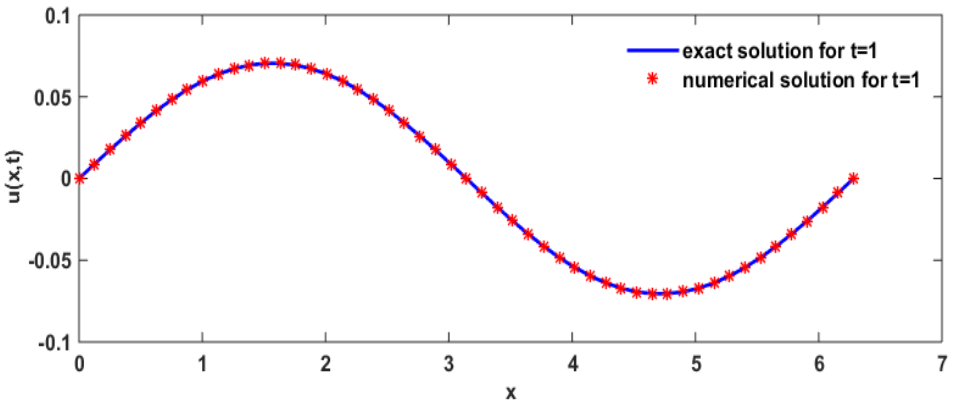

Figure 4.2: The physical representation of comparison of exact and numerical solutions of Example 4.1 for N=51 at t=1.

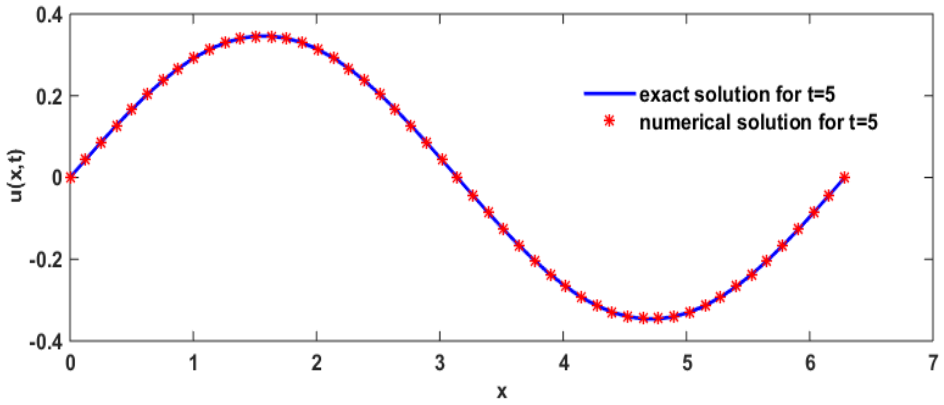

Figure 4.3: The physical representation of comparison of exact and numerical solutions of Example 4.1 for N=51at t=5.

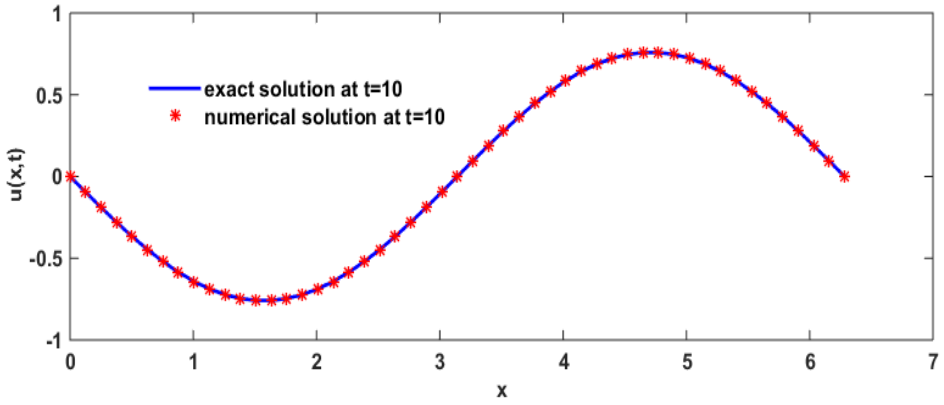

Figure 4.4: The physical representation of comparison of exact and numerical solutions of Example 4.1 for N=51 at t=10.

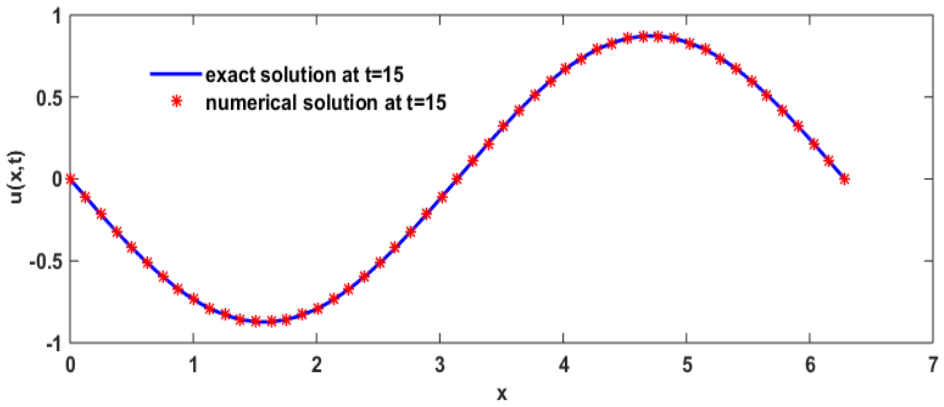

Figure 4.5: The physical representation of comparison of exact and numerical solutions of Example 4.1 for N=51 at t=15.

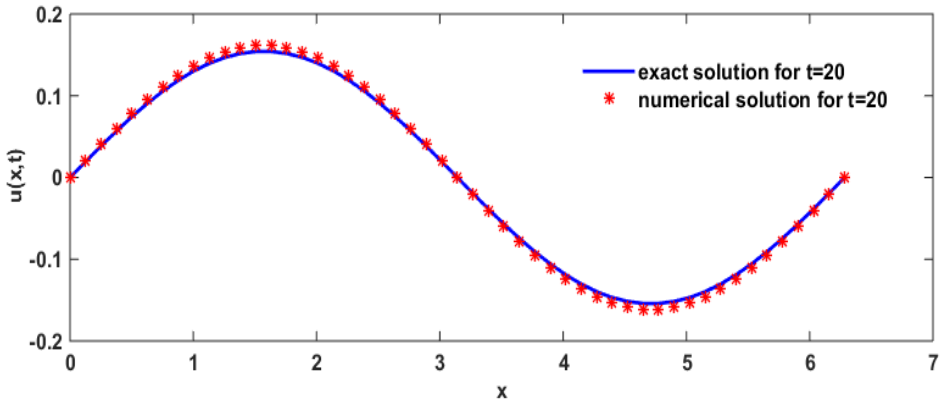

Figure 4.6: The physical representation of comparison of exact and numerical solutions of Example 4.1for N=51 at t=20.

Example 4.2: Consider NLS equation (4.1) with $\alpha = 1,,\ \beta = 2,\ g(x,t) = 0,$

$x \in [-15,15]$ and $t > 0$.

The exact solution is given as [26]:

$u(x,t) = \exp\big(-i(2x + 4 - 3t)\big)\,\mathrm{sech}(x + 2 - 4t),$

with the initial condition: $u(x,0) = \exp\big(-i(2x + 4)\big)\,\mathrm{sech}(x + 2),$

and boundary conditions: $u(-15,t) = 0 = u(15,t).$

The physical representation of comparison of numerical and exact solutions is shown in the figures 4.7-4.9 at different times. The results presented in Table 4.3 has been calculated by L_∞ error norm using $\Delta t = 0.0001$, and $N = 301$ (node points). It can be seen that the present methodology is effective and similar to results reported in the literature, for the ideal value of parameter, $\epsilon = 1.500110$ that has been calculated with the help of PSO approach, which helps to minimize the errors and is comparable to results available in literature [26]. Table 4.4 represents the comparative analysis of PSO and LOOCV with parameter value $\epsilon = 1.500110$ and $\epsilon = 3.000066$ respectively by calculated L_∞ error norm at different time level. The results of LOOCV approach is better than PSO approach.

Table 4.3: Comparative analysis of solutions of Example 4.2 with error norm.

Time	**Arora et al. [26] (N = 200)**	**Present (N= 301)**
t	L_∞	
0.5	2.54e-04	2.7559e-04
1.0	1.97e-04	2.3285e-04
1.5	2.32e-04	1.8752e-04
2.0	3.40e-04	1.4692e-04
2.5	4.49e-04	1.1676e-04
3.0	6.68e-04	2.7559e-04

Table 4.4: Comparative analysis of PSO and LOOCV of Example 4.2 by calculated different error norms.

Time	**PSO ($\epsilon = 1.500110$)**	**LOOCV ($\epsilon = 3.000066$)**
t	L_∞	
0.5	2.7559e-04	2.4820e-04
1.0	2.3285e-04	1.8289e-04
1.5	1.8752e-04	1.3055e-04
2.0	1.4692e-04	1.2879e-04
2.5	1.1676e-04	2.0734e-04
3.0	2.7559e-04	3.1204e-04

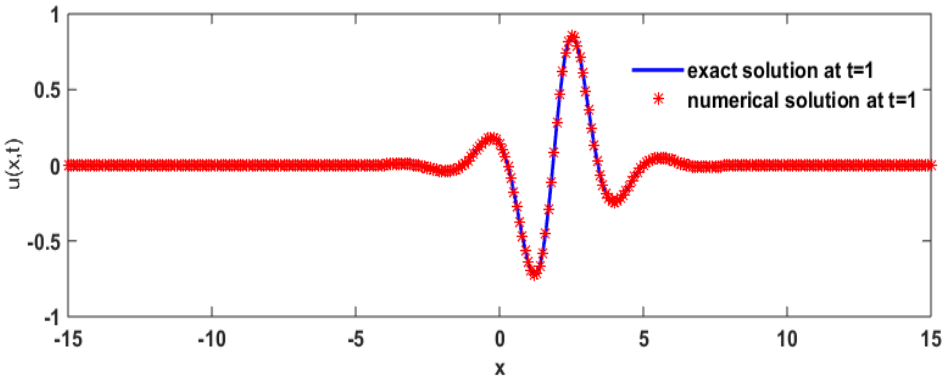

Figure 4.7: The physical representation of comparison of exact and numerical solutions of Example 4.2 for N=301 at t=1.

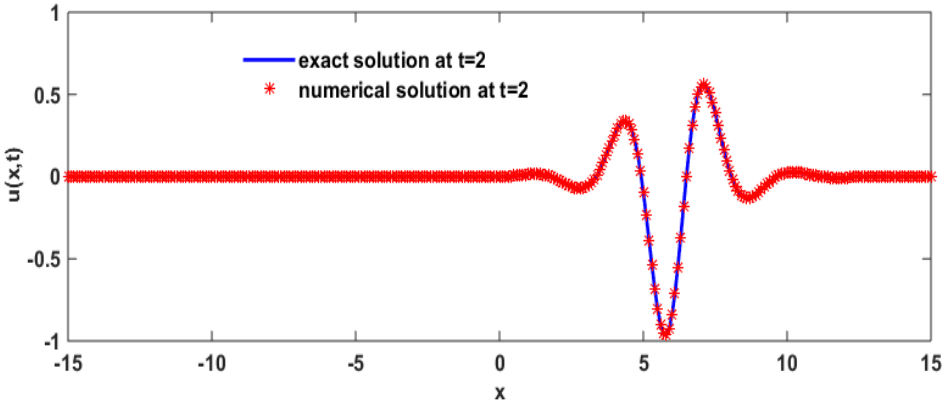

Figure 4.8: The physical representation of comparison of exact and numerical solutions of Example 4.2 for N=301 at t=2.

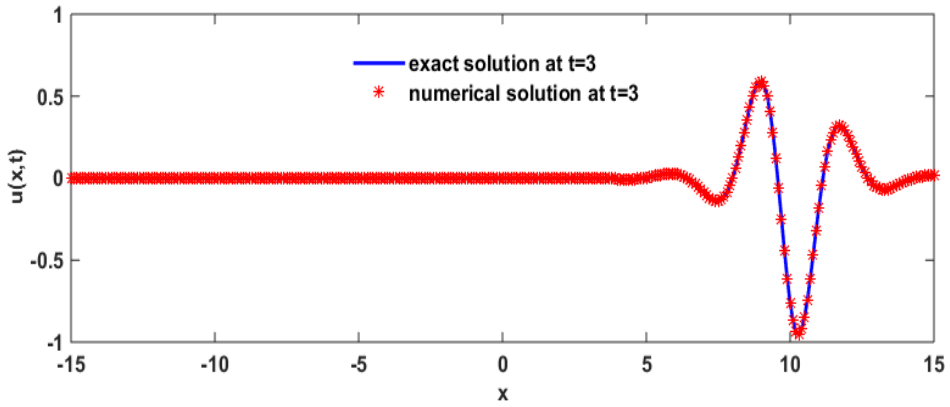

Figure 4.9: The physical representation of comparison of exact and numerical solutions of Example 4.2 for N=301 at t=3.

4.3.2 Implementation of the proposed scheme on numerical of the nonlinear Sine-Gordon equation

The SG equation is given as:

$$u_{tt} + \alpha\, u_t = \beta\ u_{xx} + \eta(x)\sin(u) \qquad (4.2)$$

with the initial conditions:

$$u(x,0) = \phi_1(x)\ and\ u_t(x,0) = \phi_2(x)$$

and values defined at the boundaries.

Here, α and β are real constants and $\eta(x,y)$ parameter depicts the Josephson current density. The constant α represents the dissipative term that plays an important role in converting equation from damped $(\alpha \geq 0)$ to undamped for $(\alpha = 0)$.

Applications and literature review of SG equation is already presented in chapter 3 briefly where this equation is solved numerically by another technique.

Example 4.3: Consider the SG equation (4.2) in domain $x \in [-20,20]$ for $\alpha = 0$, $\beta = 1$ and $\eta(x) = -1$,

with initial conditions:

$$\phi_1(x) = 4\tan^{-1}(c\sinh(\gamma x)),$$

and

$$\phi_2(x) = 0$$

The exact solution of the equation is given by:

$$u(x,t) = 4\tan^{-1}(c\sinh(\gamma x)\,\mathrm{sech}(\gamma c t))$$

here, γ is a parameter that depends on speed of a solitary wave is expressed as:

$$\gamma = \frac{1}{\sqrt{1-c^2}}$$

and the boundary conditions are calculated from exact solutions.

The physical representation of comparison of numerical and exact solutions is shown in the figures 4.10-4.11 at different times. The results are calculated using parameters $c = 0.5, k = 0.001$ and number of node points as $N = 300$. The errors are shown in Table 4.5 and compared with the research findings [102] in order to verify the outcomes. From the results it can be seen that the present methodology is efficient and is comparable to results in literature [102] for the ideal value of parameter, $\epsilon = 1$ that has been calculated with the help of PSO approach which helps to minimize the errors. Table 4.6 displays the rate of convergence of the proposed scheme, evaluated using the L_∞ error norm at different time level. Table 4.7 represents the comparative analysis of L_2, L_∞, and RMS error norms at different time level calculated by PSO and LOOCV with parameter value $\epsilon = 1$ and $\epsilon = 0.011702$ respectively. The results of LOOCV approach is better than PSO approach.

Table 4.5: Comparative analysis of solutions of Example 4.3 with different error norms.

Time	**Present results**			**Mittal and Bhatia** [102]	
t	$\boldsymbol{L_2}$	$\boldsymbol{L_\infty}$	$\boldsymbol{RMS}$	$\boldsymbol{L_2}$	$\boldsymbol{L_\infty}$
1	1.048e-05	6.845e-06	1.652e-06	---	---
2	1.077e-05	7.919e-06	1.698e-06	2.564e-05	1.818e-05
5	1.780e-05	1.415e-05	2.805e-06	---	---
10	3.190e-05	2.047e-05	5.027e-06	8.850e-05	5.228e-05
20	6.289e-05	3.616e-05	9.911e-06	1.713e-04	9.438e-05

Table 4.6: The ROC of numerical scheme with Example 4.3 at t = 1, 2, and 5.

	t=1		t=2		t=5	
N	L_∞	**ROC**	L_∞	**ROC**	L_∞	**ROC**
50	4.48e-03	---	1.81e-02	---	1.97e-02	---
100	6.13e-04	2.870395	6.94e-04	4.708085	1.35e-03	3.864084
200	3.62e-05	4.080218	4.14e-05	4.067404	7.41e-05	4.192326
400	2.16e-06	4.069812	2.52e-06	4.037465	4.49e-06	4.043202

Table 4.7: Comparative analysis of PSO and LOOCV of Example 4.3 by calculated different error norms.

Time	**PSO ($\epsilon = 1$)**			**LOOCV ($\epsilon = 0.011702$)**		
t	L_2	L_∞	***RMS***	L_2	L_∞	***RMS***
1	1.048e-05	6.845e-06	1.652e-06	8.5768e-06	5.6434e-06	1.3516e-06
2	1.077e-05	7.919e-06	1.698e-06	8.3200e-06	6.0814e-06	1.3111e-06
5	1.780e-05	1.415e-05	2.805e-06	1.2807e-05	1.0619e-05	2.0183e-06
10	3.190e-05	2.047e-05	5.027e-06	2.2668e-05	1.4979e-05	3.5722e-06
20	6.289e-05	3.616e-05	9.911e-06	4.4854e-05	2.6284e-05	7.0685e-06

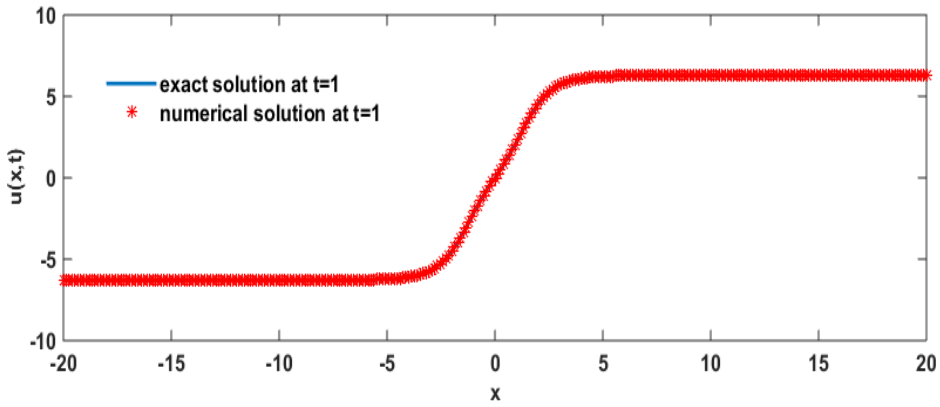

Figure 4.10: The physical representation of comparison of exact and numerical solutions of Example 4.3 for N=301 at t=1.

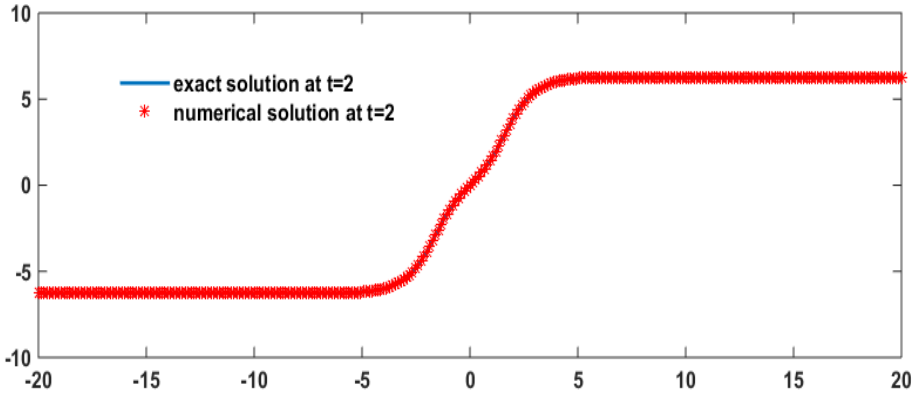

Figure 4.11: The physical representation of comparison of exact and numerical solutions of Example 4.3 for N=301 at t=2.

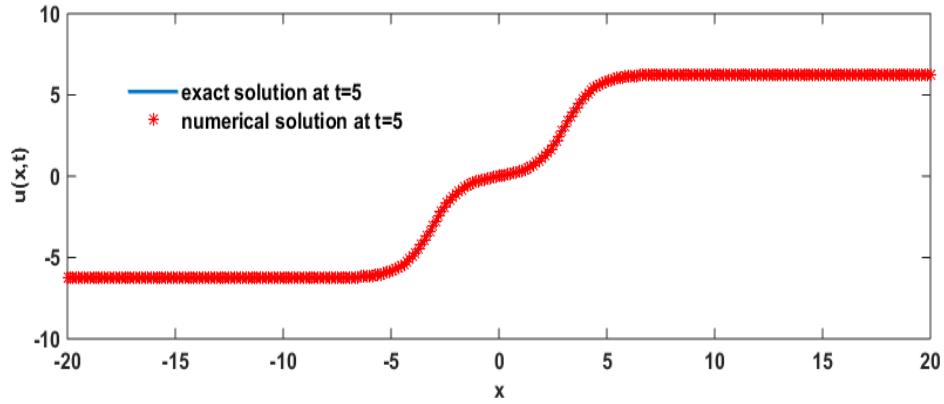

Figure 4.12: The physical representation of comparison of exact and numerical solutions of Example 4.3 for N=301 at t=5.

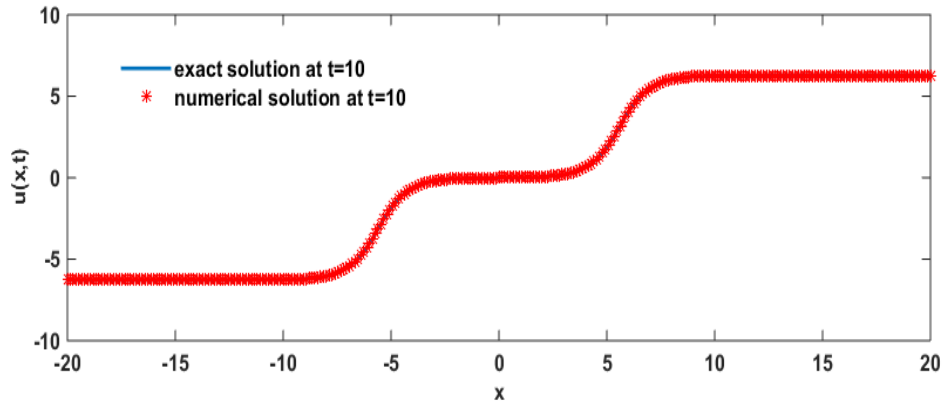

Figure 4.13: The physical representation of comparison of exact and numerical solutions of Example 4.3 for N=301 at t=10.

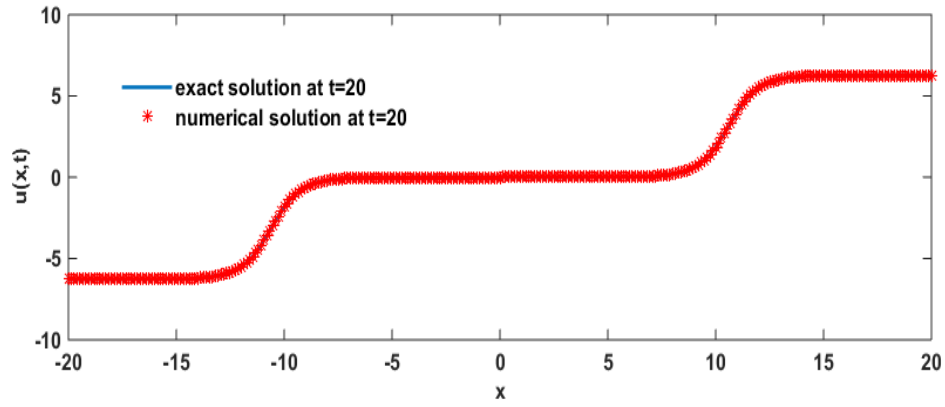

Figure 4.14: The physical representation of comparison of exact and numerical solutions of Example 4.3 for N=301 at t=20.

Example 4.4: Consider the SG equation (4.2) in domain $x \in [-3,3]$ for $\alpha = 0$, $\beta = 1$ and $\eta(x) = -1$,

with initial conditions:

$$\phi_1(x) = 4\tan^{-1}(\exp(\gamma x)),$$

and

$$\phi_2(x) = \frac{-4\gamma \exp(\gamma x)}{1 + \exp(2\gamma x)}$$

The exact solution of the equation is given by:

$$u(x,t) = 4\tan^{-1}\big(\exp\big(\gamma(x - 0.5t)\big)\big)$$

here, γ is a parameter that depends on speed of a solitary wave is expressed as:

$$\gamma = \frac{1}{\sqrt{1 - c^2}}$$

and the boundary conditions are calculated from exact solutions.

The physical representation of comparison of numerical and exact solutions is shown in the figures 4.15-4.16 at different times. The results are calculated using parameters $c = 0.5, k = 0.0001$ and number of node points as $N = 151$. The errors are shown in Table 4.8 and compared with the research findings [102] in order to verify the outcomes. From the results it can be seen that the present methodology is efficient and

is comparable to results in literature [102] for the ideal value of parameter, $\epsilon = 0.557934$ that has been calculated with the help of PSO approach which helps to minimize the errors. Table 4.9 represents the comparative analysis of L_2, L_∞, and RMS error norms at different time level calculated by PSO and LOOCV with parameter value $\epsilon = 0.557934$ and $\epsilon = 0.040996$ respectively. The results of LOOCV approach is better than PSO approach.

Table 4.8: Comparative analysis of solutions of Example 4.4 with different error norms.

Time	**Present results**		**Mittal and Bhatia** [102]	
t	$\boldsymbol{L_2}$	$\boldsymbol{L_\infty}$	$\boldsymbol{L_2}$	$\boldsymbol{L_\infty}$
0.25	6.47e-06	1.37e-05	3.66e-05	4.90e-05
0.50	8.68e-06	1.41e-05	9.00e-05	7.55e-05
0.75	9.99e-06	1.42e-05	1.60e-04	1.43e-04
1.0	1.08e-05	1.41e-05	2.27e-04	2.10e-04

Table 4.9: Comparative analysis of PSO and LOOCV of Example 4.4 by calculated different error norms.

Time	**PSO ($\epsilon = 0.557934$)**		**LOOCV ($\epsilon = 0.040996$)**	
t	$\boldsymbol{L_2}$	$\boldsymbol{L_\infty}$	$\boldsymbol{L_2}$	$\boldsymbol{L_\infty}$
0.25	6.47e-06	1.37e-05	6.4671e-06	1.3759e-05
0.50	8.68e-06	1.41e-05	8.6897e-06	1.4149e-05
0.75	9.99e-06	1.42e-05	9.9927e-06	1.4242e-05
1.0	1.08e-05	1.41e-05	1.0807e-05	1.4056e-05

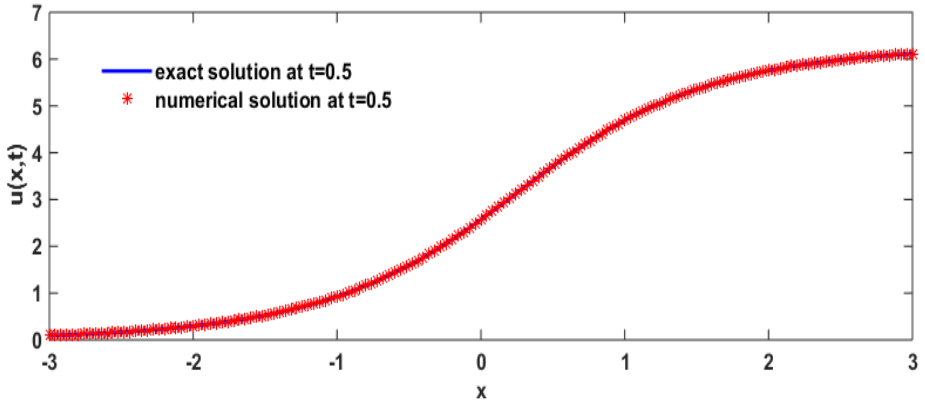

Figure 4.15: The physical representation of comparison of exact and numerical solutions of Example 4.4 for N=151 at t=0.5.

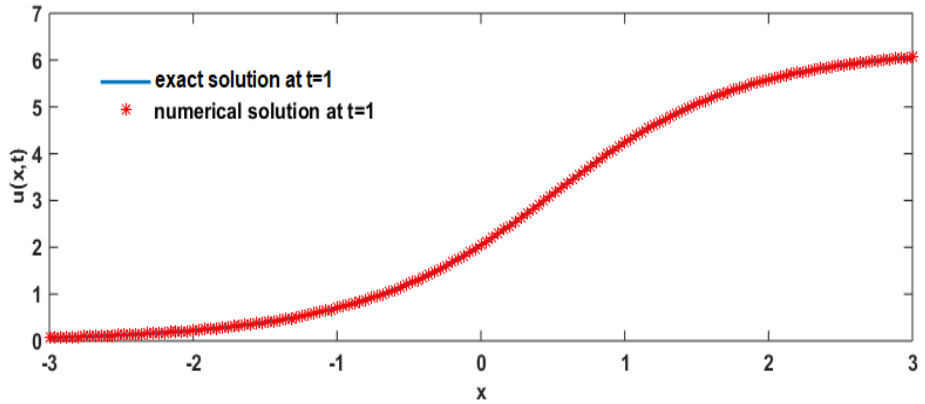

Figure 4.16: The physical representation of comparison of exact and numerical solutions of Example 4.4 for N=151 at t=1.

Example 4.5: Consider the SG equation (4.2) in domain $x \in [-20,20]$ for $\alpha = 0$, $\beta = 1$ and $\eta(x) = -1$,

with initial conditions:

$$\phi_1(x) = 4\tan^{-1}(\exp(\gamma x)),$$

and

$$\phi_2(x) = \frac{-4\gamma c exp(\gamma x)}{1+\exp(2\gamma x)}$$

The exact solution of the equation is given by:

$$u(x,t) = 4\tan^{-1}\big(\exp\big(\gamma(x-ct)\big)\big)$$

here, γ is a parameter that depends on speed of a solitary wave is expressed as:

$$\gamma = \frac{1}{\sqrt{1-c^2}}$$

and the boundary conditions are calculated from exact solutions.

The physical representation of comparison of numerical and exact solutions is shown in the figures 4.17-4.20 at different times. The results are calculated using parameters $c = 0.5, k = 0.01$ and number of node points as $N = 501$. The errors are shown in Table 4.10 and compared with the research findings [150] in order to verify the outcomes. From the results it can be seen that the present methodology is efficient and is comparable to results in literature [150] for the ideal value of parameter, $\epsilon = 0.1000$ that has been calculated with the help of PSO approach which helps to minimize the errors. Table 4.11 displays the rate of convergence of the proposed scheme, evaluated using the L_∞ error norm at different time level. Table 4.12 represents the comparative analysis of $L_2, L_\infty,$ and RMS error norms at different time level calculated by PSO and LOOCV with parameter value $\epsilon = 0.1000$ and $\epsilon = 0.012557$ respectively. The results of LOOCV approach is better than PSO approach.

Table 4.10: Comparative analysis of solutions of Example 4.5 with different error norms.

Time	**Present results**			**Shiralizadeh et al.** [150]		
t	L_2	L_∞	RMS	L_2	L_∞	RMS
0.25	1.1224e-07	1.2635e-07	7.9048e-10	1.1209e-07	1.2617e-07	1.7688e-08
0.50	3.5709e-07	3.9989e-07	2.5149e-09	3.5654e-07	3.9927e-07	5.6261e-08
0.75	5.6940e-07	6.3980e-07	4.0102e-09	5.6832e-07	6.3866e-07	8.9680e-08
1	7.0450e-07	8.2380e-07	4.9617e-09	7.0289e-07	8.2197e-07	1.1092e-07
2	1.0006e-06	1.1872e-06	7.0471e-09	9.9756e-07	1.1835e-06	1.5741e-07
5	1.6399e-06	1.4628e-06	1.1549e-08	1.6328e-06	1.4574e-06	2.5765e-07
10	3.2316e-06	2.7776e-06	2.2760e-08	3.2190e-06	2.7674e-06	5.0795e-07
15	5.2932e-06	4.3000e-06	3.7280e-08	5.2748e-06	4.2855e-06	8.3235e-07
20	7.9080e-06	6.1593e-06	5.5695e-08	7.8827e-06	6.1400e-06	1.2439e-06

Table 4.11: The ROC of numerical scheme with Example 4.5 at t = 1, 2, and 5.

	t=1		t=2		t=5	
N	L_∞	**ROC**	L_∞	**ROC**	L_∞	**ROC**
50	1.45e-02	---	2.61e-02	---	3.27e-02	---
100	5.95e-04	4.604882	9.34e-04	4.806783	9.14e-04	5.161404
200	3.42e-05	4.122454	4.82e-05	4.276137	5.47e-05	4.063054
400	2.07e-06	4.040960	2.94e-06	4.036637	3.45e-06	3.985120

Table 4.12: Comparative analysis of PSO and LOOCV of Example 4.5 by calculated different error norms.

Time	**PSO ($\epsilon = 0.1000$)**			**LOOCV ($\epsilon = 0.012557$)**		
t	L_2	L_∞	RMS	L_2	L_∞	RMS
0.25	1.1224e-07	1.2635e-07	7.9048e-10	2.4100e-04	1.1894e-04	1.0778e-05
0.50	3.5709e-07	3.9989e-07	2.5149e-09	3.4300e-04	1.2227e-04	1.5339e-05
0.75	5.6940e-07	6.3980e-07	4.0102e-09	4.1281e-04	1.2225e-04	1.8461e-05
1	7.0450e-07	8.2380e-07	4.9617e-09	4.6189e-04	1.2046e-04	2.0657e-05
2	1.0006e-06	1.1872e-06	7.0471e-09	5.1809e-04	1.1437e-04	2.3170e-05
5	1.6399e-06	1.4628e-06	1.1549e-08	4.3038e-04	1.3423e-04	1.9247e-05
10	3.2316e-06	2.7776e-06	2.2760e-08	5.1966e-04	1.7801e-04	2.3240e-05
15	5.2932e-06	4.3000e-06	3.7280e-08	6.5199e-04	2.3543e-04	2.9158e-05
20	7.9080e-06	6.1593e-06	5.5695e-08	8.4070e-04	3.1339e-04	3.7579e-05

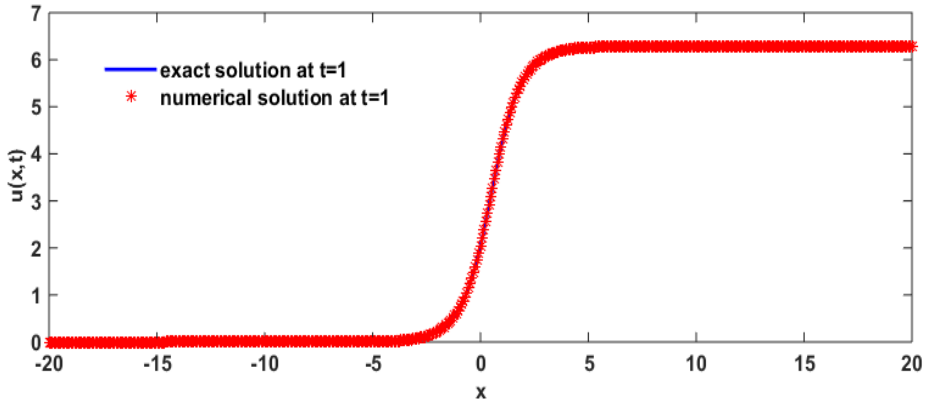

Figure 4.17: The physical representation of comparison of exact and numerical solutions of Example 4.5 for N=501 at t=1.

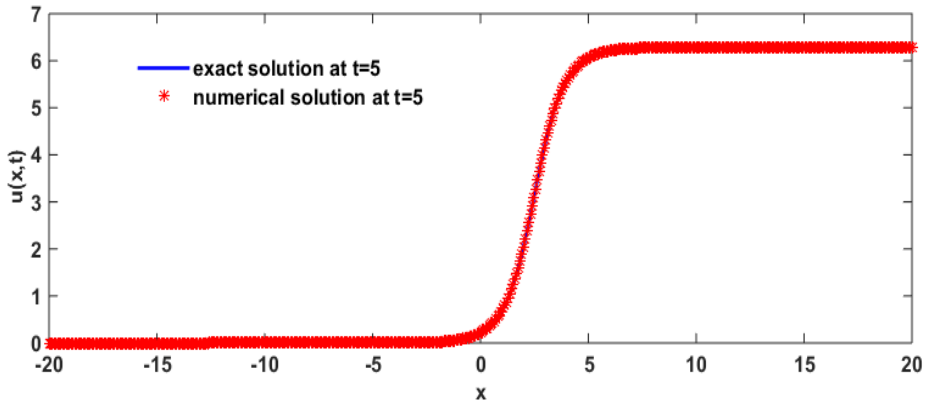

Figure 4.18: The physical representation of comparison of exact and numerical solutions of Example 4.5 for N=501 at t=5.

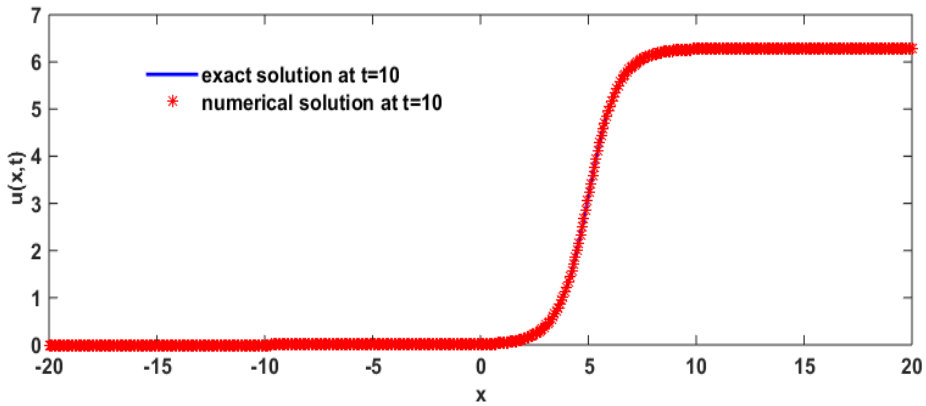

Figure 4.19: The physical representation of comparison of exact and numerical solutions of Example 4.5 for N=501 at t=10.

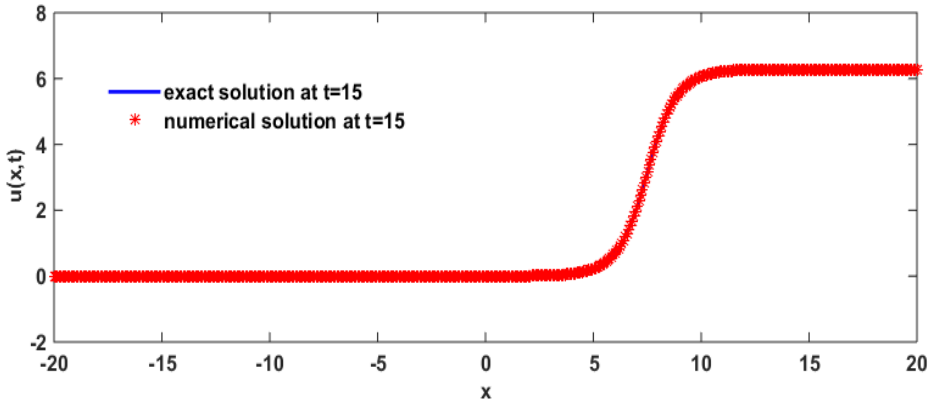

Figure 4.20: The physical representation of comparison of exact and numerical solutions of Example 4.5 for N=501 at t=15.

Example 4.6: Consider the SG equation (4.2) in domain $x \in [-20,20]$ for $\alpha = 0$, $\beta = 1$ and $\eta(x) = -1$,

with initial conditions:

$$\phi_1(x) = 4\tan^{-1}(\exp(\gamma x)),$$

and

$$\phi_2(x) = \frac{-4\gamma c exp(\gamma x)}{1+\exp(2\gamma x)}$$

The exact solution of the equation is given:

$$u(x,t) = 4\tan^{-1}\big(\exp\big(\gamma(x-ct)\big)\big)$$

here, γ is a parameter that depends on speed of a solitary wave is expressed as:

$$\gamma = \frac{-1}{\sqrt{1-c^2}}$$

and the boundary conditions are calculated from exact solutions.

The physical representation of comparison of numerical and exact solutions is shown in the figures 4.21-4.24 at different times. The results are calculated using parameters $c = 0.95, k = 0.01$ and number of node points as $N = 501$. The errors are shown in Table 4.13 and compared with the research findings [147] in order to verify the outcomes. From the results it can be seen that the present methodology is efficient and is comparable to results in literature [150] for the ideal value of parameter, $\epsilon = 1.0000$ that has been calculated with the help of PSO approach which helps to

minimize the errors. Table 4.14 represents the comparative analysis of $L_2, L_\infty,$ and RMS error norms at different time level calculated by PSO and LOOCV with parameter value $\epsilon = 1.0000$ and $\epsilon = 0.012557$ respectively. The results of LOOCV approach is better than PSO approach.

Table 4.13: Comparative analysis of solutions of Example 4.6 with different error norms.

Time	**Present results**			**Shiralizadeh et al.** [150]		
t	L_2	L_∞	RMS	L_2	L_∞	RMS
0.25	1.8083e-05	3.5466e-05	1.2735e-07	3.9330e-04	1.3086e-04	1.7589e-05
0.50	3.2542e-05	7.1808e-05	2.2919e-07	4.9815e-04	1.4274e-04	2.2278e-05
0.75	4.8376e-05	1.0762e-04	3.4070e-07	5.9493e-04	1.9470e-04	2.6606e-05
1	6.4267e-05	1.4344e-04	4.5263e-07	7.0399e-04	2.5476e-04	3.1483e-05
5	3.1211e-04	6.2588e-04	2.1982e-06	1.2000e-03	5.1335e-04	5.1525e-05
10	6.2221e-04	8.4379e-04	4.3821e-06	3.2000e-03	1.4000e-03	1.4163e-04
15	9.0612e-04	1.2000e-03	6.3817e-06	7.4000e-03	2.6000e-03	3.3026e-04
20	2.3000e-03	4.9000e-03	1.5891e-05	1.2000e-03	4.9000e-03	5.3738e-04

Table 4.14: Comparative analysis of PSO and LOOCV of Example 4.6 by calculated different error norms.

Time	**PSO ($\epsilon = 0.10000$)**			**LOOCV ($\epsilon = 0.012557$)**		
t	L_2	L_∞	RMS	L_2	L_∞	RMS
0.25	1.8083e-05	3.5466e-05	1.2735e-07	1.7667e-05	3.4727e-05	1.2443e-07
0.50	3.2542e-05	7.1808e-05	2.2919e-07	3.1706e-05	6.9928e-05	2.2330e-07
0.75	4.8376e-05	1.0762e-04	3.4070e-07	4.7193e-05	1.0470e-04	3.3238e-07
1	6.4267e-05	1.4344e-04	4.5263e-07	6.2698e-05	1.3951e-04	4.4158e-07
5	3.1211e-04	6.2588e-04	2.1982e-06	3.0092e-04	6.0438e-04	2.1193e-06
10	6.2221e-04	8.4379e-04	4.3821e-06	5.9195e-04	8.0423e-04	4.1690e-06
15	9.0612e-04	1.2000e-03	6.3817e-06	8.6128e-04	1.1118e-03	6.0659e-06
20	2.3000e-03	4.9000e-03	1.5891e-05	2.2213e-03	4.8656e-03	1.5644e-05

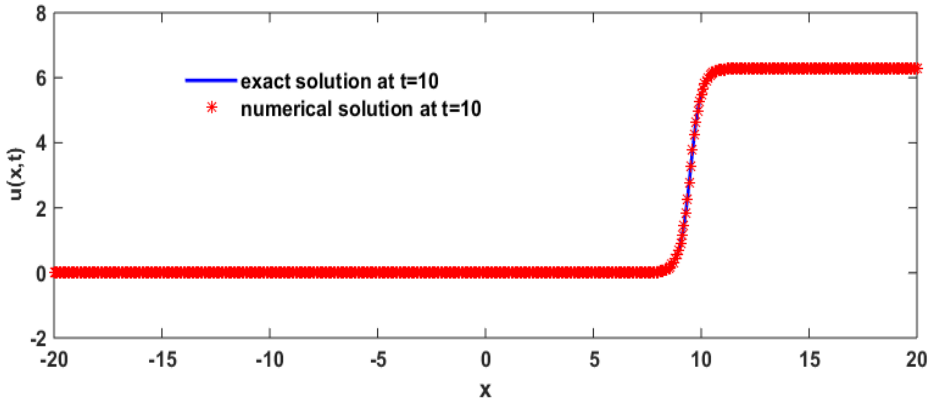

Figure 4.21: The physical representation of comparison of exact and numerical solutions of Example 4.6 for N=501 at t=1.

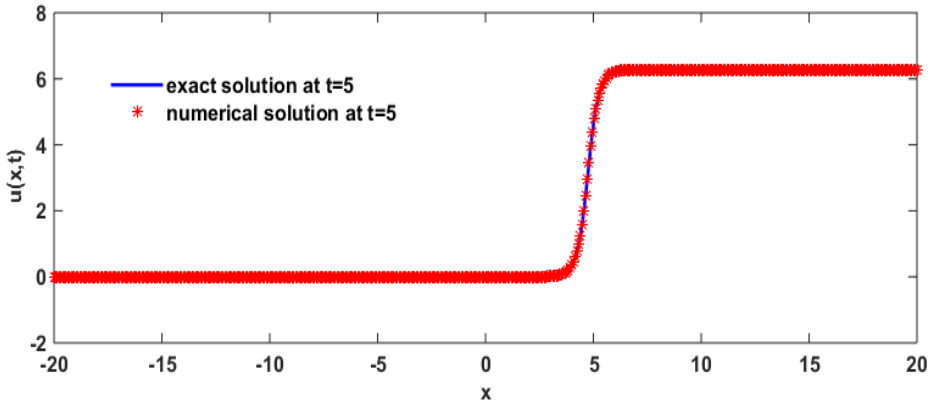

Figure 4.22: The physical representation of comparison of exact and numerical solutions of Example 4.6 for N=501 at t=5.

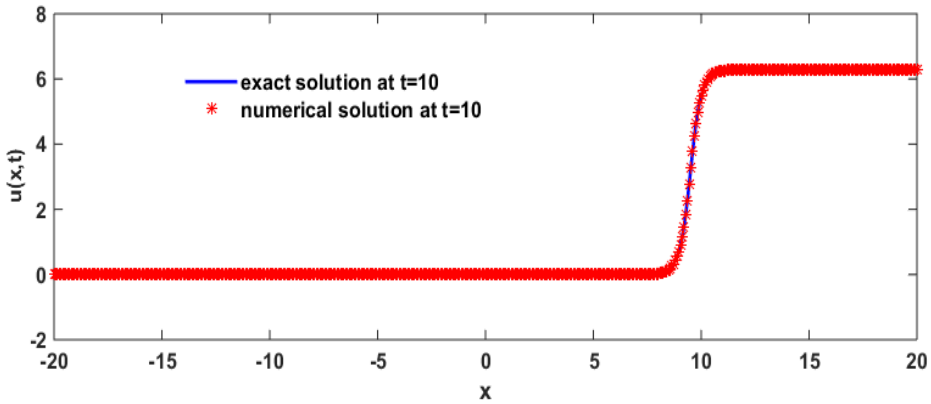

Figure 4.23: The physical representation of comparison of exact and numerical solutions of Example 4.6 for N=501 at t=10.

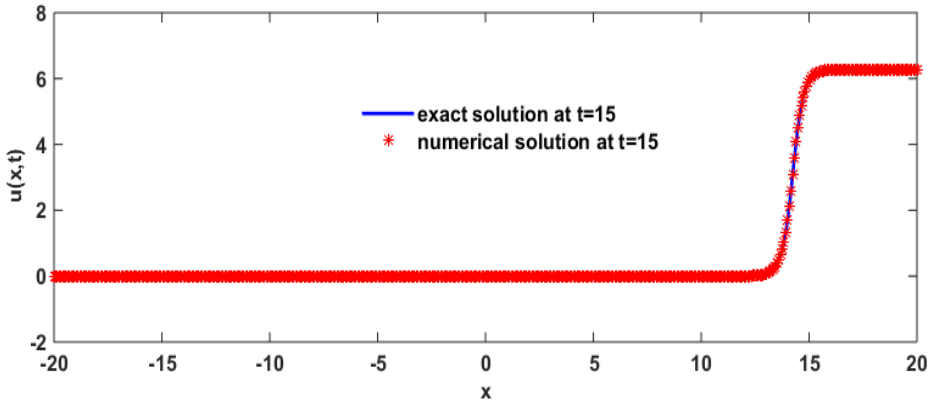

Figure 4.24: The physical representation of comparison of exact and numerical solutions of Example 4.6 for N=501 at t=15.

Example 4.7: Consider the SG equation (4.2) in domain $x \in [-10,10]$ for $\alpha = 0$, $\beta = 1$ and $\eta(x) = -1$,

with initial conditions:

$$\phi_1(x) = 0,$$

and

$$\phi_2(x) = 4\,\mathrm{sech}(x)$$

The exact solution of the equation is given by:

$$u(x,t) = 4\tan^{-1}(\mathrm{sech}(x)\,t)$$

and the boundary conditions are calculated from exact solutions.

The physical representation of comparison of numerical and exact solutions is shown in the figures 4.25-4.28 at different times. The results are calculated using parameters $k = 0.01$ and number of node points as $N = 401$. The errors are shown in Table 4.15 and compared with the research findings [150] in order to verify the outcomes. From the results it can be seen that the present methodology is efficient and is comparable to results in literature [150] for the ideal value of parameter, $\epsilon = 0.096455$ that has been calculated with the help of PSO approach which helps to minimize the errors. Table 4.16 represents the comparative analysis of $L_2, L_\infty,$ and RMS error norms at different time level calculated by PSO and LOOCV with parameter value $\epsilon = 0.096455$. and $\epsilon = 0.999934$ respectively. The results of LOOCV approach is better than PSO approach.

Table 4.15: Comparative analysis of solutions of Example 4.7 with different error norms.

Time	**Present results**			**Shiralizadeh et al.** [150]		
t	L_2	L_∞	RMS	L_2	L_∞	RMS
0.25	1.9450e-06	3.6320e-06	2.1638e-08	1.4400e-04	3.0169e-05	7.1908e-06
0.50	2.5475e-06	3.6320e-06	2.8340e-08	2.4339e-04	4.6806e-05	1.2154e-05
0.75	2.9747e-06	3.6320e-06	3.3093e-08	3.0422e-04	5.1706e-05	1.5192e-05
1	3.2771e-06	3.6320e-06	3.6457e-08	3.5484e-04	5.2994e-05	1.7720e-05
2	3.5973e-06	3.6320e-06	4.0019e-08	6.7163e-04	7.8976e-05	3.3540e-05
5	2.9320e-06	3.6320e-06	3.2618e-08	3.0000e-03	3.2159e-04	1.4923e-04
10	3.7994e-06	3.6320e-06	4.2267e-08	1.2600e-02	1.4000e-03	6.2974e-04
15	6.2894e-06	3.6320e-06	6.9968e-08	2.8900e-02	3.2000e-03	1.4000e-03
20	1.0231e-05	4.8680e-06	1.1381e-07	5.1700e-02	5.8000e-03	2.6000e-03

Table 4.16: Comparative analysis of PSO and LOOCV of Example 4.7 by calculated different error norms.

Time	**PSO ($\epsilon = 0.096455$)**			**LOOCV ($\epsilon = 0.999934$)**		
t	L_2	L_∞	RMS	L_2	L_∞	RMS
0.25	1.9450e-06	3.6320e-06	2.1638e-08	1.9450e-06	3.6320e-06	4.3383e-07
0.50	2.5475e-06	3.6320e-06	2.8340e-08	2.5475e-06	3.6320e-06	5.6822e-07
0.75	2.9747e-06	3.6320e-06	3.3093e-08	2.9748e-06	3.6320e-06	6.6354e-07
1	3.2771e-06	3.6320e-06	3.6457e-08	3.2777e-06	3.6320e-06	7.3108e-07
2	3.5973e-06	3.6320e-06	4.0019e-08	3.6014e-06	3.6320e-06	8.0328e-07
5	2.9320e-06	3.6320e-06	3.2618e-08	2.9577e-06	3.6320e-06	6.5971e-07
10	3.7994e-06	3.6320e-06	4.2267e-08	4.0544e-06	3.6320e-06	9.0432e-07
15	6.2894e-06	3.6320e-06	6.9968e-08	7.0675e-06	3.6320e-06	1.5764e-06
20	1.0231e-05	4.8680e-06	1.1381e-07	1.1713e-05	5.6180e-06	2.6126e-06

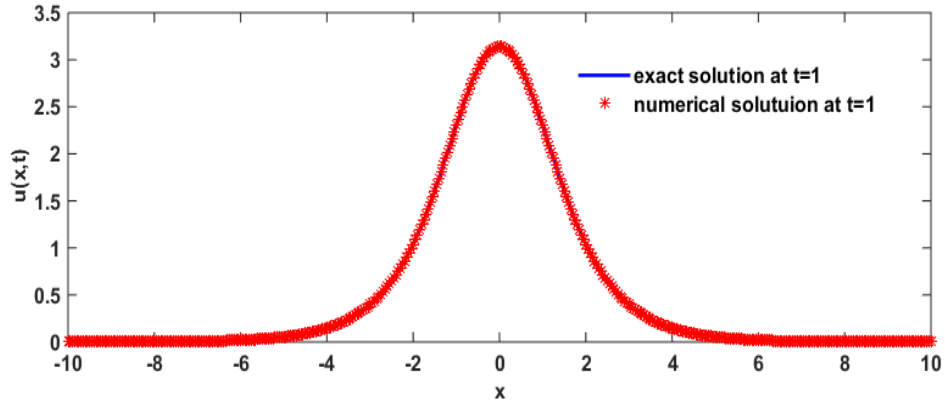

Figure 4.25: The physical representation of comparison of exact and numerical solutions of Example 4.7 for N=401 at t=1.

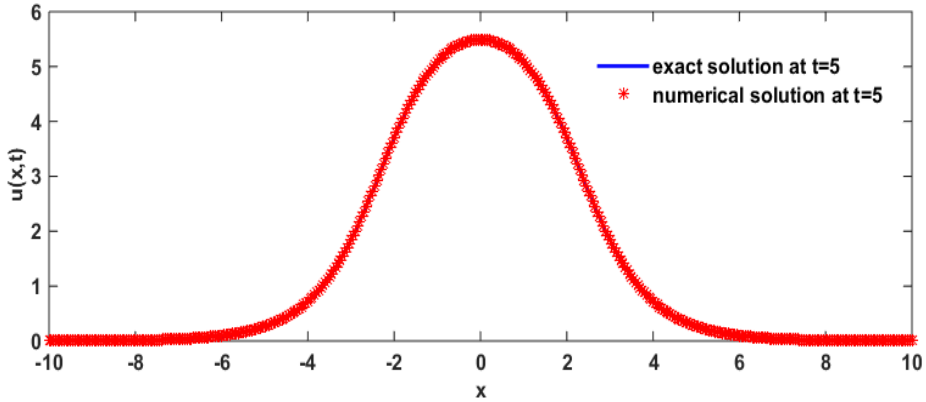

Figure 4.26: The physical representation of comparison of exact and numerical solutions of Example 4.7 for N=401 at t=5.

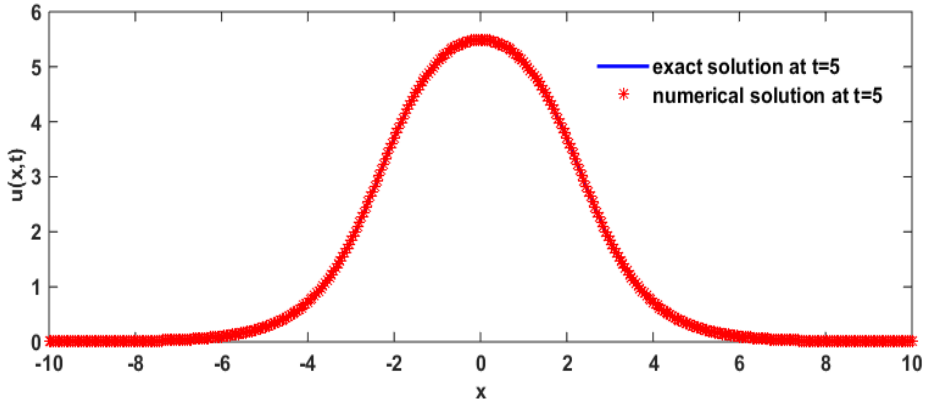

Figure 4.27: The physical representation of comparison of exact and numerical solutions of Example 4.7 for N=401 at t=10.

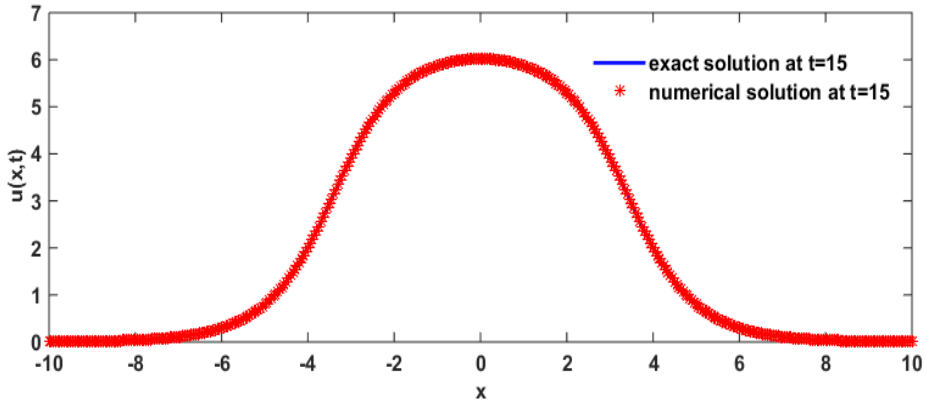

Figure 4.28: The physical representation of comparison of exact and numerical solutions of Example 4.7 for N=401 at t=15.

Example 4.8: Consider the SG equation (4.2) in domain $x \in [-2,2]$ for $\alpha = 0$, $\beta = 1$ and $\eta(x) = -1$,

with initial conditions:

$$\phi_1(x) = 0,$$

and

$$\phi_2(x) = 4\,\mathrm{sech}(x)$$

The exact solution of the equation is given by:

$$u(x,t) = 4\tan^{-1}(\mathrm{sech}(x)\,t)$$

and the boundary conditions are calculated from exact solutions.

The physical representation of comparison of numerical and exact solutions is shown in the figures 4.29-4.32 at different times. The results are calculated at $k = 0.0001$ and number of node points as $N = 101$. The errors are shown in Table 4.17 and compared with the research findings [27] in order to verify the outcomes. From these results it can be seen that the present methodology is efficient and is comparable to results in literature [27] for the ideal value of parameter, $\epsilon = 0.999934$ that has been calculated with the help of PSO approach which helps to minimize the errors. Table 4.18 represents the comparative analysis of $L_2, L_\infty,$ and RMS error norms at different time levels calculated by PSO and LOOCV with parameter value $\epsilon = 0.999934$ and

$\epsilon = 0.999934$ respectively. In this example the parameter value is same even after applying two different techniques which means that the value is the best value of this parameter in this range.

Table 4.17: Comparative analysis of solutions of Example 4.8 with different error norms.

Time	**Present results**			**Arora et al.** [27]		
t	L_2	L_∞	***RMS***	L_2	L_∞	***RMS***
0.3	5.5495e-05	1.0565e-04	2.7203e-06	5.55e-05	1.05e-04	2.72e-06
0.6	6.6122e-05	1.0368e-04	3.2413e-06	6.61e-05	1.03e-04	3.24e-06
1	7.0831e-05	7.0831e-05	3.4721e-06	7.08e-05	9.93e-05	3.47e-06
1.5	7.6553e-05	9.1739e-05	3.7901e-05	---	---	---
2	8.7983e-05	8.2896e-05	4.3129e-06	---	---	---

Table 4.18: Comparative analysis of PSO and LOOCV of Example 4.8 by calculated different error norms.

Time	**PSO ($\epsilon = 0.999934$)**			**LOOCV ($\epsilon = 0.999934$)**		
t	L_2	L_∞	***RMS***	L_2	L_∞	***RMS***
0.3	5.5495e-05	1.0565e-04	2.7203e-06	5.5495e-05	1.0565e-04	2.7474e-05
0.6	6.6122e-05	1.0368e-04	3.2413e-06	6.6124e-05	1.0368e-04	3.2736e-05
1	7.0831e-05	7.0831e-05	3.4721e-06	7.0836e-05	9.9306e-05	3.5069e-05
1.5	7.6553e-05	9.1739e-05	3.7901e-05	7.6557e-05	9.1739e-05	3.7901e-05
2	8.7983e-05	8.2896e-05	4.3129e-06	8.7977e-05	8.2896e-05	4.3555e-05

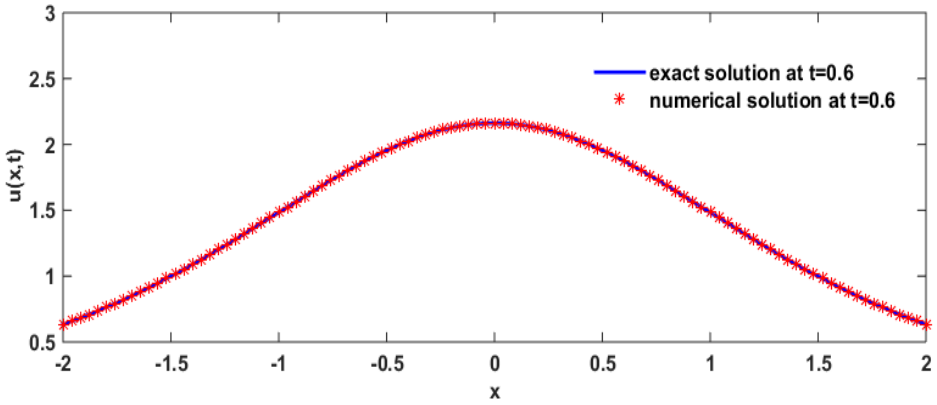

Figure 4.29: The physical representation of comparison of exact and numerical solutions of Example 4.8 for N=101 at t=0.6.

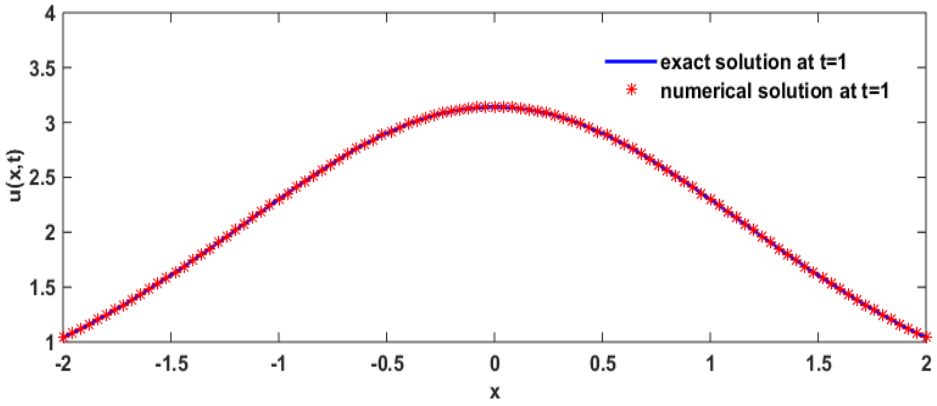

Figure 4.30: The physical representation of comparison of exact and numerical solutions of Example 4.8 for N=101 at t=1.

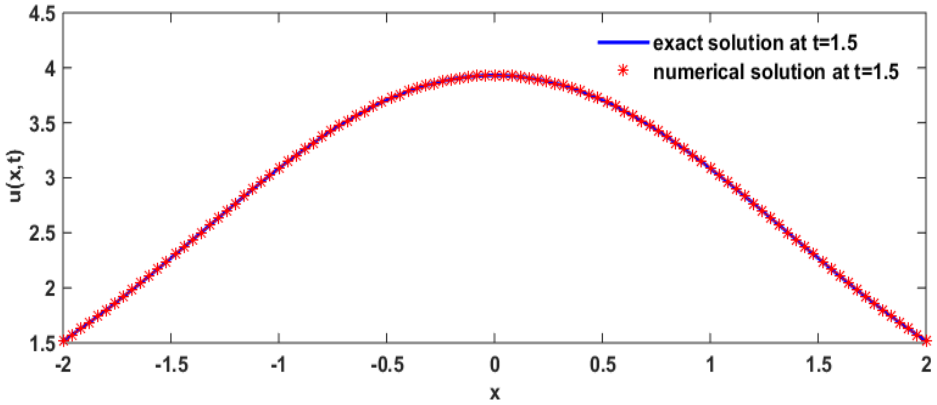

Figure 4.31: The physical representation of comparison of exact and numerical solutions of Example 4.8 for N=101 at t=1.5.

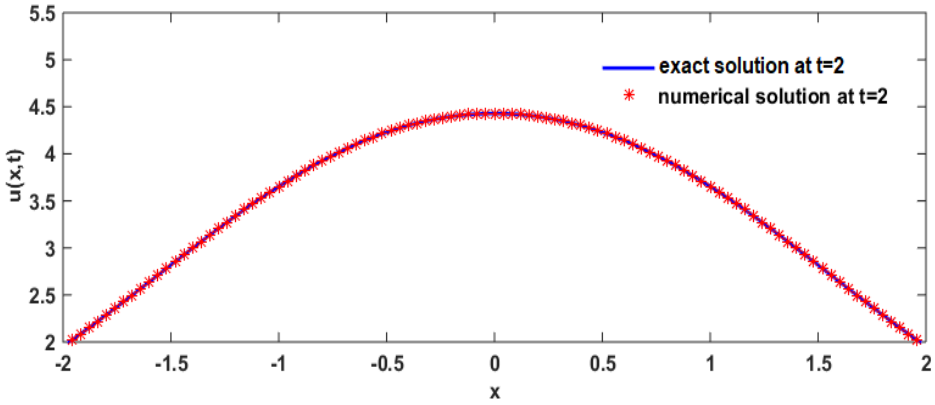

Figure 4.32: The physical representation of comparison of exact and numerical solutions of Example 4.8 for N=101 at t=2.

LOOCV and PSO are two different types of techniques. LOOCV serves as a model evaluation method, whereas PSO works as an optimization algorithm. Furthermore, the working processes of the techniques is also different, LOOCV computes the average performance for the final result, while PSO identifies the optimal value based on the best performance. Although the results obtained from both techniques are approximately similar, but also the LOOCV outcomes exhibit a slight superior, as shown in the comparison tables represented in this chapter.

4.4 Summary

This chapter presents an impressive approach to find solutions of the NLEEs using the "Exponential modified cubic B-spline differential quadrature method with PSO technique". In this chapter, the exponential modified differential quadrature method is combined with the PSO technique. Using the PSO approach, the optimal value of the parameter associated with the basis functions is estimated, to improve the accuracy of results of present method. PSO is an efficient and effective global optimization method that has been successfully applied in various fields, including engineering, smart cities, healthcare, the environment, industry, and business.

The proposed approach has been used to find soliton solutions of two important nonlinear evolutionary equations (NLS equation and SG equation), numerically. That demonstrated to be highly accurate and effective by calculating the error norms test L_2, L_∞, and RMS. The numerical solutions obtained using this combined

methodology are very close to the exact solution and are comparable to other numerical approaches that have been published previously, the results are shown in form of figures and tables. The rate of convergence of the numerical scheme is also calculated by the L_∞ error norm, which is on an average 4. It seems that the proposed approach has a fast convergence rate.

The success of this combined methodology, makes it an attractive research idea for future studies. The PSO-based method is capable of assessing the parameter in a search space that allows for global search.

Chapter-5

Role of soliton solutions of mathematical equations in optical fiber communication and Josephson junctions

5.1 Introduction

NLS equation, and SG equation are two important nonlinear evolutionary equations. One of the most interesting features of these two equations is the existence of soliton solutions, which are localized, stable, and nonlinear waves that propagate without dispersion. These equations are used in many mathematical models because of important properties of solutions. The important applications and literature review of these equations have been discussed briefly in chapter 3.

This chapter is divided into two parts: in the first part a brief discussion is done about the importance of optical fiber communications and Josephson junction is discussed in the second part. Optical fibers are related to the soliton solutions of the NLS equation to function correctly. Optical solitons have the remarkable ability to propagate over long distances without dispersion. This property makes them an interesting subject of study in optical fiber communication.

Josephson junctions, on the other hand, depend on soliton solutions of the SG equation to operate effectively. These electronic components are essential to a wide range of modern technological devices, including quantum computers, voltage standards, sensors, and high-speed digital circuits.

5.2 Brief study of one of important applications of nonlinear Schrödinger equation

5.2.1. Introduction to optical fiber communication

In earlier times many countries were dependent on industrial era. But with the changes from industrial era to informational era, there comes the need of information. The necessity of information generates for its transition/delivery which can be effectively utilized when used in correct place, time and form. This succeeds

telecommunication in to picture which infers that communication technology is one of the best prevailing technologies which use light for its communication due to its amazing speed because of the well-known fact that light travels faster than everything.

In today's era, people heavily rely on wireless communication networks such as the internet on mobile phones, e-shopping, e-business, and downloading large files, which demand high bandwidth for information transmission. Optical fiber communication (OFC) is an ideal solution to meet these requirements. OFC offers the advantage of fast transmission speed, as fast as that of light, which is much faster than any other communication mode. Additionally, OFC travels faster than copper cable communication. However, one of the significant issues with OFC is its dispersion. The more dispersion occurs, the lower the quality achieved or received because the pulses travelling in optical fibers scatter and interfere with each other after a certain time. This reduces the reliability of carrying information. While several fibers can reduce dispersion, none of them can entirely eliminate it. Here the optical soliton comes in to picture, which is invented by using setup of electromagnetic dispersion in anomalous regime with nonlinear effect known as self-phase modulation. Soliton do not disperse and when it encounters with a perturbation, it usually leaves behind the soliton unaltered. One of the best methods for favorable outcome of communication without dispersion is optical soliton. The equation of nonlinear Schrödinger is the perfect equation for narrating the propagation of light in optical fibers [103].

5.2.2. Role of Nonlinear Schrödinger equation

The NLS equation is a fundamental equation in optical fiber communication that describes the propagation of optical pulses in an optical fiber, accounting for the effects of dispersion and nonlinearity. The NLS equation is used to model and analyze the behavior of light waves in optical fibers, including different fiber types, laser sources, and modulation schemes [162-166]. The NLS equation enables researchers and engineers to optimize optical fiber communication systems by predicting their performance and minimizing dispersion while maximizing bandwidth. Recently, Alharbi et al. [162] presented new and effective solitary applications in the Schrödinger equation using the Brownian motion process with physical coefficients of

fiber optics. One critical application of the NLS equation in optical fiber communication is the soliton solution [129, 163]. Solitons are self-reinforcing solitary waves that can travel long distances without dispersion or distortion. Solitons are generated through the balance between the dispersive and nonlinear effects of the fiber. In optical fiber communication systems, solitons can transmit information over long distances without distortion or loss of signal quality.

The soliton solution of the NLS equation is directly proportional to the fiber's dispersion and the pulse's power, enabling efficient transmission of high-speed data and high-bandwidth applications. Solitons in optical fibers have revolutionized the field of communication, making it possible to support high-bandwidth applications such as video streaming, cloud computing, and telemedicine.

In summary, the NLS equation and its soliton solution play crucial roles in optical fiber communication. The NLS equation enables the optimization of communication systems by predicting their behavior and minimizing dispersion while maximizing bandwidth. The soliton solution of the NLS equation allows for the efficient transmission of high-speed data over long distances without distortion or loss of signal quality, making it a preferred solution for high-bandwidth applications.

5.2.3. Optical Soliton

The best characteristic of solitary wave is that they remain intact in their shape and velocity even if they collide with each other. It does not terminate, outstretch or loose firmness over distance which makes it productive in used for fiber optic communication networks. Now, optical soliton is finally enumerated as a pulse which can travel several miles along with information which can be carried out without dispersion. The nonlinear regime can only perceive such solitons.

5.2.4. Optical Fiber Communication (OFC)

In optical fiber communication system, the input can first encoded in to a binary sequence of electrical pulse which can be stimulated to moderate laser beam which can give rise to a sequence of zeros and ones which shows absence and presence of light respectively. In this the rate of transfer of information is expressed as bit rate which means number of bits transferred per second.

Fiber optic communication technology has become ubiquitous in today's life, finding use in a variety of fields such as telephone communication, television broadcasting, fax transmission, banking transactions via ATMs, and internet browsing. This technology is highly efficient in handling two-way communication traffic, enabling seamless and reliable communication across various applications.

It has advantage over copper wire (both twisted paid and coaxial). Optical fiber has technological superiority and has 10000 time more bandwidth than that of coaxial cables. It is lighter and occupies less volume than that of coaxial cables. It has technological superiority as well as it is economical.

Optical fiber cables are specialized communication cables that consist of one or more strands of optical fibers enclosed within a protective covering. Figure 5.1 shows optical fiber cable. These cables are designed to transmit information in the form of light signals over long distances with minimal signal loss and distortion.

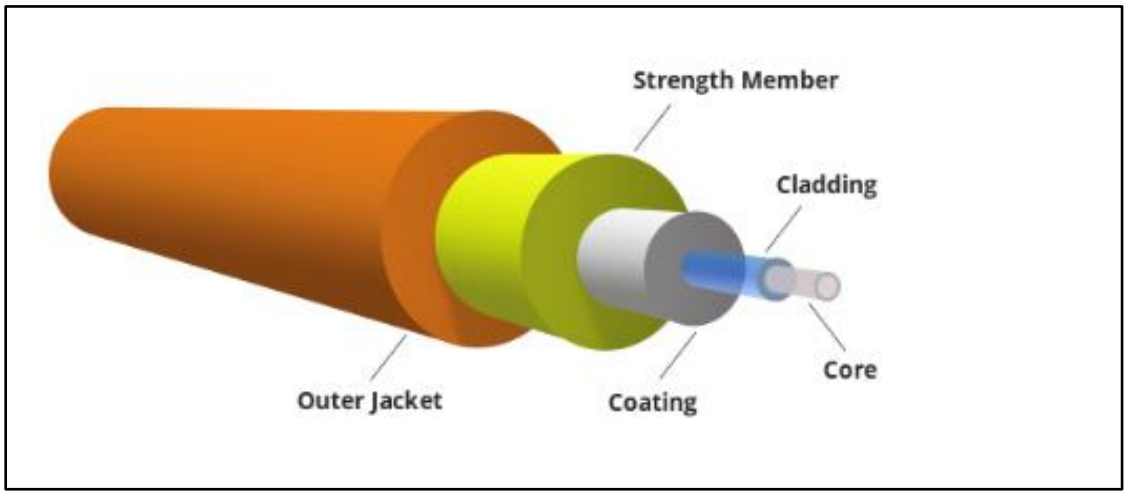

Figure 5.1 Optical Fiber Cable*

The core of an optical fiber is the central region through which light signals travel. It is typically made of high-quality glass or plastic material with a high refractive index. The cladding is the outer layer surrounding the core of the optical fiber. It is made of a different material than the core, typically glass or plastic with a lower refractive index. The remaining layers serve as a protective covering, providing strength to the central part.

*https://images.app.goo.gl/iMDi12oktQpAqmU38

Optical fiber communication is a technology that enables the transmission of information over long distances using optical fibers, which are thin strands of glass or plastic that transmit light signals. This technology has revolutionized communication, offering high-speed data transfer, high bandwidth capacity, and low attenuation rates compared to traditional copper wire communication systems. It also has a special characteristic that it is a perfect insulator as it is made of silica-based glass or plastic and current is flowing in it. Subsequently these fibers are resistant to electromagnetic interference. It has an important property that it does not corrode. It is a challenge to handle optical fibers as it needs a great deal of skill and it is very expensive.

In optical fiber communication, data is transmitted as light pulses that travel through the optical fibers. The fibers are designed to minimize signal loss and maintain the quality of the signal over long distances by using advanced techniques such as dispersion compensation, polarization mode dispersion compensation, and amplifier repeaters. Optical fibers also offer greater security and immunity to electromagnetic interference, making them suitable for sensitive applications such as military and healthcare.

Optical fiber communication technology has found widespread use in various fields, including telecommunications, internet communication, broadcasting, medical equipment, and aerospace applications. The technology has enabled the development of high-speed data transfer networks, high-definition television, and medical equipment for remote diagnosis and treatment. Optical fiber communication has also contributed to reducing the digital divide by making internet access available in remote areas.

Overall, optical fiber communication technology is a critical component of modern communication systems, enabling high-speed data transfer and reliable communication over long distances. As technology continues to advance, optical fiber communication is expected to play an even greater role in shaping the future of communication and information exchange.

5.2.5. Need of Soliton in fibers

The amount of information through fibers can be increased by reducing the width of pulse to its shortest, so that larger information can be sent through fiber. But if a large number of pulses are injected in to fiber, then there will be problem of overlapping of pulses after travelling some distances so that ultimately it becomes difficult to differentiate between pulses and information will no longer be useful.

Such situation can be handled if one handles the effects of nonlinearity. When the pulse is strong, the width of pulse is shortened when it is strong and the pulse is compressed too. It results in retaining the shape of pulse for long propagation distance. These steady waves came to be known as optical solitons. Many researchers are currently working on this topic, as it has gained significant attention in recent times. Mohammed et al. [164] presented technique of analyzing dispersion using a span of dispersion compensation fiber is used to ease the problems of chromatic dispersion and attenuation. They designed an approximate Gaussian pulse propagation model for analysis of dispersion compensation in a single mode optical fiber communication system, which is obtained from nonlinear Schrödinger equation to represent the effects of chromatic dispersion and attenuation which is solved using split-step Fourier Method. Hasegawa [165] presented a detailed study on the role of soliton-based communications on present-day ultrahigh-speed communications.

5.2.6. Advantages of Solitons in optical fiber communications

Some advantages are shown here [165, 166]:

a) Solitons are unaffected by an effect called polarization mode dispersion (PMD) has no effect on solitons. But if that wave travels over larger distances and in high-speed networks, it becomes less effective.

b) To overcome the less usage of solitons in high-speed networks, the travelling signal need not be electrified so that it can be more effective and useful in high-speed networks which include routing, de-multiplexing and switching which are used in optical domain.

c) If solitons are taken care of properly then they can be highly robust than non-return to zero (NRZ) pulse. The amplifiers which boost signaling also create noise

which can be controlled by using schemes that allows separation between amplifiers multiple times.

d) The use of in-line absorbers suppress the noise created by the signals.

e) Solitons have the capacity to stay together even during polarization which makes it efficient to use them in high-speed network.

f) Solitons can carry a large amount of data over long distances without the need for repeaters or amplifiers.

g) Solitons maintain their shape and speed over long distances, which helps reduce signal distortion.

h) Solitons require less power compared to other transmission methods, which can lead to cost savings.

i) Solitons are less susceptible to external interference, such as noise or distortion from other signals.

5.2.7. Disadvantages of solitons in optical fiber communications

However, soliton-based optical fiber communications also have several advantages it also has disadvantages. Some of these disadvantages include [165, 166]:

Complex technology: Solitons require complex technology to generate, control, and detect, which can make them more expensive and challenging to implement.

Challenging to manage: Soliton-based systems are challenging to manage because they require precise control over the signal parameters, such as the pulse width and repetition rate. This can make it difficult to maintain optimal performance, especially in complex systems with multiple soliton channels.

5.2.8. Characteristics of Solitons based optical fibers

Here the characteristics of solitons based optical fibers are [165,166]**:**

Enormous Bandwidth: Optical Fibers have high data transmission bandwidth, which further increases by wavelength division multiplexing method.

Low transmission loss: If the ultra-low loss and silica fibers which are erbium doped are being used as optical amplifiers then this contributes to achievement of loss less transmission.

Immunity to cross talk: Optical fibers are immune to cross talk means they are interference free i.e., from EMI and RFI as optical fibers are dielectric wave guides.

Electric Isolation: Optical Fibers exhibits insulation as they are made of silica.

Small size and weight: This size of optical fiber is very small and light in weight which makes them to use in satellites and aircrafts.

Signal Security: Optical fibers provide 100% security to travelling signal due to its capacity of non-radiation.

Ruggedness and Flexibility: Fiber cables retain their originality even after twisting or bending.

Low cost and availability: These fibers are available in abundance in market so they are not costly.

Reliability: The data sent via fibers is most reliable because of the following qualities:

a) Optical fibers are highly reliable because they do not disperse.

b) Optical fibers are neither corrosive nor chemically reactive as they are made of silicon glass.

5.2.9. Applications of Soliton based optical fibers in real life

Some important applications of soliton based optical fibers in real life are [165, 166]:

Telephone: Fiber Optic cables are much smaller than old metal cables i.e., four metal cable capacities equal to one fiber cable. That's why these cables are used in telephone lines and fit in to underground duct which also have high transmission capacity and low signal attenuation.

Fiber cables are made up of no electrical conductors and signals in these pulses does not carry Electromagnetic interference.

Submarine fiber cables: These fiber cables completely outdate coaxial cables in terms of transmission capacity which is 10 times more than the coaxial cables.

Computer data communications: Fibers are used for data communications where wire links would not work properly because of electromagnetic interference that can block wire or radio transmission, whereas fiber cables are immune to electromagnetic

interference. Further fiber cables which do not carry conductors are also immune to power surges from lightning strikes which can damage electronic equipment.

Ships Automobiles and Airplanes: The three magical properties of fibers i.e., light weight, small size and immune to EMI attracted makers of ships, automobiles and planes. As the electronic content of the ships, automobiles and planes have increased; the need of communications arises too. Automakers have studied the fiber to control signals i.e., from steering wheel to accessories such as power windows or radios.

Military System: Military Systems also replaced bulky 26 pair wire cables by optical fibers to have better and effective communication systems. The fiber cable is more reliable than metal cable which often gets broken and hence causes loss in communication system. Military planners are also working on fiber optic systems for guiding battlefield missiles to their targets.

Coded and decoded secret information: Optical fiber communication plays a crucial role in the transmission of coded and decoded secret information. Optical fibers provide a highly secure and reliable means of communication, making them ideal for transmitting sensitive information that needs to be kept confidential.

One of the primary advantages of optical fiber communication is that it is highly resistant to external interference and eavesdropping. The light signals that are transmitted through the fiber are confined within the fiber's core, which makes it difficult for unauthorized parties to intercept or tamper with the signals.

Moreover, the use of encryption techniques in combination with optical fiber communication adds an extra layer of security, ensuring that the information being transmitted is only accessible to authorized parties. Encryption involves the use of mathematical algorithms to convert plain text into a coded format that can only be decoded by authorized parties.

Optical fiber communication is used extensively in military and government applications, where the transmission of sensitive information is critical. For example, optical fiber communication is used by intelligence agencies to transmit classified information securely between different locations.

5.2.10. Summary

Optical fiber communication has revolutionized the way we communicate in our daily lives. It offers several advantages such as high bandwidth, low signal loss, and immunity to electromagnetic interference. However, one of the major challenges in optical fiber communication is dispersion, which can be overcome by using soliton solutions of the NLS equation.

The study of the soliton solutions of the NLS equation is of utmost importance in the field of optical fiber communication. It enables researchers and engineers to design and optimize optical fibers, laser sources, and modulation schemes to achieve faster and more efficient communication. By understanding the behavior of solitons, researchers can develop communication systems that can transmit data over long distances without loss of signal quality.

Optical solitons are self-reinforcing solitary waves that can travel long distances in optical fibers without dispersion or distortion. They are crucial for the efficient transmission of high-speed data and high-bandwidth applications over long distances. Soliton-based optical communication is used in many applications such as long-distance telephone networks, high-speed internet, video streaming, cloud computing, and telemedicine.

In day-to-day life, optical fiber communication technology is used in various applications such as making telephone calls, watching television, sending documents over fax, withdrawing money from bank ATMs, and surfing the internet. Optical fiber communication has become an essential part of our daily life, and its importance will continue to increase as technology advances further.

In addition to military and government applications, optical fiber communication is also used in the banking and finance sector to transmit confidential financial information securely. For example, banks use optical fiber communication to transmit credit card data, online banking transactions, and other sensitive financial information securely between different branches and data centers.

Overall, the secure and reliable nature of optical fiber communication makes it an indispensable technology for the transmission of coded and decoded secret information in various applications.

5.3. Brief study of one of important applications of Sine-Gordon equation

5.3.1. Introduction

The SG equation is a nonlinear PDE that arises in various areas of physics, including condensed matter physics, field theory, and soliton theory. One of the interesting features of the SG equation is that it supports soliton solutions, which are localized wave-like structures that behave as particles. A number of applications of the soliton solutions of the SG equation that play a key role in science and engineering have been addressed discussed in chapter 3 briefly. The Josephson junction is particularly significant and is briefly explained in this chapter. Here, the importance of soliton in Josephson junctions is discussed, along with some of its advantages and disadvantages.

5.3.2. Josephson junction

Josephson junctions [94] are devices that consist of two superconductors separated by a thin insulating barrier. Figure 5.2 represent the pictorial representation of Josephson junctions, when a voltage is applied across the junction, a supercurrent flows through the barrier, and the junction exhibits a variety of interesting and useful phenomena. One of these phenomena is the formation of solitons, which are self-reinforcing solitary waves that can travel through the junction [168, 169].

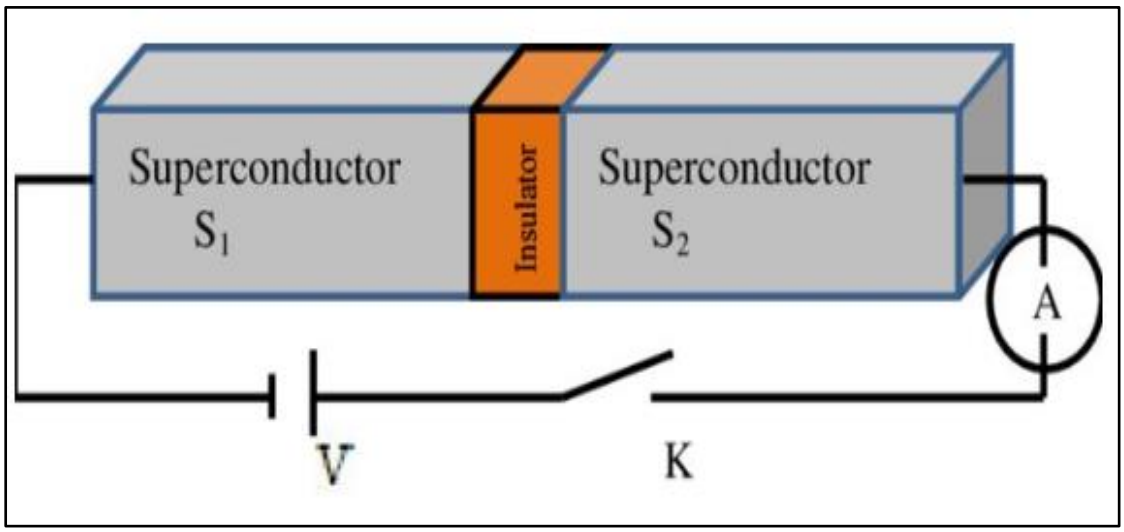

Figure 5.2 Josephson junctions*

*https://images.app.goo.gl/jhdr84G9cqpVEhct9

Where V is Voltage, A is ammeter, and K is key.

In new technologies, Josephson junctions are used in various ways, such as in superconducting electronics, quantum computing, and medical imaging. For example, in quantum computing, Josephson junctions are used as qubits, which are the building blocks of quantum computers. By controlling the flow of superconducting current through the junction, researchers can manipulate the state of the qubit and perform quantum operations. Trabelsi et al. [168] presented physical behavior of superconductivity phenomenon in their work.

If Josephson junctions did not exist, many of these technologies would not be possible or would require alternative approaches that may not be as efficient or effective. For example, quantum computing without Josephson junctions would require the use of other types of qubits, such as those based on trapped ions or superconducting resonators, which have different properties and challenges. Medical imaging without superconducting quantum interference devices (SQUIDs) would require alternative magnetic field detectors, which may not be as sensitive or versatile.

Josephson junctions are essential components of many modern technologies, and without them, these technologies would not exist or would be significantly different.

5.3.3. Role of soliton solution in Josephson junction

When a voltage is applied to the junction, a supercurrent can flow through the barrier, and the junction can exhibit a variety of interesting and complex behaviors, such as oscillations, chaos, and soliton formation.

Soliton solutions are particularly important in the study of Josephson junctions because they can arise spontaneously and persist for long periods of time, even in the presence of noise and other sources of perturbation. This makes them useful for a wide range of applications, such as signal processing, data storage, and quantum computing.

One of the key advantages of soliton solutions in Josephson junctions is their stability. Unlike other types of waves, solitons do not dissipate or spread out over time, which means that they can carry information over long distances without losing their coherence. This makes them useful for transmitting signals in noisy or unstable

environments, and for maintaining the coherence of quantum information in quantum computing applications.

In addition to their practical applications, solitons in Josephson junctions have also been the subject of intense theoretical study. They provide a rich source of complex dynamical behavior, and their properties can be analyzed using a variety of mathematical techniques, including perturbation theory, bifurcation analysis, and numerical simulations. As a result, they have helped to advance our understanding of many important phenomena in nonlinear physics, such as chaos, pattern formation, soliton, and synchronization [169].

5.3.4. Applications of solitons in Josephson junction

Solitons are self-reinforcing waves that maintain their shape and velocity while propagating through a medium. They have found several applications in various fields of physics, including the study of Josephson junctions, which are devices that allow the flow of a supercurrent between two superconductors separated by a thin insulating layer. Here are some applications of solitons in Josephson junctions [168, 169]:

Voltage standards: Josephson junctions play a critical role in the creation of highly accurate voltage standards. Voltage standards are used to calibrate voltage-measuring instruments and to ensure the accuracy of voltage measurements in a wide range of applications in industries such as power grid management, telecommunications, and medical equipment. Josephson junctions are used to create a highly stable and precise reference voltage. When a Josephson junction is subjected to a microwave frequency, it generates a voltage that is proportional to the frequency. This voltage is known as the Josephson voltage, and it is highly stable and predictable. By using Josephson junctions in a specially designed circuit, known as a Josephson voltage standard (JVS), a highly accurate and stable voltage reference can be created. The JVS can then be used to calibrate voltage-measuring instruments and to provide a reference voltage for other applications.

Voltage-controlled Josephson soliton oscillators: Solitons in Josephson junctions can be used to create oscillators that generate stable and coherent microwave signals.

By applying an external voltage to the junction, the soliton can be controlled to oscillate at a specific frequency.

Digital signal processing: Josephson junctions can be used to perform ultrafast digital signal processing. This can be useful in applications such as high-speed data communication, radar systems, and image processing.

High-speed communication: Solitons can be used to transmit information at high speeds through Josephson junctions. This is because they can propagate over long distances without losing their shape, making them ideal for carrying information without distortion.

Magnetic flux quantization: Solitons can also play a role in the quantization of magnetic flux in Josephson junctions. When a soliton passes through a Josephson junction, it can induce a phase shift in the superconducting order parameter, resulting in the quantization of magnetic flux.

Quantum computing: Solitons in Josephson junctions have also been proposed as a possible building block for quantum computing. By manipulating solitons with external voltages, it may be possible to create qubits that can be used for quantum information processing.

Superconductivity: Josephson junction-based devices are used for making high-temperature superconducting electronic components coupled with Josephson junctions used in making Josephson voltage standards. These are also used in the study of phase transition. These junctions help in the study of the properties of layered superconducting materials.

5.3.5. Role of Josephson junction in new technologies

The role of Josephson junctions in improving new technology in day-to-day life is significant. Here are some ways Josephson junctions are contributing to technological advancements that impact our daily lives [171, 172]:

Improved efficiency of electronics: Josephson junctions can be used to create low-power, high-speed electronics, which are essential for modern electronic devices. By improving the efficiency of electronic devices, Josephson junctions help to reduce

energy consumption and improve battery life, leading to longer-lasting and more sustainable technology.

Faster and more accurate communication: Josephson junctions can be used to create highly stable and accurate microwave signals, which are essential for communication technology. This enables faster and more reliable communication, leading to better connectivity and improved data transfer rates.

Medical imaging and diagnostics: Josephson junctions are used in SQUIDs, which are highly sensitive detectors of magnetic fields. SQUIDs are used in medical imaging, such as MRI, to detect the magnetic fields produced by the body's tissues. This allows for highly detailed images of the body's internal structures, leading to improved diagnostics and treatment planning.

Advancements in quantum computing: Josephson junctions are essential components of superconducting qubits, which are used in quantum computing. Quantum computing has the potential to solve complex problems that classical computers cannot, leading to advancements in fields such as drug discovery, material science, and cryptography.

High-speed data processing: Josephson junctions can be used to create ultrafast data processing devices, which are essential for high-speed data processing applications such as image and video processing. This enables faster data processing and more responsive technology, leading to improved user experiences and productivity.

Josephson junctions are contributing to technological advancements that impact our daily lives in many ways, from improved energy efficiency and communication to better medical diagnostics and quantum computing.

5.3.6. Advantages and Disadvantages of Solitons in Josephson Junctions

Here are some advantages and disadvantages of solitons in Josephson junctions [173, 174]:

5.3.6.1. Advantages

Stability: Solitons in Josephson junctions are topologically stable and can persist for long periods of time without dissipating. This makes them useful for carrying information in quantum computing and communication applications.

Nonlinear behavior: Solitons exhibit nonlinear behavior and can interact with each other in interesting ways. This allows for the manipulation and control of the soliton waveforms, which can be used for information processing and signal modulation.

High-speed transmission: Solitons can travel through the Josephson junction at high speeds without losing their shape or amplitude. This makes them useful for high-speed data transmission in electronic circuits.

5.3.6.2. Disadvantages

Difficult to generate: Generating solitons in Josephson junctions requires careful tuning of the junction parameters, such as the bias voltage and temperature. This can be challenging and time-consuming.

Sensitivity to noise: Solitons in Josephson junctions are sensitive to noise and other environmental perturbations. This can cause the soliton waveform to degrade or even disappear, leading to errors in signal transmission.

Limited applications: While solitons in Josephson junctions have many potential applications, their use is currently limited to certain areas of research and development, such as quantum computing and high-speed data transmission. Their implementation in commercial applications is still in its early stages.

5.3.7. Summary

The connection between the SG equation and Josephson junctions comes from the fact that the SG equation arises as an effective description of the dynamics of the phase difference between the two superconducting electrodes in a Josephson junction. This phase difference plays a crucial role in determining the behavior of the junction, and the SG equation provides a way to model its dynamics.

The accuracy of voltage measurements is critical in many fields, including power grid management, telecommunications, and medical equipment. By using Josephson

junctions to create highly accurate voltage standards, it is possible to ensure the reliability and accuracy of voltage measurements in these and other applications. Overall, Josephson junctions have a wide range of applications in areas such as quantum computing, sensing, and digital electronics, and ongoing research is exploring new ways to utilize and optimize their unique properties.

Solitons have a wide range of applications in the study of Josephson junctions and may have the potential for future technological advances in the field of electronics. Overall, the SG equation has many applications in various fields of physics and mathematics, and its study continues to be an active area of research.

Chapter-6

Conclusion

Two novel numerical methodologies: "Exponential modified cubic B-spline differential quadrature method with LOOCV approach" and "Exponential modified cubic B-spline differential quadrature method with PSO approach", have been established in this thesis.

The optimal value of the parameter ϵ employed in the basis functions of the "exponential cubic B-spline" is determined for the first time ever in literature. Researchers will benefit greatly from this breakthrough. The ideal value of the parameter ϵ in the exponential cubic B-spline basis functions is determined through the use of optimization techniques. Up till now, the value of parameter ϵ has been determined by the hit-and-trial approach, which leads to unstable results.

The LOOCV approach is used in the "Exponential modified cubic B-spline differential quadrature method (Expo-MCB-DQM) with LOOCV approach" methodology to identify the optimal value of the parameter ϵ that is utilized in the exponential cubic B-spline basis functions and improves the results. The application of this combined approach on two PDEs (NLS equation and SG equation) ensures its validity. Accuracy evaluation of the technique is performed using error norms tests, with the results presented in tables and figures. The outcomes are really amazing, according to observations. The results are close to exact solutions and comparable to results of other numerical methods that have been previously published. The established methods will be successfully used in the future to numerically solve various issues, assisting researchers in their future work.

PSO is a quick, accurate, and successful method of optimization. PSO, a well-known potential global optimization technique, has been used to tackle issues in many fields: engineering, smart cities, healthcare, the environment, business, and industry.

The PSO algorithm is used in the "Exponential modified cubic B-spline differential quadrature method (Expo-MCB-DQM) with PSO approach" methodology to identify

the optimal value of the parameter ϵ that is utilized in the exponential cubic B-spline basis functions and improves the results. The application of this combined approach on two PDEs (NLS equation and SG equation) ensures its validity. Accuracy evaluation of the technique is performed using error norms tests, with the results presented in tables and figures. The outcomes are really amazing, according to observations. The results are close to exact solutions and comparable to results of other numerical methods that have been previously published. The established methods will be successfully used in the future to numerically solve various issues, assisting researchers in their future work.

This study not only provides numerical methods for solving NLEEs numerically, but also focuses on applications of these equations in field of science and engineering. Solitons solutions of NLEEs have been covered in the current work along with a short history of their existence. Solitons have been used in a number of scientific and engineering fields, and this has been explored in this thesis. To spark the attention of the readers, the several sorts of solitons for the well-known NLEEs have also been covered. The importance of two specific NLEEs (NLS equation and SG equation) is briefly explained. These two NLEEs are also used to apply soliton solutions of NLEEs to various field of scientific and engineering, with a focus on two applications discussed in detail: optical fiber communication and Josephson junctions.

The following is a brief description of the work conducted in this thesis:

1. Two novel numerical approaches have been developed using optimization techniques.

2. The thesis discusses the significance of NLEEs and their applications in science and engineering. Additionally, it highlights the importance of applications of soliton solutions of NLEEs, exemplified through Josephson junctions and optical fiber communication.

Future scope

In future this research work may be extended as follows:

1. In this research work LOOCV and PSO technique has been used with the "Exponential cubic B-spline differential quadrature method" to find the best value

of the parameter ϵ in the basis function. More basis function may be explored in which any parameter value needs to be optimized can further be extended, for example hyperbolic tension B-spine basis function.

2. In this research work the exponential cubic B-spline differential quadrature method has been used with LOOCV and PSO technique to find the best value of the parameter ϵ in the basis function. More optimization techniques can be explored to optimize parameter value ϵ in the basis function, for example ABC, GA optimization techniques, and many more.
3. The numerical solutions in this thesis are calculated only for partial differential equations. Fractional-order partial differential equations may also be explored to implement these techniques.
4. The equations solved in this research work are in one dimension. These methods may further be extended to solve two and higher-dimensional equations appearing in various applications of science and engineering.
5. In this research work discussion about different types of solutions of NLEEs, particularly one of them i.e., soliton type solution has been explored. This may further be extended to explore more type of solutions of PDE's like pattern formation, population dynamics, epidemiology, finance, climate science, and many more.
6. In this research work application of soliton solution of NLS equation in optical fiber and SG in Josephson junction equation has been briefed. This research may further be extended by exploring application of solutions of more equations like KdV equation, BBM equation, and many more which are discussed in this work.

References

[1] G. Arora and G. S. Bhatia, *A Meshfree Numerical Technique Based on Radial Basis Function Pseudospectral Method for Fisher's Equation*, Int. J. Nonlinear Sci. Numer. Simul. **21**(2020), no. 1, 37–49, doi: 10.1515/ijnsns-2018-0091.

[2] J. A. Koupaei, M. Firouznia, and S. M. M. Hosseini, *Finding a good shape parameter of RBF to solve PDEs based on the particle swarm optimization algorithm,* Alexandria Eng. J. **57**(2018), no. 4, 3641–3652, doi: 10.1016/j.aej.2017.11.024.

[3] E. Perracchione and I. Stura, *An RBF-PSO based approach for modeling prostate cancer,* in AIP Conference Proceedings. **1738**(2016), 1–7, doi: 10.1063/1.4952182.

[4] R. Cavoretto and A. D. Rossi, *An adaptive LOOCV-based refinement scheme for RBF collocation methods over irregular domains An adaptive LOOCV-based refinement scheme for RBF collocation methods over irregular domains,* Appl. Math. Lett. **103**(2020), 106178 doi: 10.1016/j.aml.2019.106178.

[5] R. E. Bellman and J. Casti, *Differential quadrature and long-term integration,* J. Math. Anal. Appl. **34**(1971), 235–238.

[6] R. E. Bellman, B. G. Kashef, and J. Casti, *Differential quadrature: a technique for the rapid solution of nonlinear partial differential equation*, J. Comput. Phys. **10**(1972), 40–52.

[7] C. W. Bert, S. K. Jang, and A. G. Striz, *Two new approximate methods for analyzing free vibration of structural components,* AIAA J. **26**(1988), 612–618.

[8] C. W. Bert and M. Malik, *Differential quadrature in computational mechanics: A review,* Appl. Mech. Rev. **49**(1996), no. 1, 1–27.

[9] C. Shu, *Differential quadrature and its application in engineering*, Springer-Verlag London Ltd. 2000.

[10] J. R. Quan and C. T. Chang, *New insights in solving distributed system equations by the quadrature method-I,* Comput. Chem. Eng. **13**(1989), 779–788.

[11] R. C. Mittal and S. Dahiya, *Numerical simulation of three-dimensional telegraphic equation using cubic B-spline differential quadrature method,* Appl. Math. Lett. **313**(2017), 442–452.

[12] A. Korkmaz and I. Dag, *Polynomial based differential quadrature method for numerical solution of nonlinear Burger's equation,* J. Franklin Inst. **348**(2011), no. 10, 2863–2875.

[13] A. H. Msmali, M. Tamsir, and A. A. H. Ahmadini, *Crank-Nicolson-DQM based on cubic exponential B-splines for the approximation of nonlinear Sine-Gordon equation,* Ain Shams Eng. J. **12**(2021), no. 4, 4091–4097, doi: 10.1016/j.asej.2021.04.004.

[14] A. Krowiak, *Hermite type radial basis function-based differential quadrature method for higher order equations,* Applied Mathematical Modellin, **40**(2016), 2421–2430, doi: 10.1016/j.apm.2015.09.069.

[15] A. H. Msmali, M. Tamsir, N. Dhiman, and M. A. Aiyashi, *New trigonometric B-spline approximation for numerical investigation of the regularized long-wave equation,* Open Phys. **19**(2021), no. 1, 758–769, doi: 10.1515/phys-2021-0087.

[16] A. Bashan, N. M. Yagmurlu, Y. Ucar, and A. Esen, *An effective approach to numerical soliton solutions for the Schrödinger equation via modified cubic B-spline differential quadrature method,* Chaos, Solitons and Fractals, **100**(2017), 45–56, doi: 10.1016/j.chaos.2017.04.038.

[17] A. Bashan, *An effective application of differential quadrature method based on modified cubic B-splines to numerical solutions of the KdV equation,* Turkish J. Math. **42**(2018), no. 1, 373–394, doi: 10.3906/mat-1609-69.

[18] A. Bashan, *Modification of quintic B-spline differential quadrature method to nonlinear Korteweg-de Vries equation and numerical experiments,* Appl. Numer. Math. **167**(2021), 356–374, doi: 10.1016/j.apnum.2021.05.015.

[19] A. Bashan, Y. Ucar, N. Murat Yagmurlu, and A. Esen, *A new perspective for quintic B-spline based Crank-Nicolson-differential quadrature method algorithm for numerical solutions of the nonlinear Schrödinger equation,* Eur. Phys. J. Plus. **133**(2018), no. 1, 12. doi: 10.1140/epjp/i2018-11843-1.

[20] A. Korkmaz and I. Dag, *Numerical Simulations of Boundary-Forced RLW Equation with Cubic B-Spline-based Differential Quadrature Methods,* Arab. J. Sci. Eng. **38**(2013), no. 5, 1151–1160, doi: 10.1007/s13369-012-0353-8.

[21] A. Korkmaz, A. M. Aksoy, and I. Dag, *Quartic B-spline differential quadrature method,* Int. Nonlinear Sci. **11**(2011), no. 4, 403–411.

[22] A. Korkmaz and I. Dag, *Shock wave simulations using sinc differential quadrature method,* Eng. Comput. Int. J. Comput. Aided Eng. Softw. **28**(2011), no. 6, 654–674.

[23] M. Tamsir, V. K. Srivastava, and R. Jiwari, *An algorithm based on exponential modified cubic B-spline differential quadrature method for nonlinear Burgers' equation,* Appl. Math. Comput. **290**(2016), 111–124, doi: 10.1016/j.amc.2016.05.048.

[24] M. Tamsir, V. K. Srivastava, N. Dhiman, and A. Chauhan, *Numerical Computation of Nonlinear Fisher's Reaction–Diffusion Equation with Exponential Modified Cubic B-Spline Differential Quadrature Method,* Int. J. Appl. Comput. Math. **4**(2018), no. 1, 1–13, doi: 10.1007/s40819-017-0437-y.

[25] G. Arora and V. Joshi, *Simulation of generalized nonlinear fourth order partial differential equation with Quintic Trigonometric Differential Quadrature Method,* Mathematical Models and Computer Simulations, **11**(2019), no. 6, 1059-1083, doi:10.1134/S207004821906005X.

[26] G. Arora, V. Joshi, and R. C. Mittal, *Numerical simulation of nonlinear Schrödinger Equation in One and Two Dimensions,* Math. Model. Comput. Simulations. **11**(2019), no. 4, 634–648, doi: 10.1134/S2070048219040070.

[27] G. Arora, V. Joshi, and R. C. Mittal, *a Spline-Based Differential Quadrature Approach To Solve Sine-Gordon Equation in One and Two Dimension,* Fractals, **30**(2022), no. 7, 1–14, doi: 10.1142/S0218348X22501535.

[28] G. Arora and V. Joshi, *Comparison of Numerical Solution of 1D Hyperbolic Telegraph Equation using B-Spline and Trigonometric B-Spline by Differential Quadrature Method,* Indian J. Sci. Technol. **9**(2016), no. 45, 1–8, doi: 10.17485/ijst/2016/v9i45/106356.

[29] H. S. Shukla and M. Tamsir, *Numerical solution of nonlinear Sine-Gordon equation by using the modified cubic B-spline differential quadrature method,* Beni-Suef Univ. J. Basic Appl. Sci. **7**(2018), no. 4, 359–366, doi: 10.1016/j.bjbas.2016.12.001.

[30] H. S. Shukla and M. Tamsir, *An exponential cubic B-spline algorithm for multi-dimensional convection-diffusion equations,* Alexandria Eng. J. **57**(2018), no. 3, 1999–2006, doi: 10.1016/j.aej.2017.04.011.

[31] M. Kapoor and V. Joshi, *Numerical regime "Uniform Algebraic Hyperbolic tension B-spline DQM" for the solution of Fisher's Reaction-Diffusion equation,* 3rd Int. Conf. Appl. Res. Eng. Sci. Technol. Paris, Fr. Diam. Sci. Publ. (2020), 20–22.

[32] M. Kapoor, *Numerical simulation of Burgers' equations via quartic HB-spline DQM,* Nonlinear Eng. **12**(2023), no. 1, 20220264.

[33] M. Kapoor and V. Joshi, *Numerical solution of coupled 1D Burgers' equation by employing Barycentric Lagrange interpolation basis function-based differential quadrature method,* Int. J. Comput. Methods Eng. Sci. Mech. **23**(2022), no. 3, 263–283, doi: 10.1080/15502287.2021.1954726.

[34] S. Kumar, R. Jiwari, R. C. Mittal, and J. Awrejcewicz., *Dark and bright soliton solutions and computational modeling of nonlinear regularized long wave model,* Nonlinear Dyn. **104**(2021), no. 1, 661–682, doi: 10.1007/s11071-021-06291-9.

[35] C. De Boor, *On calculating with B-splines,* Journal of Approximation theory, **6** (1972), no. 1, 50-62.

[36] I. J. Schoenberg, *Contribution to the problem of approximation of equidistant data by analytical functions,* Quart. Appl. Math. **4**(1946), 45-99.

[37] B. K. Singh and P. Kumar, *An algorithm based on a new DQM with modified exponential cubic B-splines for solving hyperbolic telegraph equation in (2 + 1) dimension*, Nonlinear Eng. **7**(2018), no. 2, 113–125, doi: 10.1515/nleng-2017-0106.

[38] R. Spiteri and S. Ruuth, *A new class of optimal high-order strong stability-preserving time-stepping schemes*, SIAM J. Numer. Anal. **40**(2002), no. 2, 469–491.

[39] M. Ghasemi, *High order approximations using spline-based differential quadrature method: Implementation to the multi-dimensional PDEs*, Applied Mathematical Modelling, **46**(2017), 63-80.

[40] M. K. Jain, *Numerical Solution of Differential Equations*, second ed., Wiley, New York, NY, 1983.

[41] R. Eberhart and J. Kennedy, *A new optimizer using particle swarm theory*, MHS'95. Proc. Sixth Int. Symp. Micro Mach. Hum. Sci. (1995), 39–43.

[42] J. S. Russell, *Report on Waves, The report of the meeting of the British Association for the advancement of science*, Nature, (1844), 311–390, doi: 10.1038/002124a0.

[43] R. L. Horne, *A (Very) Brief Introduction to Soliton Theory in a class of Nonlinear PDEs*, Mathematical Sciences Proceedings, 2002, doi: 10.13140/RG.2.1.2314.0962.

[44] M. Wadati, *Introduction to solitons*, Pramana, **57**(2001), no. 5–6,841–847,doi: 10.1007/s12043-001-0002-3.

[45] D. J. Korteweg and G. de Vries, *XLI. On the change of form of long waves advancing in a rectangular canal, and on a new type of long stationary waves*, London, Edinburgh, Dublin Philos. Mag. J. Sci. **39**(1895), no. 240, 422–443, doi: 10.1080/14786449508620739.

[46] E. Fermi, J. R. Pasta, and S. M. Ulam, *Studies of Non-Linear Prolems (Technical Report)*, Collect. Work. E. Fermi. **2**(1965), no. May, 978–988.

[47] N. J. Zabuskal and M. D. Kruskal, *Interaction of 'Solitons' in a collisionless plasma and the recurrence of initial states N.*, Phys. Rev. Lett. **15**(1965), no. 6, 240–243.

[48] P. D. Lax, *Integrals of nonlinear equations of evolution and solitary waves,* Commun. Pure Appl. Math. **21**(1968), no. 5, 467–490, doi: 10.1002/cpa.3160210503.

[49] A. B. Shabat and V. E. Zakharov, *Exact theory of two-dimensional self-focussing and one-dimensional self-modeulation of waves in nonlinear media,* Sov. Phys. Jept. **34**(1972), no. 1, 62, doi: 10.1515/znb-2005-0905.

[50] M. J. Ablowitz, D. J. Kaup, A. C. Newell, and H. Segur, *Inverse Scattering Transform-Fourier Analysis for Nonlinear Problems.,* Stud. Appl. Math. **53**(1974), no. 4, 249–315, doi: 10.1002/sapm1974534249.

[51] Y. Yousefi and K. K. Muminov, *A Simple Classification of Solitons,* arXiv preprint arXiv:1206. **1294**(2012), 1–18.

[52] G. P. Agrawal and C. Headley, *Kink solitons and optical shocks in dispersive nonlinear media,* Phys. Rev. A. **46**(1992), no. 3, 1573–1577.

[53] A. L. Fabian, R. Kohl, and A. Biswas, *Perturbation of topological solitons due to Sine-Gordon equation and its type,* Commun. Nonlinear Sci. Numer. Simul. **14**(2009), no. 4, 1227–1244, doi: 10.1016/j.cnsns.2008.01.013.

[54] M. M. Khater, *Diverse solitary and Jacobian solutions in a continually laminated fluid with respect to shear flows through the Ostrovsky equation,* Mod. Phys. Lett. B. **35**(2021), no. 13, 2150220.

[55] S. Johnson and A. Biswas, *Breather dynamics of the Sine-Gordon equation,* Commun. Theor. Phys. **59**(2013), no. 6, 664–670, doi: 10.1088/0253-6102/59/6/02.

[56] M. Tajiri and Y. Watanabe, *Breather solutions to the focusing nonlinear Schrödinger equation,* Phys. Rev. E. **57**(1998), no. 3, 3510–3519, doi: 10.1103/PhysRevE.57.3510.

[57] R. Carretero and J. Frantzeskakis, *Nonlinear Waves in Bose-Einstein Condensates: Physical Relevance and Mathematical Techniques,* Nonlinearity, **21**(2008), no. 7, 139.

[58] A. B. Aceves, *Optical gap solitons : Past, present, and future ; theory and experiments,* Chaos, **584**(2011), no. 2000, 584–589, doi: 10.1063/1.1287065.

[59] Y. S. Kivshar, *Stable vector solitons composed of bright and dark pulses,* Opt. Lett. **17**(1992), no. 19, 1322–1324, doi: 10.1364/ol.17.001322.

[60] R. Radhakrishnan and M. Lakshmanan, *Bright and dark soliton solutions to coupled nonlinear Schrödinger equations,* J. Phys. A. Math. Gen. **28**(1995), no. 9, 2683–2692, doi: 10.1088/0305-4470/28/9/025.

[61] A. R. Seadawy and D. Lu, *Bright and dark solitary wave soliton solutions for the generalized higher order nonlinear Schrödinger equation and its stability,* Results Phys. **7**(2017), 43–48, doi: 10.1016/j.rinp.2016.11.038.

[62] K. Hosseini, M. Mirzazadeh, D. Baleanu, S. Salahshour, and L. Akinyemi, *Optical solitons of a high-order nonlinear Schrödinger equation involving nonlinear dispersions and Kerr effect,* Opt. Quantum Electron. **54**(2022), no. 3, 1–12, doi: 10.1007/s11082-022-03522-0.

[63] M. M. A. Khater and B. Ghanbari, *On the solitary wave solutions and physical characterization of gas diffusion in a homogeneous medium via some efficient techniques,* Eur. Phys. J. Plus, **136**(2021), no. 4, 1–28, doi: 10.1140/epjp/s13360-021-01457-1.

[64] M. M. Khater, L.Akinyemi, S. K. Elagan, M. A. El-Shorbagy, S. H., Alfalqi, J. F. Alzaidi, and N. A. Alshehri, *Bright–dark soliton waves' dynamics in pseudo spherical surfaces through the nonlinear kaup–kupershmidt equation,* Symmetry, **13**(2021), no. 6, 1–20, doi: 10.3390/sym13060963.

[65] L. Najera, M. Carrillo, and M. A. Aguero, *Non-classical solitons and the broken hydrogen bonds in DNA vibrational dynamics,* Adv. Stud. *Theor. Phys.* **4**(2010), no. 9–12, 495–510.

[66] J. Chen, J. Chen, and J. Zhou, *Compacton, Peakon and Solitary Wave Solutions of the Osmosis K (3,2) Equation,* J. Sci. Res. Reports. **5**(2015), no. 4, 275–284, doi: 10.9734/jsrr/2015/14958.

[67] S. S. Behzadi, *Numerical solution of fuzzy Camassa-Holm equation by using homotopy analysis methods,* J. Appl. Anal. Comput. **1**(2011), no. 3, 315–323.

[68] J. Li and Y. Zhang, *Exact loop solutions, cusp solutions, solitary wave solutions and periodic wave solutions for the special CH-DP equation,* Nonlinear Anal. Real World Appl. **10**(2009), no. 4, 2502–2507, doi: 10.1016/j.nonrwa.2008.05.006.

[69] A. C. Scott, *Davydov's soliton,* Phys. D Nonlinear Phenom. **51**(1991), no. 1–3, 333–342, doi: 10.1016/0167-2789(91)90243-3.

[70] W. Alka, A. Goyal, and C. Nagaraja Kumar, *Nonlinear dynamics of DNA - Riccati generalized solitary wave solutions,* Phys. Lett. Sect. A Gen. At. Solid State Phys. **375**(2011), no. 3, 480–483, doi: 10.1016/j.physleta.2010.11.017.

[71] M. Peyrard, *Nonlinear dynamics and statistical physics of DNA,* Nonlinearity,**17**(2004), no. 2, p. R1, 2004, doi: 10.1088/0951-7715/17/2/R01.

[72] J. S. Song, *Theory of Magnetic Monopoles and Electric-Magnetic Duality: A Prelude to S -Duality,* J. Undergrad. Sci. **3**(1996), 47–55.

[73] H. G. Abdelwahed, E. K. El-Shewy, M. A. E. Abdelrahman, and A. F. Alsarhana, *On the physical nonlinear $(n+1)$-dimensional Schrödinger equation applications,* Results Phys. **21**(2021), 103798, doi: 10.1016/j.rinp.2020.103798.

[74] V. E. Zakharov, *Collapse of Langmuir Waves,* Sov. Phys. JETP. **35**(1972), no. 5, 908–914.

[75] E. A. Kuznetsov, A. M. Rubenchik, and V. E. Zakharov, *Soliton stability in plasmas and hydrodynamics,* Phys. Rep. **142**(1986), no. 3, 103–165, doi: 10.1016/0370-1573(86)90016-5.

[76] M. Tajiri and M. Tuda, *On Large Amplitude Ion Acoustic Solitons in Plasma with Negative Ions,* Journal of the Physical Society of Japan, **54**(1985), no. 1, 19–22, doi: 10.1143/JPSJ.54.19.

[77] M. M. A. Khater and A. E. S. Ahmed, *Strong langmuir turbulence dynamics through the trigonometric quintic and exponential B-spline schemes,* AIMS Math. **6**(2021), no. 6, 5896–5908, doi: 10.3934/math.2021349.

[78] M. M. A. Khater, T. A. Nofal, H. Abu-Zinadah, M. S. M. Lotayif, and D. Lu, *Novel computational and accurate numerical solutions of the modified Benjamin–Bona–Mahony (BBM) equation arising in the optical illusions field,* Alexandria Eng. J. **60**(2021), no.1, 1797–1806, doi: 10.1016/j.aej.2020.11.028.

[79] D. H. Peregrine, *Water waves, nonlinear Schrödinger equations and their solutions,* J. Aust. Math. Soc. Ser. B. Appl. Math. **25**(1983), no. 1, 16–43, doi: 10.1017/s0334270000003891.

[80] V. E. Zakharov, *Stability of periodic waves of finite amplitude on the surface of a deep fluid,* J. Appl. Mech. Tech. Phys. **9**(1986), no. 2, pp. 190–194, doi: 10.1007/BF00913182.

[81] A. Larraza and S. Putterman, *Theory of non-propagating surface-wave solitons,* J. Fluid Mech. **148**(1984), 443–449.

[82] M. Longuet-Higgins, *Capillary-gravity waves of solitary type on deep water,* J. Fluid Mech. **252**(1993), 703–711, doi: 10.1063/1.869315.

[83] M. D. Maiden, D. V. Anderson, N. A. Franco, G. A. El, and M. A. Hoefer, *Solitonic Dispersive Hydrodynamics: Theory and Observation,* Phys. Rev. Lett. **120**(2018), no. 14, 1–8, doi: 10.1103/PhysRevLett.120.144101.

[84] M. Y. Wang, *Optical solitons of the perturbed nonlinear Schrödinger equation in Kerr media*, Optik, **243**(2021), 167382, doi: 10.1016/j.ijleo.2021.167382.

[85] A. Hasegawa, *An historical review of application of optical solitons for high speed communications,* Chaos: An Interdisciplinary Journal of Nonlinear Science, **10**(2000), no. 3, 475–485, doi: 10.1063/1.1286914.

[86] T. Shi and S. Chi, *Nonlinear photonic switching by using the spatial soliton collision,* Opt. Lett. **15**(1990), no. 20, 1123, doi: 10.1364/ol.15.001123.

[87] M. N. Islam, *Ultrafast all-optical logic gates based on soliton trapping in fibers,* Opt. Lett. **14**(1989), no. 22, 1257–1259, doi: 10.1364/ol.14.001257.

[88] G. Arora, R. Rani, and H. Emadifar, *Numerical solutions of nonlinear Schrödinger equation with applications in optical fiber communication,* Optik, **266**(2022), 169661, 2022.

[89] M. M. A. Khater, A. E. S. Ahmed, S. H. Alfalqi, J. F. Alzaidi, S. Elbendary, and A. M. Alabdali, *Computational and approximate solutions of complex nonlinear Fokas–Lenells equation arising in optical fiber,* Results Phys. **25**(2021), 104322, doi: 10.1016/j.rinp.2021.104322.

[90] M. Khater, *Recent electronic communications; optical quasi–monochromatic soliton waves in fiber medium of the perturbed Fokas–Lenells equation,* Opt. Quantum Electron. **59**(2022), no. 9, 1–12.

[91] M. M. Khater, *Abundant wave solutions of the perturbed Gerdjikov–Ivanov equation in telecommunication industry,* Mod. Phys. Lett. B. **35**(2021), no. 26, 2150456.

[92] M. M. A. Khater, K. S. Nisar, and M. S. Mohamed, *Numerical investigation for the fractional nonlinear space-time telegraph equation via the trigonometric Quintic B-spline scheme,* Math. Methods Appl. Sci. **44**(2021), no. 6, 4598–4606, doi: 10.1002/mma.7052.

[93] M. M. Khater and D. Lu, *Analytical versus numerical solutions of the nonlinear fractional time–space telegraph equation,* Mod. Phys. Lett. B. **35**(2021), no. 19, 2150324.

[94] L. V. Ginzburg, I. E. Batov, V. V. Bol'ginov, S. V. Egorov, V. I. Chichkov, A. E. Shchegolev, N. V. Klenov, I. I. Soloviev, S. V. Bakurskiy, and M. Y. Kupriyanov, *Determination of the Current–Phase Relation in Josephson Junctions by Means of an Asymmetric Two-Junction SQUID,* JETP Lett. **107**(2018), no. 1, 48–54, doi: 10.1134/S0021364018010058.

[95] L. Ferrari, *Approaching Bose-Einstein condensation,* Eur. J. Phys. **32**(2011), no. 6, 1547–1557, doi: 10.1088/0143-0807/32/6/009.

[96] J. Rogel-Salazar, *The Gross-Pitaevskii equation and Bose-Einstein condensates,* Eur. J. Phys. **34**(2013), no. 2, 247–257, doi: 10.1088/0143-0807/34/2/247.

[97] J. S. He, E. G. Charalampidis, P. G. Kevrekidis, and D. J. Frantzeskakis, *Rogue waves in nonlinear Schrödinger models with variable coefficients: Application to Bose-Einstein condensates,* Phys. Lett. Sect. A Gen. At. Solid State Phys. **378**(2014), no. 5–6, 577–583, doi: 10.1016/j.physleta.2013.12.002.

[98] K. B. Davis, M. O. Mewes, M. R. Andrews, N. J. van Druten, D. S. Durfee, D. M. Kurn, and W. Ketterle, *Bose-Einstein Condensation in a Gas of Sodium Atoms, Physical review letters*. **75**(1995), no. 22, 3969–3972.

[99] M. H. Anderson, J. R. Ensher, M. R. Matthews, C. E. Wieman, and E. A. Cornell, *Observation of bose-einstein condensation in a dilute atomic vapor,* Collect. Pap. Carl Wieman. **269**(1995), no. 5221, 453–456, doi: 10.1142/9789812813787_0062.

[100] K. Abedi, V. Ahmadi, S. Gholmohammadi, E. Darabi, and M. H. Yavari, *Soliton solution of nonlinear Schrödinger equation with application to Bose-Einstein condensation using the FD method,* Second Int. Conf. Adv. Optoelectron. Lasers. **7009**(2008), 125–131, doi: 10.1117/12.793329.

[101] A. M. Wazwaz, *Compactons dispersive structures for variants of the K(n,n) and the KP equations,* Chaos, Solitons and Fractals. **13**(2002), no. 5, 1053–1062, doi: 10.1016/S0960-0779(01)00109-6.

[102] R. C. Mittal and R. Bhatia, *Numerical solution of nonlinear Sine-Gordon equation by modified cubic B-Spline Collocation Method,* Int. J. Partial Differ. Equations. **2014**(2014), no. 1, 1–8, doi: 10.1155/2014/343497.

[103] H. A. Alkhidhr, *Closed-form solutions to the perturbed NLSE with Kerr law nonlinearity in optical fibers,* Results Phys. **22**(2021), 103875, doi: 10.1016/j.rinp.2021.103875.

[104] K. Hosseini, K. Sadri, M. Mirzazadeh, Y. M. Chu, A. Ahmadian, B. A. Pansera, and S. Salahshour, *A high-order nonlinear Schrödinger equation with the weak non-local nonlinearity and its optical solitons,* Results Phys. **23**(2021), 104035, doi: 10.1016/j.rinp.2021.104035.

[105] S. Malik, S. Kumar, K. S. Nisar, and C. Ahamed Saleel, *Different analytical approaches for finding novel optical solitons with generalized third-order nonlinear Schrödinger equation,* Results Phys. **29**(2021), 104755, doi: 10.1016/j.rinp.2021.104755.

[106] M. S. Osman, H. Almusawa, K. U. Tariq, S. Anwar, S. Kumar, M. Younis, and W. X. Ma, *On global behavior for complex soliton solutions of the perturbed nonlinear Schrödinger equation in nonlinear optical fibers,* J. Ocean Eng. Sci. **7**(2022), no. 5, 431-443, doi: 10.1016/j.joes.2021.09.018.

[107] M. M. A. Khater, S. Anwar, K. U. Tariq, and M. S. Mohamed, *Some optical soliton solutions to the perturbed nonlinear Schrödinger equation by modified Khater method,* AIP Adv. **11**(2021), no. 2, 025130, 2021, doi: 10.1063/5.0038671.

[108] M. M. Khater, S. K. Elagan, A. A. Mousa, M. A. El-Shorbagy, S. H. Alfalqi, J. F. Alzaidi, and D. Lu, *Sub-10-fs-pulse propagation between analytical and numerical investigation,* Results Phys. **25**(2021), 104133, doi: 10.1016/j.rinp.2021.104133.

[109] R. Camassa and D. D. Holm, *An integrable shallow water equation with peaked solitons,* Phys. Rev. Lett. **71**(1993), no. 11, 1661–1664, doi: 10.1103/PhysRevLett.71.1661.

[110] G. Gui, Y. Liu, P. J. Olver, and C. Qu, *Wave-Breaking and Peakons for a Modified Camassa-Holm Equation,* Commun. Math. Phys. **319**(2013), no. 3, 731–759, doi: 10.1007/s00220-012-1566-0.

[111] M. M. A. Khater, M. S. Mohamed, and R. A. M. Attia, *On semi analytical and numerical simulations for a mathematical biological model; the time-fractional nonlinear Kolmogorov–Petrovskii–Piskunov (KPP) equation,* Chaos, Solitons and Fractals, **144**(2021), 110676, doi: 10.1016/j.chaos.2021.110676.

[112] Y. Chu, M. M. A. Khater, and Y. S. Hamed, *Diverse novel analytical and semi-analytical wave solutions of the generalized (2+1)-dimensional shallow water waves model,* AIP Adv. **11**(2021), no. 1, 015223, doi: 10.1063/5.0036261.

[113] M. M. A. Khater, A. E. S. Ahmed, and M. A. El-Shorbagy, *Abundant stable computational solutions of Atangana–Baleanu fractional nonlinear HIV-1 infection of CD4+ T-cells of immunodeficiency syndrome,* Results Phys. **22**(2021), 103890, doi: 10.1016/j.rinp.2021.103890.

[114] M. M. Mostafa, M. S. Mohamed, and S. K. Elagan, *Diverse accurate computational solutions of the nonlinear Klein–Fock–Gordon equation,* Results Phys. **23**(2021), 104003, doi: 10.1016/j.rinp.2021.104003.

[115] M. M. A. Khater, A. A. Mousa, M. A. El-Shorbagy, and R. A. M. Attia, *Analytical and semi-analytical solutions for Phi-four equation through three recent schemes,* Results Phys. **22**(2021), 103954, doi: 10.1016/j.rinp.2021.103954.

[116] M. M. A. Khater, A. Bekir, D. Lu, and R. A. M. Attia, *Analytical and semi-analytical solutions for time-fractional Cahn–Allen equation,* Math. Methods Appl. Sci. **44**(2021), no. 3, 2682–2691, doi: 10.1002/mma.6951.

[117] M. M. A. Khater, A. A. Mousa, M. A. El-Shorbagy, and R. A. M. Attia, *Abundant novel wave solutions of nonlinear Klein–Gordon–Zakharov (KGZ) model,* Eur. Phys. J. Plus. **136**(2021), no. 5, 1–11, 2021, doi: 10.1140/epjp/s13360-021-01385-0.

[118] M. M. A. Khater and A. M. Alabdali, *Multiple novels and accurate traveling wave and numerical solutions of the (2+1) dimensional fisher-kolmogorov-petrovskii-piskunov equation,* Mathematics. **9**(2021), no. 12, 1–13, 2021, doi: 10.3390/math9121440.

[119] K. Hosseini, D. Baleanu, S. Rezapour, S. Salahshour, M. Mirzazadeh, and M. Samavat, *Multi-complexiton and positive multi-complexiton structures to a generalized B-type Kadomtsev−Petviashvili equation,* J. Ocean Eng. Sci. (2022), doi: 10.1016/j.joes.2022.06.020.

[120] K. Hosseini, M. Mirzazadeh, L. Akinyemi, D. Baleanu, and S. Salahshour, *Optical Solitons to the Ginzburg – Landau Equation Including the Parabolic Nonlinearity,* Optical and Quantum Electronics, **54**(2021), no. 10, 631.

[121] C. Yue, D. Lu, and M. M. A. Khater, *Abundant wave accurate analytical solutions of the fractional nonlinear hirota–satsuma–shallow water wave equation,* Fluids. **6**(221), no. 7, 1–13, doi: 10.3390/fluids6070235.

[122] W. Li, L. Akinyemi, D. Lu, and M. M. A. Khater, *Abundant traveling wave and numerical solutions of weakly dispersive long waves model,* Symmetry (Basel). **13**(2021), no. 6, 1–15, doi: 10.3390/sym13061085.

[123] M. M. Khater, *Diverse bistable dark novel explicit wave solutions of cubic–quintic nonlinear Helmholtz model,* Mod. Phys. Lett. B. **35**(2021), no. 26, 2150441, 2021.

[124] M. M. Khater, *Abundant breather and semi-analytical investigation: On high-frequency waves' dynamics in the relaxation medium,* Mod. Phys. Lett. B. **35**(2021), no. 22, 2150372, 2021.

[125] S. Rippa, *An algorithm for selecting a good parameter c in radial basis function interpolation,* Adv. Comput. Math. **11**(1999), 193–210, doi: 10.1023/A.

[126] G. E. Fasshauer and J. G. Zhang, *'optimal' shape parameters for RBF approximation,* Numer. Algorithms, **45**(2007), 345–365.

[127] A. Bekir and E. H. M. Zahran, *New visions of the soliton solutions to the modified nonlinear Schrödinger equation,* Optik, **232**(2021), 166539, doi: 10.1016/j.ijleo.2021.166539.

[128] H. Abdillah, N. Nasaruddin, M. Ikhwan, N. Nurmaulidar, and M. Ramli, *Soliton dynamics in optical fiber based on nonlinear Schrödinger equation,* Heliyon, **9**(2023), no. 3, e12122, doi: 10.1016/j.heliyon.2023.e14235.

[129] A. Biswas, H. Triki, Q. Zhou, S. P. Moshokoa, M. Z. Ullah, and M. Belic, *Cubic–quartic optical solitons in Kerr and power law media,* Optik, **144**(2017), 357–362, doi: 10.1016/j.ijleo.2017.07.008.

[130] S. Kumar, S. Malik, A. Biswas, Y. Yıldırım, A. S. Alshomrani, and M. R. Belic, *Optical solitons with generalized anti-cubic nonlinearity by Lie symmetry,* Optik, **206**(2020), 163638, doi: 10.1016/j.ijleo.2019.163638.

[131] I. D. Remizov and M. F. Starodubtseva, *Quasi-Feynman Formulas providing Solutions of Multidimensional Schrödinger Equations with Unbounded Potential,* Math. Notes. **104**(2018), no. 5–6, 767–772, doi: 10.1134/S0001434618110214.

[132] I. D. Remizov, *Solution of the Schrödinger equation with the use of the translation operator,* Math. Notes. **100**(2016), no. 3–4, 499–503, doi: 10.1134/S0001434616090200.

[133] H. Bulut, Y. Pandir, and S. Tuluce Demiray, *Exact solutions of nonlinear Schrödingers equation with dual power-law nonlinearity by extended trial equation method,* Waves in Random and Complex Media, **24**(2014), no. 4, 439–451,doi: 10.1080/17455030.2014.939246.

[134] M. Javidi and A. Golbabai, *Numerical studies on nonlinear Schrödinger equations by spectral collocation method with preconditioning,* J. Math. Anal. Appl. **333**(2007), no. 2, 1119–1127, doi: 10.1016/j.jmaa.2006.12.018.

[135] H. Wang, *Numerical studies on the split-step finite difference method for nonlinear Schrödinger equations,* Appl. Math. Comput. **170**(2005), no. 1, 17–35, doi: 10.1016/j.amc.2004.10.066.

[136] A. Bashan, *A mixed method approach to Schrödinger equation: Finite difference method and quartic B-spline based differential quadrature method,* Int. J. Optim. Control Theor. Appl. **9**(2021), no. 2, 223–235, doi: 10.11121/IJOCTA.01.2019.00709.

[137] A. Iqbal, N. N. A. Hamid, and A. I. M. Ismail, *Numerical solution of nonlinear Schrödinger equation with Neumann boundary conditions using quintic B-spline Galerkin method,* Symmetry, **11**(2019), no. 4, 469, doi: 10.3390/sym11040469.

[138] O. Ersoy Hepson and I. Dag, *Numerical investigation of the solutions of Schrödinger equation with exponential cubic B-spline finite element method,* Int. J. Nonlinear Sci. Numer. Simul. **22**(2021), no. 2, 119–133, doi: 10.1515/ijnsns-2016-0179.

[139] T. Povich and J. Xin, *A Numerical Study of the Light Bullets Interaction in the (2 + 1) Sine-Gordon Equation*, J. Nonlinear Sci. **15**(2005), no. 1, 11–25, doi: 10.1007/s00332-003-0588-y.

[140] L. Di, M. Villari, G. Marcucci, M. C. Braidotti, and C. Conti, *Sine-Gordon soliton as a model for Hawking radiation of moving black holes and quantum soliton evaporation*, J. Phys. Commun. **2**(2018), no. 5, 055016.

[141] V. G. Bykov, *Sine-Gordon equation and its application to tectonic stress transfer*, J. Seismol. **18**(2014), no. 3, 497–510, doi: 10.1007/s10950-014-9422-7.

[142] D. Kaya, *An application of the modified decomposition method for two dimensional sine-Gordon equation*, Appl. Math. Comput. **159**(2004), no. 1, 1–9, doi: 10.1016/S0096-3003(03)00820-8.

[143] U. Yucel, *Homotopy analysis method for the sine-Gordon equation with initial conditions*, Appl. Math. Comput. **203**(2008), no. 1, 387–395, 2008, doi: 10.1016/j.amc.2008.04.042.

[144] M. Dehghan and A. Shokri, *A Numerical Method for One-Dimensional Nonlinear Sine-Gordon Equation Using Collocation and Radial Basis Functions*, Numer. Methods Partial Differ. Equations. **24**(2008), no. 2, 687–698, doi: 10.1002/num.

[145] J. Rashidinia and R. Mohammadi, *Tension spline solution of nonlinear sine-Gordon equation*, Numer. Algorithms. **56**(2011), no. 1, 129–142, doi: 10.1007/s11075-010-9377-x.

[146] M. Lotfi and A. Alipanah, *Legendre spectral element method for solving Sine-Gordon equation*, Adv. Differ. Equations. **2019**(2019), 1–15, doi: 10.1186/s13662-019-2059-7.

[147] D. Adak and S. Natarajan, *Virtual element method for semilinear Sine-Gordon equation over polygonal mesh using product approximation technique*, Math. Comput. Simul. **172**(2019), 224–243.

[148] R. Jiwari, *Barycentric rational interpolation and local radial basis functions based numerical algorithms for multidimensional sine-Gordon equation,*

Numer. Methods Partial Differ. Equ. **37**(2020), no. 3, 1965–1992, doi: 10.1002/num.22636.

[149] B. K. Singh and M. Gupta, *A New Efficient Fourth Order Collocation Scheme for Solving Sine-Gordon Equation*, Int. J. Appl. Comput. Math. **123**(2021), no. 7, 138, doi: 10.1007/s40819-021-01089-0.

[150] M. Shiralizadeh, A. Alipanah, and M. Mohammadi, *Numerical solution of one-dimensional Sine-Gordon equation using rational radial basis functions,* J. Math. Model. **10**(2022), no. 3, 387–405, doi: 10.22124/jmm.2021.20458.1780.

[151] A. T. Abed and A. S. Y. Aladool, *Appling Particle Swarm Optimization Based on Pade Approximant to Solve Ordinary Differential Equation*, Numer. Algebr. Control Optim. **12**(2022), no. 2, 321–337, doi: 10.3934/naco.2021008.

[152] A. G. Gad, *Particle Swarm Optimization Algorithm and Its Applications: A Systematic Review,* Arch. Comput. Methods Eng. **29**(2022), no. 5, 2531–2561, doi: 10.1007/s11831-021-09694-4.

[153] J. Robinson and Y. Rahmat-Samii, *Particle swarm optimization in electromagnetics, IEEE* Trans. Antennas Propag. **52**(2004), no. 2, 397–407, doi: 10.1109/TAP.2004.823969.

[154] P. Wang, L. Xie, and Y. Sun, *Application of PSO algorithm and RBF neural network in electrical impedance tomography,* in 9th International Conference on Electronic Measurement and Instruments, (2009), 2-517–2-521. doi: 10.1109/ICEMI.2009.5274525.

[155] R. V Kulkarni and G. K. Venayagamoorthy, *Particle swarm optimization in wireless-sensor networks: A brief survey*, IEEE Trans. Syst. Man Cybern. Part C Appl. Rev. **41**(2011), no. 2, 262–267, doi: 10.1109/TSMCC.2010.2054080.

[156] R. Barbieri, N. Barbieri, and K. F. De Lima, *Some applications of the PSO for optimization of acoustic filters,* Appl. Acoust. **89**(2015), 62–70, doi: 10.1016/j.apacoust.2014.09.007.

[157] H. Yang, Y. Xu, G. Peng, G. Yu, M. Chen, W. Duan, Y. Zhu, Y. Cui, and X. Wang, *Particle swarm optimization and its application to seismic inversion of igneous rocks*, Int. J. Min. Sci. Technol. **27**(2017), no. 2, 349–357, doi: 10.1016/j.ijmst.2017.01.019.

[158] R. Kalatehjari, N. Ali, M. Hajihassani, and M. Kholghi Fard, *The application of particle swarm optimization in slope stability analysis of homogeneous soil slopes*, Int. Rev. Model. Simulations. **5**(2012), no. 1, 458–465.

[159] B. T. Pham, C. Qi, L. S. Ho, T. Nguyen-Thoi, N. Al-Ansari, M. D. Nguyen, H. D. Nguyen, H. B. Ly, H. Van Le, and I. Prakash, *A novel hybrid soft computing model using random forest and particle swarm optimization for estimation of undrained shear strength of soil*, Sustainability, **12**(2020), no. 6, 2218, doi: 10.3390/su12062218.

[160] Z. Cui, J. Zhang, D. Wu, X. Cai, H. Wang, W. Zhang, and J. Chen, *Hybrid many-objective particle swarm optimization algorithm for green coal production problem*, Inf. Sci. (Ny). **518**(2020), 256–271, doi: 10.1016/j.ins.2020.01.018.

[161] M. Juneja and S. K. Nagar, *Particle swarm optimization algorithm and its parameters : A review,* 6 Int. Conf. Control. Comput. Commun. Mater. (2016), 1–5.

[162] Y. F. Alharbi, E. K. El-Shewy, and M. A. Abdelrahman, *New and effective solitary applications in Schrödinger equation via Brownian motion process with physical coefficients of fiber optics*, AIMS Math, **8**(2023), no. 2, 4126-40.

[163] G. Arora, R. Rani, and H. Emadifar, *Numerical solutions of nonlinear Schrodinger equation with applications in optical fiber communication*, Optik, **266** (2022), 169661.

[164] S. A. Mohammed, Y. Adamu, and M. K. Luka, *Analysis of Dispersion Compensation in a Single Mode Optical Fiber Communication System*, Int. J. Adv. Acad. Res. **5**(2019), no. 1, 12-19.

[165] A. Hasegawa, *Soliton-based optical communications: an overview,* in IEEE Journal of Selected Topics in Quantum Electronics, **6**(2000), no. 6, 1161-1172, doi: 10.1109/2944.902164.

[166] A. Hasegawa, *Optical soliton: Review of its discovery and applications in ultra-high-speed communications,* Frontiers in Physics, **10***(*2022), 1210.

[167] Y. Song, X. Shi, C. Wu, D. Tang, and H. Zhang, *Recent progress of study on optical solitons in fiber lasers*, Applied Physics Reviews, **6**(2019), no. 2, 1-20.

[168] Z. Trabelsi, E. Hannachi, S. A. Alotaibi, Y. Slimani, M. A. Almessiere, and A. Baykal, *Superconductivity Phenomenon: Fundamentals and Theories,* In Superconducting Materials: Fundamentals, Synthesis and Applications, (2022), 1-27, Singapore: Springer Nature Singapore.

[169] G. Arora, R. Rani, and H. Emadifar, *Soliton: A dispersion-less solution with existence and its types*, Heliyon, **e12122**(2022).

[170] S. M. Anlage, *Microwave superconductivity*, IEEE Journal of Microwaves, **1**(2021), no. 1, 389-402.

[171] R. S. Souto, M. Leijnse, and C. Schrade, *Josephson diode effect in supercurrent interferometer,* Physical Review Letters, **129**(2022), no. 26, 267702.

[172] J. J. Mazo, and A. V. Ustinov, *The Sine-Gordon equation in Josephson-junction arrays,* The Sine-Gordon Model and Its Applications: From Pendula and Josephson Junctions to Gravity and High-Energy Physics, (2014), 155-175.

[173] D. De Santis, C. Guarcello, B. Spagnolo, A. Carollo, and D. Valenti, *Generation of travelling sine-Gordon breathers in noisy long Josephson junctions*, Chaos, Solitons & Fractals, **158** (2022), 112039.

[174] F. S. V. Causanilles, H. M. Baskonus, J. L. G. Guirao, and G. R. Bermudez, *Some important points of the Josephson effect via two superconductors in complex bases*, Mathematics, **10**(2022), no. 15, 2591.

List of Published and Communicated Papers/ Book Chapter/ List of Attended Conferences

List of Published and Communicated Papers

1. Arora, G., Rani, R., & Emadifar, H. (2022). Numerical solutions of nonlinear Schrodinger equation with applications in optical fiber communication. *Optik, 266*, p.169661,

   https://doi.org/10.1016/j.ijleo.2022.169661.

   (Scopus and SCI, Impact Factor-3.1, SJR 2022-0.54, Q2, CiteScore-5.7, Print ISSN: 0030-4026, Online ISSN: 1618-1336,

   Web link of journal-

   https://www.sciencedirect.com/journal/optik/about/insights#abstracting-and-indexing)

2. Arora, G., Rani, R., & Emadifar, H. (2022). Soliton: A dispersion-less solution with existence and its types. *Heliyon*,

   https://doi.org/10.1016/j.heliyon.2022.e12122.

   (Scopus and SCIE, Impact Factor-4.0, SJR 2022-0.61, Q1, CiteScore-5.6, Online ISSN- 2405-8440,

   Web link of journal- https://www.sciencedirect.com/journal/heliyon)

3. Rani, R., Arora, G., Emadifar, H., & Khademi, M. (2023). Numerical simulation of one-dimensional nonlinear Schrodinger equation using PSO with exponential B-spline. *Alexandria Engineering Journal*, *79*, pp.644-651,

   https://doi.org/10.1016/j.aej.2023.08.050.

   (Scopus and SCIE, Impact Factor-6.8, SJR 2022-0.93, Q1, CiteScore-9.1, Online ISSN: 2090-2670, Print ISSN: 1110-0168,

   Web link of journal- https://www.sciencedirect.com/journal/alexandria-engineering-journal)

4. Numerical solution of one-dimensional nonlinear Sine-Gordon equation by using LOOCV with exponential B-spline and its application in Josephson junctions. (Communicated)

5. Particle Swarm Optimization Numerical Simulation with Exponential modified cubic B-spline DQM. (Communicated)

Book Chapter

Rani, R., & Arora, G., (2022). "Role of Soliton Solutions of Mathematical Model in Optical Fiber Communication". Published by Studera Press in Recent Advances in Mathematical and Computer Sciences, ISBN 978-93-91854-48-5.

List of Attended Conferences

1. Presented a paper entitled "Role of Soliton Solutions of Mathematical Model in Optical Fiber Communication" in National conference "RAMCS-2021" held at Govt. College, Nalwa (Hisar) on 27 Nov., 2021.
2. Presented a paper entitled "Overview of Soliton and its Applications" in 2nd international conference on "CSMCS-2022" held at Manipal Institute of Technology, Manipal, on 28-30 March, 2022.
3. Presented a paper entitled "A brief on Particle Swarm Optimization and its applications" in "International conference on evolution in pure and applied mathematics" held at Akal University, Talwandi Sabo, Bathinda, Punjab, on 16-18 November, 2022.
4. Presented a paper entitled "Role of soliton solutions of nonlinear Sine-Gordon equation in Josephson junction" in 4th international conference on "RAFAS-2023" held at Lovely Professional University, Punjab, on 24-25 March, 2023.